University of Stavanger

FACULTY OF SCIENCE AND TECHNOLOGY

MASTER'S THESIS

Study programme/Specialisation: Petroleum Engineering/Drilling and Well Engineering	Spring semester, 2020 Open
Author: Tat, Thea Hang Ngoc	…………………………………………… (Author's signature)

Supervisor(s): Fjelde, Kjell Kåre
Title of master's thesis: A Numerical Study of Pressure Build Up due to Kick Migration in a Closed Well Filled with Water-Based Mud
Credits (ECTS): 30

Keywords: Transient flow model Gas migration velocity Pressure build up Suspended gas AUSMV scheme	Number of pages: 107 + supplemental material/other: 48 Stavanger, June 15th, 2020

I

Abstract

There has been considerable and diverging discussion in the academic literature regarding the real gas kick velocity. This thesis contributes to improving and sharing the knowledge about the real gas kick velocity. It is demonstrated that estimating gas kick migration velocities using pressure build up slopes is an unreliable method. In Non-Newtonian drilling fluids, some of the gas volumes may be suspended in the mud, which can explain why there has been reported large discrepancies on what the gas kick migration velocity can be. This is one potential explanation, but future research should investigate this topic even further.

A transient flow model based on the drift flux model supplemented with a gas slip relation was used. The transient flow model was solved by an explicit numerical scheme (AUSMV) in MATLAB. The slope limiter concept was applied, and numerical diffusion was reduced to obtain optimal results. In the existing numerical scheme, the old model, a fixed gas slip model was implemented, i.e. the slug model. Hence, the gas migration velocity was a constant value. As for the new model, different flow patterns were included, i.e. suspended gas, bubble flow, slug flow, and the transition to one-phase gas. Appropriate transition intervals were linearly interpolated. Pressure build up for kick migration in a closed well was studied to observe how it varied from the impact of having a gas slip model which varied depending on what kind of flow pattern that was present at different locations in the well. A closed well of constant geometry was considered in order to study the pressure evolution. A sensitivity analysis was performed by varying kick sizes, suspension limits, and changing the transition intervals between the flow patterns. The analysis helped identifying the variables that were of major influence.

Simulation results showed that the slope of the pressure build up was influenced by suspension effects; the slope was reduced for increasing suspension limits. For cases where substantial suspension effects were considered, the pressures reached stable values quite early. The gas volume fraction depth profiles revealed that the gas kick was fully suspended in the well. In cases where the kicks were still able to migrate, the gas kick bulks migrated at the same velocity as long as they were in the same flow regime despite the different suspension limits that affected the pressure build up slopes differently. It seems impossible to determine a unique gas velocity from different pressure build up slopes. Nevertheless, they could be used to predict flow pattern transitions as abrupt changes in the slope were observed when flow pattern transitions occurred.

Acknowledgement

I would like to express my gratitude towards my supervisor Professor Kjell Kåre Fjelde for giving me the opportunity to be a part of this project. I am genuinely grateful for the great guidance and valuable feedback he dedicatedly provided to me throughout the process.

I would also like to thank my family and my partner Kåre-André for their support during the two last years.

Lastly, to all friends who in one way or another made the last few years enjoyable, thank you!

<div align="center">

Thea Hang Ngoc Tat

Stavanger, 15th of June 2020

</div>

Table of contents

List of tables

List of figures

List of Abbreviations

O&G – oil and gas

E&P – exploration and production

HSE – health, safety, and environment

BOP – blow out preventer

AUSMV- advection upwind splitting method

WBM – water-based mud

CML – controlled mud level

CMCD – controlled mud cap drilling

PMCD – pressurized mud cap drilling

BHP – bottom hole pressure

WHP – wellhead pressure

List of Symbols

α_l – phase volume fraction of liquid at new time level [dimensionless]

α_g – phase volume fraction of gas at new time level [dimensionless]

ρ_l – liquid phase density at new time level [kg/m^3]

ρ_{lo} – liquid phase density at old time level [kg/m^3]

ρ_g – gas density at new time level [kg/m^3]

ρ_{mix} – mixture density of fluid [kg/m^3]

v_l – phase velocity of liquid at new time level [m/s]

v_g – phase velocity of gas at new time level [m/s]

v_{mix} – mixed velocity of fluid [m/s]

w – sound velocity [m/s]

p – pressure at new time level [Pa]

p_o – pressure at old time level [Pa]

p_{inlet} – pressure at inlet [Pa]

p_{outlet} – pressure at outlet [Pa]

F_w – friction gradient model [Pa/m]

f – friction factor [dimensionless]

d_i – inner diameter of well [m]

d_o – inner diameter in annulus; outer diameter of drillstring [m]

θ – well inclination [degrees]

σ – interfacial tension between phases [N/m]

μ_{mix} – viscosity of mixed fluid [cP]

Re – Reynold's number [dimensionless]

K – gas slip parameter [dimensionless]

S – gas slip parameter [m/s]

t – time variable [s]

z – spatial variable [m]

g – gravitational constant [m/s^2]

x – transition interval between flow regimes [dimensionless]

a – minimum suspension limit [fraction (0-1)]

b – maximum suspension limit [fraction (0-1)]

1. Introduction

1.1. Background

In the past decade, scientists have dedicated their research to connecting human-induced climate change and extreme weather conditions. With the increase in population and economic development, parallel with the drastic growth in energy demand, citizens and governments are desperately attempting to avert a global climate disaster as the awareness for climate is rising. Entering 2020, it is crucial for industries to transform into the low-carbon energy transition and simultaneously meet the high energy demand. With this in mind, the O&G industry is still important for the world's energy consumption. Nevertheless, it has never been as important to produce fossil fuels as clean, cost-effective, and safe as today. Despite the recognition that the fossil fuel industry still is important for the world's energy consumption, the world is recognizing the need to reduce the energy-related CO_2 emissions. In order for the O&G industry to contribute to the global energy transition, research has to be conducted to ensure that E&P activities can be conducted with minimal HSE risk.

One of the most hazardous situations occurring while drilling is kick. If not controlled properly, it can in worst case scenario develop into an uncontrolled blowout which can have a disastrous impact threatening the lives of people and the environment. The Deepwater Horizon oil spill in the Gulf of Mexico in 2010 [1] and the recent oil spill into Lake Texoma, Oklahoma [2] are examples of undesirable accidents that involve exposure of people and environment to hazardous HSE risks. As well control situation is one of the most crucial aspects of drilling and well operations, contingency procedures must be designed, and techniques for handling well control incidents must be properly applied. With a thorough strategy, risk is minimized, and appropriate procedures established to avoid reoccurrence of accidents.

When a gas kick occurs, the BOP is closed, and depending on which type of mud is being used, the gas kick will migrate upwards in the well towards the closed BOP. Usually, a well kill procedure is initiated before the kick reaches the BOP in a closed well. In order to implement appropriate measures to regain well control, it is an advantage to know the behavior of the fluid. Useful knowledge includes gas migration velocity, which can affect the distribution of gas, and consequently gas holdup. It will also have impact on how fast the pressure builds up in a closed well. An important effect that has to be considered is that for Non-Newtonian drilling fluids,

free gas can be trapped or suspended by the mud. In some situations, the kick will not be able to reach the surface at all without additional circulation. A special dangerous situation can occur if a gas kick enters the riser before the BOP is closed where a worst-case scenario will be that the riser is unloaded.

After the Macondo blowout in 2010, early kick detection technology was considered critical for well control operations. However, since sensor readings must be interpreted correctly, kick detection can be complicated. Kick detection technologies can be improved by developing smart detection systems that also work under various conditions besides the conventional drilling and circulating operations. Improved reliability can lead to automation of kick detection systems, but in order to develop new technology, standards have to be defined. Since accuracy of gas migration velocity models has been discussed, there is still no well-defined standard for these measurements that also can be applied in the field. In [3], it was highlighted that current kick detection technology rely on measurements from the rig, yet the ultimate solution would be kick detection from the bottom of the wellbore, passing through sensors along its way up. The development of a networked kick detection system relies on more data about the occurrence of kicks and the condition in which it occurs. Eventually, new algorithms to create kick detection systems can benefit the industry.

During the production and transport of hydrocarbons through long pipelines, two-phase flow occurs frequently. Understanding the behavior of the fluid is therefore vital in the O&G industry. Two-phase flow models are used for this purpose. A basic two-fluid model involves conservation equations for mass, momentum and energy conservation, and combined with closure laws that considers the phase interactions, two-phase flow can be described [4]. Since modeling of gas-liquid flow is rather complex, a simple drift flux model can be used instead [5], [6]. The drift flux model originates from the two-fluid model. By adding the respective momentum and energy equations, mixture momentum and energy equations are obtained. Since complex terms such as phase interactions cancel, an empirical slip equation is needed to replace the missing information that describes the relation between the phase velocities [4]. The AUSMV scheme can be used to solve the drift flux model.

1.2.   Objective

The main purpose of this simulation study is to show how different modelling assumptions, numerical approximations, and specific physical effects can have significant impact on both how fast the pressures in the closed well increase, when the final pressures are reached, and at what final pressure levels the well will stabilize. Boyle's law states that the bottom hole pressure in a closed well is brought to the closed BOP when the kick migrates from bottom to the BOP. This is a conservative assumption and assumes that the mud is incompressible. In reality, some gas expansion is allowed since the mud is compressed slightly.

A transient flow model based on the drift flux model supplemented with a gas slip relation will be used to study the pressure evolution in a closed well of constant geometry when a kick migrates. The mathematical model and code used in this thesis will be based on previous work in [7] and [8]. In [7], a gas slip model based on constant slip parameters were used. In [8], the gas slip model was extended to cover different flow regimes and suspension effects. The focus of the latter paper was unloading of riser scenarios. In this work, the focus will be on pressure build up in a closed well when having a migrating kick. The same density models will be used for simplicity.

Initially, the existing numerical scheme, the old model, will be improved by addressing some mass conservation issues that were encountered in [9]. The way the boundary cells are treated in the transient flow model will affect the accuracy of the model. Previous methods will be reviewed and improved techniques of handling the slope limiters in the boundary cells will be proposed to reduce numerical liabilities.

In continuation of the work initiated in [7], the pressure build up will be studied to investigate how the pressures vary from the impact of having a gas slip model which will vary depending on what kind of flow pattern that is present at different locations in the well. In the existing numerical scheme, old model, only the slug flow model was implemented; hence, the gas velocity was fixed. In the improved numerical scheme, new model, the flow pattern that is present will be dependent on the gas fraction; different flow patterns will be considered, i.e. suspended gas, bubble flow, slug flow, and transition to one-phase gas. Appropriate transition intervals will be linearly interpolated and evaluated. Three different kick sizes will be used to show that the new model is able to consider different gas slip models depending on the flow regime.

The accuracy of the new model will be studied by varying the grid refinement. It will be demonstrated that the numerical diffusion is reduced by increasing the number of numerical cells. A recommendation on the number of cells will be provided before further simulations.

A sensitivity analysis will be performed by varying kick sizes, suspension limits, and changing the transition intervals between the flow patterns. The analysis helps identifying the variables that are of major influence.

For Non-Newtonian drilling fluids, small gas volumes can be trapped by the mud (suspended) in the mud [10]. Suspension effects for different kick volumes will be studied in detail. It will be shown that gas suspension effects will also have impact on the pressure build up [10], [7]. The more gas that is trapped, the lower the pressure build up will be. It will become clear that trying to estimate a gas slip velocity by using the slope of the pressure build up is not reliable.

Minimum suspension limits will be defined, where the gas volume will be in full suspension. The transition interval from full suspension to fully developed bubble flow will be linearly interpolated and evaluated. The gas will migrate in the bubble flow regime for gas volume fractions larger than the predefined maximum suspension limit before the gas fraction is sufficiently large to form slugs. In [10], it was reported that for Non-Newtonian fluids, the transition zone from slug to bubble flow seemed to take place for lower gas volume fractions compared to what was seen for Newtonian fluids. The effect of changing this transition zone on pressure build up slopes will be studied.

Lastly, the interpolation interval from slug flow to one-phase gas will be evaluated. This interpolation is required as there exists a singularity in the gas slip relation for gas fractions at around 0.83 when considering slug flow. This will be explained in detail in chapter 3.3. The effect of changing the interpolation interval on pressure build up slopes will be studied.

1.3. Literature Review on Kick Migration

1.3.1 Suspension Effects

Suspension effects were reviewed and studied in [10], where gas was injected into a column full of a Non-Newtonian drilling mud in a small-scale experiment to measure how much gas was trapped by the mud. Two main implications were drawn from the experiments. The experimental tests indicated that suspension of gas occurs early in the migration route, and the volume of migrating gas will be reduced on its way towards the surface as some of the gas will be left behind. The second effect was that suspended gas increases the compressibility of the mud. In paper [10], an analytical model was developed to estimate how much gas volume that could be suspended in the well based on knowing the initial kick volume at the bottom and the gas fraction suspension limit. In paper [10], the effect of suspended gas on the mud compressibility was also considered. An analytical model for the pressure build up in a closed well was derived where both the effect of suspended gas and migrating gas was taken into account. This was an extension of the model presented in [11]. The calculations using the model revealed that pressure build up decreases with increasing gas suspension. If no gas suspension is observed, pressure at surface will be much greater than if a small fraction of gas is suspended in the mud. In addition, the experimental results in paper [10] revealed that the volume of suspended gas is dependent on the mud properties, e.g. yield stress and gel strength. Paper [10] also discusses some field observations that later were published in [12]. These field tests also indicated that suspension of gas occurred, and gas only appeared as bubbles at surface after longer periods of circulation.

Field tests, e.g. [12] and [13], have shown the effect of gas suspension in Non-Newtonian drilling fluids, such as WBM. If gas is fully suspended in the mud, there is no gas slip conditions. Whether a kick becomes fully suspended or not depends on parameters such as size of the kick, well/riser length, and fluid properties, where one must also take well status into consideration since it will impact the shear stress of the mud. These experiments revealed that more advanced models needed to be implemented to predict the suspension effects.

1.3.2 Transient Drift Flux Model

In [14], a transient model with a gas slip model presented a better fit to the gas migration velocity compared to the single-bubble model. An advanced two-phase flow model was recommended for evaluations of gas migration scenarios. Paper [7] discusses the accuracy of the gas kick slippage models used in transient flow models. It presents some uncertainties related to this, and how the pressure build up is affected as a consequence of two sources of errors. The first source of error is the gas slip constants defined. The gas slip constants, K and S, will vary depending on what flow regime that is present, which again depends on the gas volume fraction. Paper [15] and [16] present variations in the K-value for bubble flow, which can possibly be a source of error. The second source of error when using a transient model is numerical diffusion caused by the numerical scheme [7]. The uncertainties related to the first order numerical scheme was possibly larger than the ones related to the gas slip model constants. The first order numerical scheme results presented in [7] had excessive numerical diffusion, especially for a rough grid, i.e. 25 cells. Calculations were more accurate when increasing the number of cells, e.g. to 50 cells or 100 cells; however, an increase in number of cells will increase the computational time. Numerical diffusion was improved by making the numerical discretization second order by using the slope limiter concept. The second order method reduced the numerical diffusion to an acceptable level without needing a very large number of cells [7].

In [8], a drift flux model was used to simulate riser unloading. The paper presents a literature review about gas migration and suspension effects. A gas slip model which takes into account both suspended gas, bubble flow and slug flow was included. A sensitivity analysis was performed to study how gas kick volumes and suspension limits affected the unloading scenario. First, grid refinement was studied to evaluate how many numerical cells that was needed for accurate calculations. An increase in the number of cells presented a reduction in numerical diffusion; yet, the accuracy of the results would not increase enough when increasing the number of cells from 100 to 200 to justify for the increase in computational time. For the riser unloading case, the simulations showed that gas expanded as it circulated, initiating a pressure drop in the hydrostatic column. When the kick left the riser, pressure again increased. When numerical diffusion was minimal, higher maximum rates were predicted. Thus, the bottom hole pressure drop was more evident.

Another effect studied in [8] was the suspension limit. In this case, there was no circulation, and the gas migrated due to the density differences between the gas and drilling fluid. The highest gas and fluid rates were reported for the no suspension case, i.e. gas fully migrating. This gave the lowest pressure at the BOP after unloading and it was the most dramatic case. The kick was fully suspended for a suspension limit somewhere between 2.5 and 3% for an 8 m^3 kick. At this suspension limit, the pressure at the BOP was nearly constant. The total liquid mass was also nearly constant, indicating that almost no liquid was unloaded from the well. Simulation results showed that the severity of the unloading is very dependent on the inclusion of suspension effects.

Paper [8] also compared kick sizes and suspension limits. The likelihood of an unloading event is sensitive to both suspension limits and kick volume, and the importance of a good gas migration model including suspension effects was highlighted.

1.3.3 Gas Migration Velocity used in New Technology

Knowledge about gas migration velocities is important for the development of technology. For example, in [17], operational procedures for controlled mud level (CML) technology and controlled mud cap drilling (CMCD) were assessed. It was evident that the field observations from pressurized mud cap drilling operations indicated a much lower gas migration velocity compared to that obtained by a transient flow model and theoretical bubble rise velocity models. In [18], it was emphasized that research about gas migration velocities is needed to improve the operational procedures for these types of drilling systems. This includes preparation for safe circulation of gas out of the riser if it has passed undetected through the BOP, especially for ultradeepwater drilling [19], and its associated surface effects. For example, a change of gas migration velocity can double the volume of the gas, and thus hydrostatic pressure is reduced. As a consequence, hydrostatic collapse can occur [20], and this can cause damage to the marine riser and in worst-case scenario create hazardous situations. Furthermore, knowledge about gas migration velocity is important in bullheading operations both in PMCD and conventional drilling systems. Gas migration velocities are used to determine the bullheading rates.

Although current models can be used to predict gas migration velocities, papers [10] and [11] highlight that it can be difficult to estimate accurate gas migration velocities. Paper [11] showed that the gas migration velocity could be underestimated more than 10 times. Paper [10] explains that this is because the velocities are often derived based on how fast the pressure builds up

under the assumption that the well is not leaking, and the mud is incompressible. By using the pressure build up rates to estimate gas migration velocities, there will in fact be difficulties because one also has to consider other parameters that affect the pressures, e.g. the presence of suspension effects. It should be mentioned that a well kill procedure would be initiated a long time before the kick reaches the BOP for the closed well conditions. The reason is that the pressures in the well could become so large that the formation breaks down. Hence, it is reasonable to assume that for the cases where field observations of pressure build rates are used to deduce what the gas migration velocity is, these data must come from the initial stages of the pressure build up.

In [7], simulations were conducted to attempt to clarify why it is difficult to estimate gas migration velocities from pressure build up slopes. Three different pressure build up slopes were presented for three different suspension values, yet the gas kick bulks migrated at approximately the same speed. This showed that one cannot deduct a unique gas migration velocity from three different pressure build up slopes. Improved knowledge about gas migration velocities under various conditions and consequently pressure build up can lead to the development of new technology that can be applied to current operational procedures.

In the next chapter, an introduction to modeling will be provided. A literature review on modeling of two-phase flow will be presented, including the details of the model that is used in this thesis.

2. Modeling of Two-Phase Flow

2.1. Introduction to modeling

Common models used in the O&G industry are empirical correlations, homogeneous models, and mechanistic models [21]. In empirical correlations, experimental data is plotted and attempted to fit a curve. Accuracy in an empirical relationship is dependent on whether the correlation is supported by proven theory or not. An example of an empirical relationship for liquid holdup (the fraction of the pipe which is occupied by liquid) for varying viscosities was presented in [22] considering two-phase flow in horizontal pipes. The Beggs-Brill model [23] can be used to calculate the liquid holdup for inclined pipes.

Homogeneous models characterize two-phase fluids in mixture properties, and hence, one can treat the fluid properties as one continuous single-phase. Drift flux models are homogeneous models supplemented with a slip model to include the effect that the two phases move with different velocities. They are derived from the more fundamental two-fluid model by combining the momentum equations into a mixture momentum equation. Hence, a gas slip relation is needed to supply the missing information. The drift-flux model proposed in [24] has been researched and applied successfully, e.g. in [25] for gas-liquid two-phase flow in pipes for varying inclinations.

The model with the least uncertainties is the mechanistic model, as the models derive from physics of the different flow patterns. The mechanistic model developed in [26] is one of the most significant models for predicting flow pattern transitions. The model is developed for gas-liquid pipe flow at inclinations varying from -90° to 90° from horizontal. The slug flow pattern was used as base for describing and predicting flow pattern transitions. As slug liquid holdup is associated with the average liquid holdup and consequently pressure gradient, a relatively complex mechanistic model for slug and liquid holdup was developed in [27] for different oil viscosities in pipes. By varying well geometry, i.e. pipe inside diameter and pipe inclination, and viscosity, other models were compared with the proposed model. The experiments showed that the liquid holdup increased with increasing superficial liquid velocity and decreased with an increase in superficial gas velocity.

Although the mechanistic model might be more accurate for liquid holdup prediction, it is based on a system of equations requiring closure laws that derive from assumptions and experimental

values. Also, in the transition zones between different flow patterns, the mechanistic model fails due to discontinuities, as discussed in [28]. An important remark is that the mechanistic models consider a steady state situation while the drift flux model is a model for the transient dynamics that can take place. It is possible to try to make an attempt to incorporate gas slip models developed by the mechanistic approach into the drift flux approach [29].

With all the common models in mind, the most complex model for flow pattern identification is the mechanistic model, since it is difficult to identify flow patterns considering gas migration and friction. In [30], a prediction model for liquid holdup in horizontal pipes was attempted to be developed for higher gas and superficial liquid velocity based on different models. Considering friction factor of the liquid phase, the gas-liquid interface, the Reynold's number of both phases, the average error of the proposed model was 4.8%.

The flow pattern transitions were first studied in [31] for vertical tubes, where the transition between the flow regimes were predefined based on mathematical models and correlated to behavior of pressure, two-phase flow, and experimental data. Later studies showed that inconsistency existed. In [32], the modeling methodology for slug flow was reviewed and compared with laboratory experiments for both horizontal and vertical pipes. It was concluded that further studies needed to be conducted to fully develop the proposed models to be able to scale up to heavy oil, as the models used in [31] were based on light oils of 0.001-0.002 Pa·s. In [33], a mechanistic model was presented for bubble, dispersed bubble, slug, and annular flow configurations for Newtonian fluids in vertical annuli. The slug-churn transition and the pressure drop predictions for this flow pattern was also discussed.

There exists a number of models for describing two-phase flow both for horizontal and vertical wells, as reviewed in [34]. Some of the existing models for two-phase flow, reviewed in [34], are presented below.

2.1.1 Pipeline models
For vertical pipes, flow pattern transitions were presented in [31] and [35]. The flow pattern transition model in [31] was extended to an inclined pipe model in [36]. Taitel and Dukler presented a model for flow pattern prediction in horizontal and near-horizontal pipes [37]. Paper [38] presented a mechanistic model for two-phase flow in horizontal and near-horizontal pipes.

2.1.2 Wellbore models

For vertical annuli, a flow regime transition model was presented in [39]. The mechanistic models presented in [16] apply for vertical annuli. [40] reviews the developments in the modelling of horizontal annuli. Different flow regimes in annulus for both vertical and inclined wells has been described in [16].

2.1.3 Unified model

In [34], an attempt was made to develop a unified model for two-phase flow, i.e. a mechanistic model for predicting flow pattern considering horizontal, inclined, and vertical pipelines and wellbores. The model provides individual models for stratified, slug, bubble, annular, and dispersed bubble flow.

2.1.4 Applied model

In this thesis, the simulations will be conducted using a drift-flux model and a gas slip relation given by the bubble and slug model specified in [16]. Gas suspension will be considered and there will be transition intervals between suspended gas and bubble flow, bubble and slug flow, and slug flow to one-phase gas. For these transition intervals gas slip constants will be found by linear interpolation using the gas volume fraction as parameter. The value of the gas volume fraction will be used to distinguish between the different flow patterns, and different values and models will be used for the gas slip constants depending on the flow pattern. By doing this, different flow patterns will exist at different locations in the well, but also at different times since we are considering a transient flow scenario. The gas slip model will be described in detail in chapter 3.

2.2. Transient Drift Flux Model

2.2.1. Conservation Laws

Under the assumption that (1) the fluid is a mixture of two phases, (2) mass exchange does not exist between the phases, (3) uniform area along the flow line, and (4) isothermal flow (constant temperature), the following nonlinear partial differential equations was used in the drift-flux model presented in [7] and [8]:

Conservation of liquid mass:

$$\frac{\partial}{\partial t}(\alpha_l \rho_l) + \frac{\partial}{\partial z}(\alpha_l \rho_l v_l) = 0 \tag{2.1}$$

Conservation of gas mass:

$$\frac{\partial}{\partial t}(\alpha_g \rho_g) + \frac{\partial}{\partial z}(\alpha_g \rho_g v_g) = 0 \tag{2.2}$$

Conservation of mixture momentum:

$$\frac{\partial}{\partial t}\left((\alpha_l \rho_l v_l + \alpha_g \rho_g v_g)\right) + \frac{\partial}{\partial z}\left((\alpha_l \rho_l v_l^2 + \alpha_g \rho_g v_g^2 + p)\right) = -(F_w + \rho_{mix} g \cos\theta) \tag{2.3}$$

2.2.2. Closure Laws

In order to be able to solve the drift flux model, the following simple equations are used:

2.2.2.1. Liquid Density Model

$$\rho_l(p) = \rho_{lo} + \frac{(p - p_o)}{a_l^2} \tag{2.4}$$

$$\left(simple\ model\text{: }for\ water\text{: }\rho_{lo} = 1000\frac{kg}{m^3}, p_o = 100000\ Pa, a_l = 1500\frac{m}{s}\right)$$

where a_l is the velocity of sound in the liquid phase.

2.2.2.2. Gas Density Model

$$\rho_g(p) = \frac{p}{a_g^2} \tag{2.5}$$

$$\left(simple\ model:for\ ideal\ gases: a_g = 316\frac{m}{s}\right)$$

where a_g is the velocity of sound in the gas phase. The models presented here are very simple, but they will be used in the simulation work presented in this thesis.

2.2.2.3. Friction Model

The Newtonian model, which is extended to two-phase flow using mixture variables, will be used in this thesis to calculate the frictional pressure loss gradient term for WBM. In general, different friction models are needed for describing Non-Newtonian fluids; however, in a shut-in situation, the friction effect is probably marginal. In [7] and [8], the following Newtonian friction model was used:

$$F_w = \left(\frac{2f\rho_{mix}v_{mix}abs(v_{mix})}{d_{out} - d_{in}}\right)\left(\frac{Pa}{m}\right) \tag{2.6}$$

To be able to calculate frictional pressure loss accurately, several factors need to be taken into consideration for a smooth transition, e.g. to distinguish between laminar and turbulent flow. For varying flow pattern, Reynold's number is used to differentiate between laminar, transient, and turbulent flow. It can be written as

$$Re = \frac{\rho_{mix}abs(v_{mix})(d_{out} - d_{in})}{\mu_{mix}} \tag{2.7}$$

The simplest way to model two-phase flow is estimating density of the mixed fluid using the gas volume fraction as an averaging parameter. Because the latter property of the fluid is dependent on flow regime, i.e. bubble or slug in this case, each flow regime has to be modeled separately to accurately estimate the density.

When Reynold's number is less than 2000, laminar flow exists. For Reynold's number between 2000 and 3000, the flow is transient. The flow is considered turbulent for Reynold's number greater than 3000. The friction factor will be different for laminar and turbulent flow and a smooth transition is needed in between.

$$f = \frac{24}{Re} \; for \; laminar \; flow \tag{2.8}$$

$$f = 0.052 Re^{-0.19} \; for \; turbulent \; flow \tag{2.9}$$

A better approach for calculating friction for Non-Newtonian fluids was presented in [41], where Newtonian and Non-Newtonian friction pressure correlations were reviewed and compared. While it was concluded that the correlations proposed by [42] and [43] were to be used for Non-Newtonian fluids in laminar flow regime in annuli, the correlations proposed by [44] was proposed for Non-Newtonian turbulent flow. The Newtonian friction model given in equation 2.6 will be used for simplicity since the friction effect is probably marginal for a closed well.

In the next chapter, the applied gas slip model is presented in detail.

3. Gas Slip Model

The slip between the two phases, namely gas and liquid, can be described by the drift-flux model. Combining two mechanisms, the drift-flux model is used to describe the interaction between the two phases. The gas slip model to be used in the drift-flux model is as follows

$$v_g = Kv_{mix} + S = K\left(\alpha_l v_l + \alpha_g v_g\right) + S \tag{3.1}$$

The velocity of the migrating gas is highest in the center of the flow, which makes the average velocity of the fluid slower than the average velocity of gas, which affects the KV_{mix}-term. This term becomes important, e.g. when there is drilling fluid circulation and when the gas expands in an open well and increasing the total flow. Both circulation and large expansion will have impact on the mixture velocity. Also, gas migrates upwards due to buoyancy, and travels through the fluid, affecting the S-value. This term will be the one representing the gas migration in a closed well since the KV_{mix}-term in that case is very close to zero.

The phase velocities are determined from the above equation in combination with the mixture momentum equations [45]. For the simulations, a gas slip relation which depends on what flow patterns that can be present will be implemented.

3.1. Suspension Effects

In Non-Newtonian fluids, gas bubbles are suspended as claimed in [10], leading to a no-slip condition where K_{susp}=1.0, S_{susp}=0 m/s. The transition from suspension to bubble flow occurs when the gas fraction is between the predefined minimum suspension limit and the predefined maximum suspension limit. For example, for 3% suspension, the minimum suspension limit is at the gas fraction 0.03 and the maximum suspension limit is at the gas fraction 0.05. The transition interval is calculated from the below equation. In this interval, the gas slip constants are interpolated:

$$x = \frac{\alpha_g - a}{b - a} \tag{3.2}$$

where a is the minimum suspension limit and b is the maximum suspension limit. The value of K and S are defined from:

$$K_{susp-bubble} = x * K_{bubble} + (1 - x)K_{susp} \qquad (3.3)$$

$$S_{susp-bubble} = x * S_{bubble} + (1 - x)S_{susp} \qquad (3.4)$$

3.2. Bubble Flow

Bubble flow is described as a homogeneous mixture of gas phase existing in the liquid phase [46]. In bubble flow, evenly distributed small bubbles migrate upwards. Before transitioning into cap bubbles (early slug), the migrating bubbles coalesce and become larger. As a consequence, they move at higher speed and force the smaller bubbles downwards. The pipe wall puts a constraint on how large the cap bubbles can become before eventually forming slugs [47]. For bubble flow, where the gas fraction is lower than 25% [33] for Newtonian fluids, the following K constant applies for vertical annuli [48]:

$$K_{bubble} = 1.0$$

The Harmathy correlation [49] gives the parameter S for bubble flow in vertical annuli:

$$S_{bubble} = 1.53 \left[\frac{g(\rho_l - \rho_g)\sigma}{\rho_l^2} \right]^{0.25} \qquad (3.5)$$

For the simulations conducted in this thesis, the interfacial tension between the phases will be $\sigma = 0.0772$ N/m, as presented and evaluated in [7].

Experiments in [33] indicated that the transition from bubble to slug flow occurs for a gas volume fraction of 0.25 for vertical *pipes*, and although experiments of [48] suggested a gas volume fraction at 0.20 for vertical pipes, a theoretical investigation [33] showed that at the experimental gas volume fraction of 0.25, slugs would appear also for Newtonian fluids in vertical *annuli* [16],[50]. The transition interval from bubble to slug flow is given below:

$$x = \frac{\alpha_g - 0.20}{0.25 - 0.20} \qquad (3.6)$$

In the transition interval, the gas slip constants are interpolated from the equations provided below:

$$K_{bubble-slug} = x * K_{slug} + (1-x)K_{bubble}$$ (3.7)

$$S_{bubble-slug} = x * S_{slug} + (1-x)S_{bubble}$$ (3.8)

3.3. Slug Flow

Slug flow is characterized by alternating flow of liquid and gas. In [30], the flow pattern is described as gas slugs separating liquid slugs. For slug flow, which applies for gas fractions larger than 25% for Newtonian fluids, the following slip parameters are established:

$$K_{slug} = 1.2 \ [15], [16]$$

$$S_{slug}^* = 0.35\sqrt{\frac{gd(\rho_l - \rho_g)}{\rho_l}} \ (\frac{m}{s})$$ (3.9)

[49],[10], [16] for vertical annular flow. d is the tubing inside diameter.

$$S_{slug} = S_{slug}^* \left(1 + \frac{0.29*d_i}{d_o}\right) * \sqrt{cos\theta}(1 + sin\theta)^2 \ (\frac{m}{s})$$ (3.10)

[16] for inclined annular flow. d_i and d_o are the annulus inside and outside diameter respectively. This equation has been implemented in the new model, but it is not used in the simulations as a vertical well of constant geometry will be considered.

A challenge encountered in the slug flow model is that a *singularity* exists [7]. The gas slip relation can be written as

$$v_g = \frac{Kv_l\alpha_l + S}{1 - K\alpha_g}$$ (3.11)

For a gas volume fraction equal to 1/K, the equation becomes undefined, i.e. for a gas volume fraction of 0.83 and a K_{slug}-value of 1.2, the gas migration velocity cannot be calculated. K will therefore be interpolated to 1.0 for gas fractions between 0.7-0.8, and S will be interpolated to

17

0 m/s for gas fractions between 0.9-1.0, which presents the no slip conditions when transitioning to one-phase gas.

3.4.   Practical Implementation of Gas Slip Models

Previous work, e.g. [7], used the *old model* to simulate different scenarios. In the initial code, the gas slip model was implemented with a fixed flow regime, i.e. the slug flow regime with gas slip parameters of K=1.2 and S=0.55 m/s (S was considered constant). In the proposed model, the *new model*, the gas slip constants will vary depending on what kind of flow pattern that is present at different locations in the well. The formulas for S for each flow pattern will depend on different parameters that will vary depending on well geometry and fluid parameters, e.g. phase densities and surface tension. The parameters are defined from equation 3.2 through equation 3.10. However, for the simulation work in this thesis, a vertical well of constant geometry will be considered, i.e. the well deviation and annular geometry corrections in equation 3.10 will be neglected. The S_{slug}-value will essentially be calculated from equation 3.9 in the new model. It was decided to keep the corrections in the MATLAB code for future studies, but as seen in Appendix B, they have been commented away.

The new model also takes suspension effects into account, where the gas will be in full suspension at the minimum suspension limit, i.e. K=1.0 and S=0 m/s. The transition interval from full suspension and fully developed bubble flow is given in equation 3.2. The gas slip parameters will be linearly interpolated in this interval depending on the gas fraction as given in equations 3.3 and 3.4. At the maximum suspension limit, fully developed bubble flow exists. For Newtonian fluids, bubble flow exists for all gas fractions below 0.25 [33]. The gas slip constant is K=1.0 and S is given by equation 3.5 for this flow regime. For gas fractions in the interval 0.20-0.25, as given in equation 3.6, an interpolation from bubble to slug flow will exist, and the gas slip parameters are calculated from equations 3.7 and 3.8. Slug flow fully exists for gas fractions larger than 0.25, where K=1.2 m/s and S can be calculated using equation 3.9. To avoid the issue of singularity explained in chapter 3.3, K will be interpolated to 1.0 for gas fractions between 0.7 and 0.8, and for gas fractions between 0.9 and 1.0, S will be interpolated to 0, i.e. K and S are interpolated to no slip conditions. The interpolation is critical for the simulation since there is a transition to pure gas in the boundary cells when the gas reaches the BOP.

Paper [10] suggested a lower transition between bubble and slug flow to consider that slug flow may take place for lower gas volume fractions when considering Non-Newtonian fluids. Paper [51] emphasizes that for Non-Newtonian fluids, suspension of gas occurs for smaller gas volumes, at approximately 10%. Gas migration velocities at 100 ft/min, or 0.51 m/s, were observed for gas concentrations larger than 10%, suggesting an early transition to slug flow. Bubble flow will be present at gas fractions below 0.10 and the transition from bubble to slug flow will occur at gas fractions between 0.10-0.15 in chapter 5.6.

4. Numerical Scheme

4.1. Discretization

To solve the conservation equations using the closure laws, one can discretize the well into several sections, N cells each with length of Δz. By solving the equations for each segment, the solution will be more accurate since the local variations in pressure, phase volume fractions phase velocities and phase densities are accounted for. Here, the explicit AUSMV scheme presented in [52] will be used.

To estimate the conservative variables at the new time level, they are updated based on values from the previous time level as represented in the figure below.
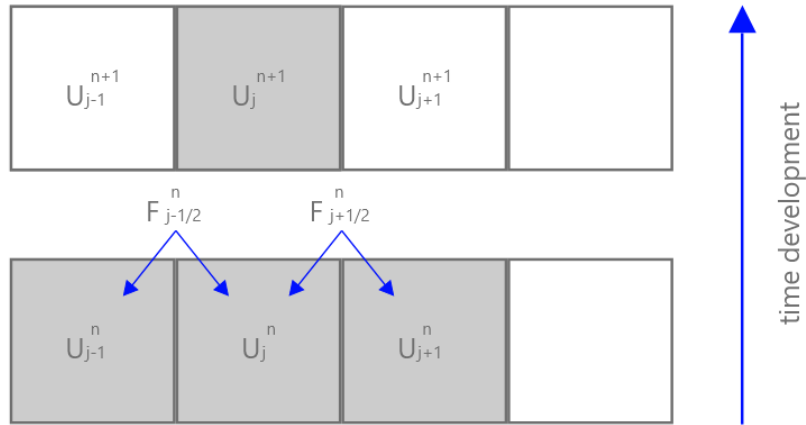
Figure 4.1 Update of discretized variables

The variables are always defined in the midpoint of the cell. To update each cell based on local variables, the following formula can be used:

$$U_j^{n+1} = U_j^n - \frac{\Delta t}{\Delta z}\left(F_{j+\frac{1}{2}}^n - F_{j-\frac{1}{2}}^n\right)\Delta t q(j,n) \tag{4.1}$$

The variable j represents the cell number, and variable n represents time level. The fluxes F in and out of the cell is predicted based on old time level. Formulas for the fluxes F being used in the AUSMV scheme can be found in [21]. The variable q is the source or sink term (inflow, leakage, phase transfer between phases). This explicit scheme allows prediction of fluid behavior by implementing recognized physical laws, e.g. calculation of K- and S-values depending on flow regime. The timestep is restricted by the CFL criterion from the equation:

$$\Delta t \leq CFL \frac{\Delta z}{\max(|\lambda_1|, |\lambda_2|, |\lambda_3|)} \tag{4.2}$$

where λ_3 corresponds to the fastest sonic wave propagating in the system. The numerical scheme has difficulties calculating for CFL values greater than 0.25 and will be kept at a fixed value of 0.1875 in the simulations.

4.1.1. Mathematical Properties of the Drift Flux Model

The conservations laws can be rewritten as:

$$\frac{\partial}{\partial t}U + \frac{\partial}{\partial z}F(U) = Q(U) \tag{4.3}$$

The vector U is a representation of the conservative variables given in the conservation equations. The numerical scheme converts the conservative variables to physical parameters.

$$U = \begin{bmatrix} u_1 \\ u_2 \\ u_3 \end{bmatrix} = \begin{bmatrix} \alpha_l \rho_l \\ \alpha_g \rho_g \\ \alpha_l \rho_l v_l + \alpha_g \rho_g v_g \end{bmatrix}$$

It is possible to analyze this nonlinear system of partial differential equations and show that it is a hyperbolic system describing propagation of waves [53]. The speed of these waves is represented by the real eigenvalues obtained by analyzing the system. They are calculated as follows:

$$\lambda_1 = v_l - w, \lambda_2 = v_g, \lambda_3 = v_l + w \tag{4.4}$$

where w is the sound velocity, and calculated as below:

$$w = \sqrt{p/(\alpha_g \rho_l (1 - C_0 \alpha_g)} \tag{4.5}$$

The first and latter eigenvalue represents the sound waves propagating with the current, i.e. upwards in a vertical well, and sound waves propagating countercurrent, i.e. downwards in a

21

vertical well, respectively. Pressure disturbances caused by varying pump rate or valve openings can cause these variations. The mass transport wave is represented by the second eigenvalue, e.g. migration of a gas bubble in a well filled with liquid.

4.2. Boundary Treatment

At the boundary cells, the inlet and outlet fluxes at the physical boundaries have to be found in other ways than using the fluxes defined by the AUSMV scheme. After determining the cell variables using the AUSMV scheme formulas, a method to determine the fluxes at the boundaries is to use extrapolation techniques using the variables defined in the midpoint of the boundary cells. This will be combined with the physical information given. For instance, at the bottom, the inlet rates in kg/s may be known. If the well is open, the pressure at the top of the well will be known.

How this will be done will depend on whether the well is open or closed. In this thesis, the well is specified as closed during kick migration, which means that the inlet and outlet mass and convective momentum fluxes are considered zero. However, the pressure at the inlet and outlet boundary has to be found. The following formulas are then used [7]:

$$p_{inlet} = p(1) + \frac{\Delta z}{2}\rho_{mix}g cos\theta + \frac{\Delta z}{2}F_w \qquad (4.6)$$

$$p_{outlet} = p(N) - \frac{\Delta z}{2}\rho_{mix}g cos\theta - \frac{\Delta z}{2}F_w \qquad (4.7)$$

4.3. Second Order AUSMV Scheme

In the numerical scheme, the physical variables like pressure, density, phase velocities and phase volume fractions are considered constant within each cell. But the variables will vary from cell to cell. When using the first order AUSMV scheme, it will tend to smear out sharp transition zones, e.g. the kick front where the gas volume fraction changes sharply to zero. This is the effect of numerical diffusion. It will tend to smear out this transition zone between two-phase and one-phase flow. One approach for reducing this problem to use a high enough number of cells. A disadvantage of increasing the number of cells would be the increase in computational time [7]. Grid effects will be studied in chapter 5.2.

4.3.1. Slope limiters

A second approach for reducing the numerical diffusion is by implementing the second order scheme using slope limiters [42]. Figure 4.2 illustrates the slope limiter concept.

First order method: Flow variables are treated as constant across a cell.

Second order method/ Slope limiter concept: Gives better resolution of gas distribution in a well.
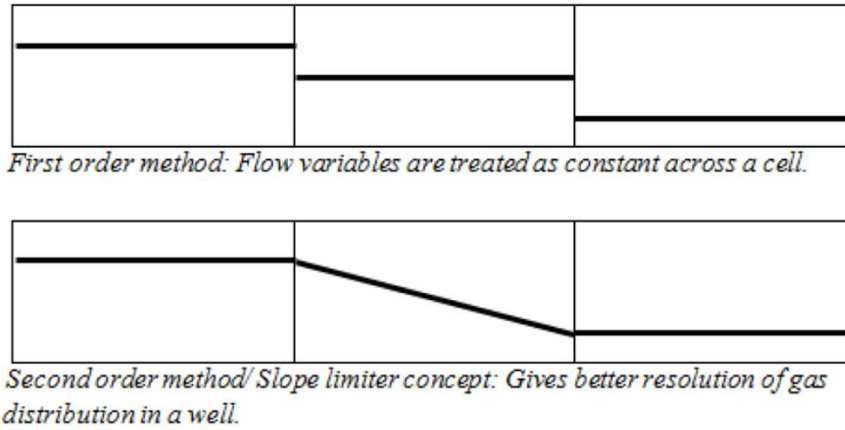
Figure 4.2 Slope limiter concept [4]

To calculate the boundary values in each cell, different slopes are defined for the physical variables. Here, slopes are calculated within the cells for phase densities, pressure and gas volume fraction, but not for the phase velocities. The left and right boundary of the cell variables are calculated from the cell averages using the corresponding slopes. With updated variables at the boundaries, the fluxes can be calculated. The physical variables at the boundaries can be calculated using slope limiters as defined in [42]:

$$P_i(z) = P_i + (z - z_i)\Delta_i \qquad (4.8)$$

$$z \in [z_{i-\frac{1}{2}}, z_{i+\frac{1}{2}}]$$

In the boundary cells, the slope limiters cannot be calculated. There are then two choices, they can either be set to zero or copied from the closest neighbor cell. In the old model, all of them were copied, but it turned out that it caused some mass conservation problems. In the new model, the slope limiter related to the gas volume fraction will be set to zero both in the inlet and outlet boundary cell. In chapter 5.1, previous and improved techniques of handling the slope limiters in the boundary cells are discussed.

5. Simulation and Numerical Results

A 4 000-meter-deep vertical well is assumed. A 12 ¼" x 5" geometry is assumed from bottom to top for simplicity. Also, the BOP is assumed to be at the top of the well. The cross-sectional area is given by:

$$A = \frac{\pi}{4}(OD^2 - ID^2) \tag{5.1}$$

where OD is the outer diameter of 12.25" given in inches and ID is the inner diameter of 5" given in inches.

With the given well geometry, the well volume of the 4 000 m deep well is 253 m³. Water is considered the drilling fluid in the system. The friction model from equation 2.6 will be used. The sonic velocity related to water is a_l=1 500 m/s, and the kick is considered an ideal gas with a sonic velocity of a_g=316 m/s, which is the simple model used in [7]. Unless specified otherwise, the initial kick volume is 4 m³, which is the result of a gas mass rate of 16 kg/s, as shown in Figure 5.1 and calculated on the next page. To introduce 8 m³ and 12 m³ kicks, the gas mass rates have to be 31 kg/s and 46 kg/s respectively. First, the well is kept static for 10 s before the gas mass rate is ramped up to 16 kg/s in 10 s. The gas influx is kept for 90 s before it is ramped down to zero in a 10 second period. After this, the well is closed. 1 600 kg of gas mass will be introduced to the system, and consequently the migrating gas will lead to a pressure increase at the wellhead. The cell lengths are specified from $\Delta z = \frac{L}{N}$, where L is the length of the well, i.e. 4 000 m and N is the number of cells chosen in the discretization. The CFL criterion is used to limit the time steps, and for simulations with 25, 50, and 100 cells, the time step is limited to 0.02, 0.01, and 0.005 respectively to keep the CFL number fixed at 0.1875.
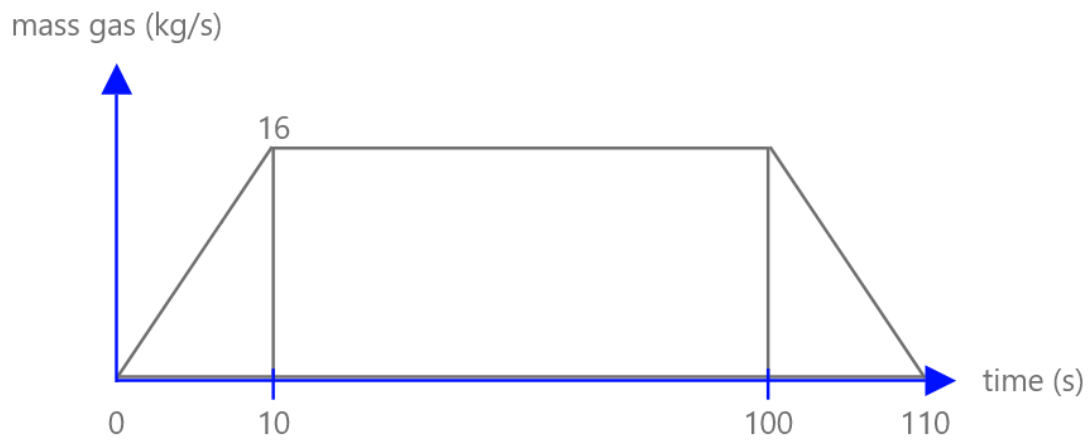
Figure 5.1 Mass of gas introduced to the well during the simulations

$$m = A = 16\frac{kg}{s} \cdot 10s + 16\frac{kg}{s} \cdot 90s = 1\,600\,kg$$

$$V = \frac{m}{\rho} = \frac{1\,600\,kg}{384\,kg/m^3} = 4.16\,m^3$$

5.1. Case 1 – Effect of Slope Limiters in the Boundary Cells

As an introduction, some issues with the slope limiters must be addressed before discussing the effect of different parameters on pressure build up. In case 1, the old model is used to address some issues encountered when activating slope limiters in the boundary cells. Later, the simulations will be run using the new model. This case is quite similar to the one studied in case 1 in [7]. Simulations were run for 12 000 s in order for the pressures to stabilize.

In previous work, it was found that if the slope limiters were set to zero in the boundary cells using a rough grid, i.e. 25 cells, the pressure in these became wrong. For the case where the slope limiters were set to zero in the boundary cells, Figure 5.2 shows that the relation between pressure and depth at depths close to the boundary cells did not become completely linear as one should expect.
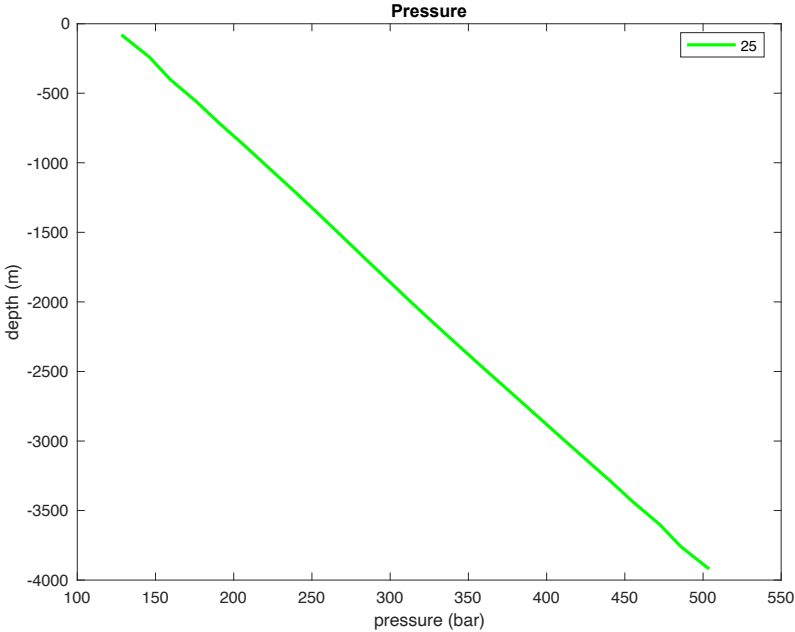
Figure 5.2 Pressure depth profile at 4 000 s for old model with 25 cells when slope limiters are set to zero

26

Figure 5.3 shows the pressure vs depth profile for the old model with varying grid refinement. As seen in Figure 5.3, the kick bulks observed at the boundary cells when using 25 cells are reduced when increasing the number of cells. As the grid is refined, it looks like the pressure vs depth profile converges to a linear curve, which is preferred. In addition, if the pressure is plotted against time, as seen in Figure 5.4, the final BHPs and WHPs for the grids of 50 and 100 cells converge to almost the same values. The final pressures should converge to the same values at steady state; however, this is not the case for 25 cells. The pressure is not linear at surface and at the bottom, which was clearly seen in Figure 5.2.
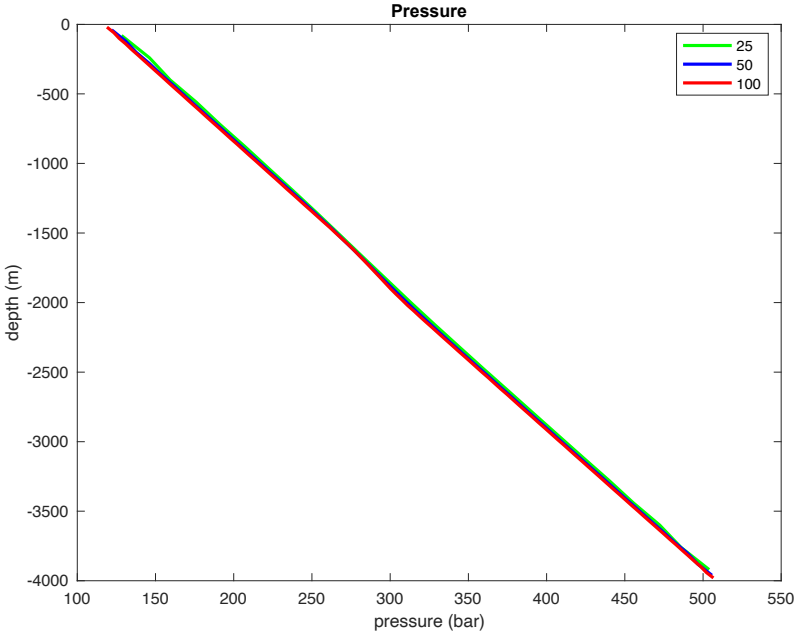
Figure 5.3 Pressure depth profile at 4 000 s for old model with varying grid refinement when slope limiters are set to zero
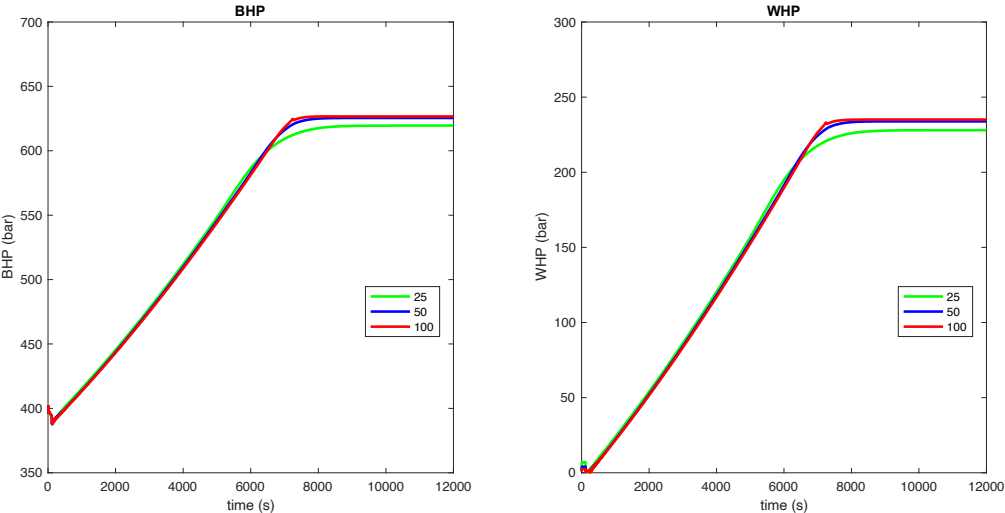
Figure 5.4 Pressure build up in well for old model with varying grid refinement when slope limiters are set to zero

In order to improve the accuracy of the pressure predictions also for rough grids, it was attempted to copy the slope limiters in the boundary cells from the closest interior cells; however, mass conservation problems were encountered, as shown in Figure 5.5. On the left-hand side, an increase in liquid mass is seen when increasing the grid refinement above 25 cells. The liquid mass conservation problem occurs at the outlet boundary cell. On the right-hand side in Figure 5.5, gas is added to the well even through the well is closed. The gas mass conservation problem occurs at the inlet boundary cell. Hence, masses are artificially added to the system and the numerical method seems to have lost its ability to conserve mass, which is a serious flaw. This approach for handling the boundary cell slope limiters gives a more correct pressure vs depth profile (Figure 5.6) and even better when refining the grid (Figure 5.7). Despite this, the mass conservation problems lead to erroneous pressure conditions in the well, which is shown in Figure 5.8.
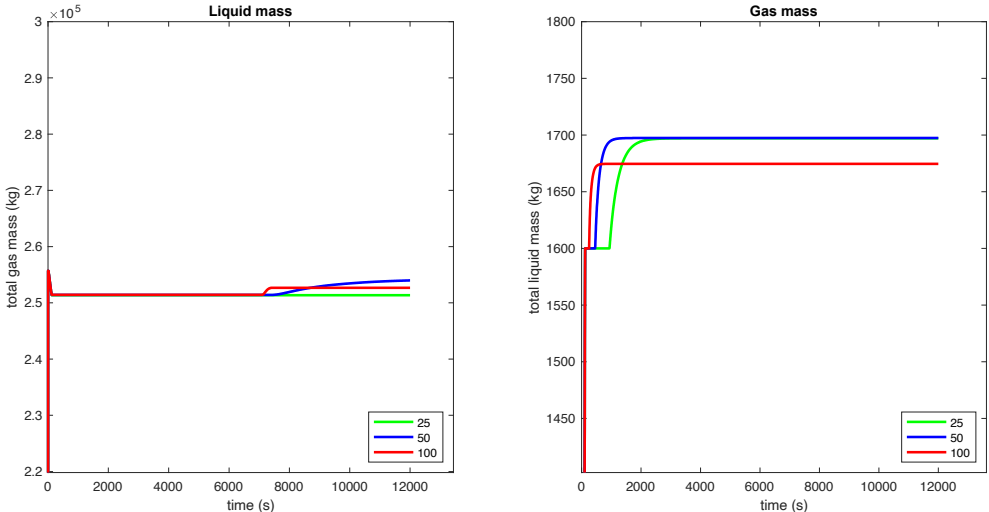
Figure 5.5 Mass of liquid and gas phase during the simulation of old model with varying grid refinement when slope limiters are copied
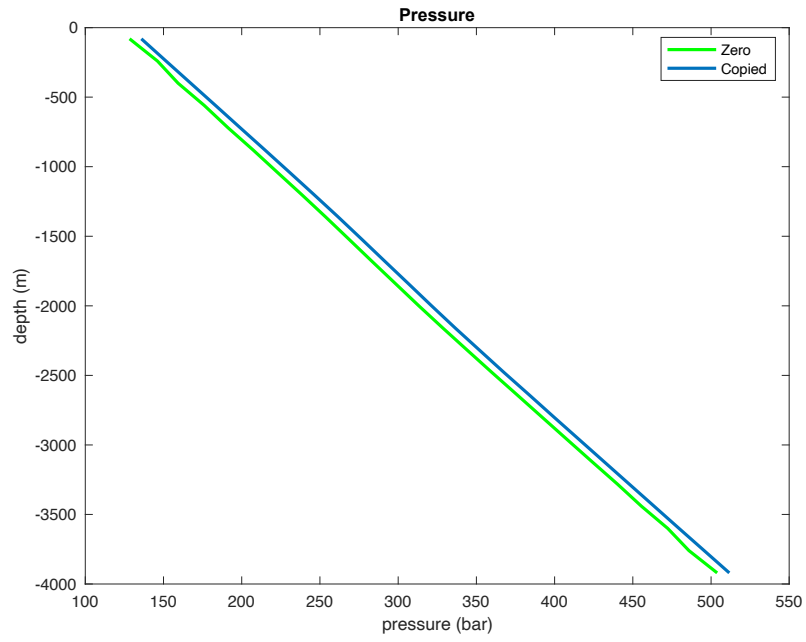
Figure 5.6 Pressure depth profile at 4 000 s for old model with 25 cells when slope limiters are set to zero and copied
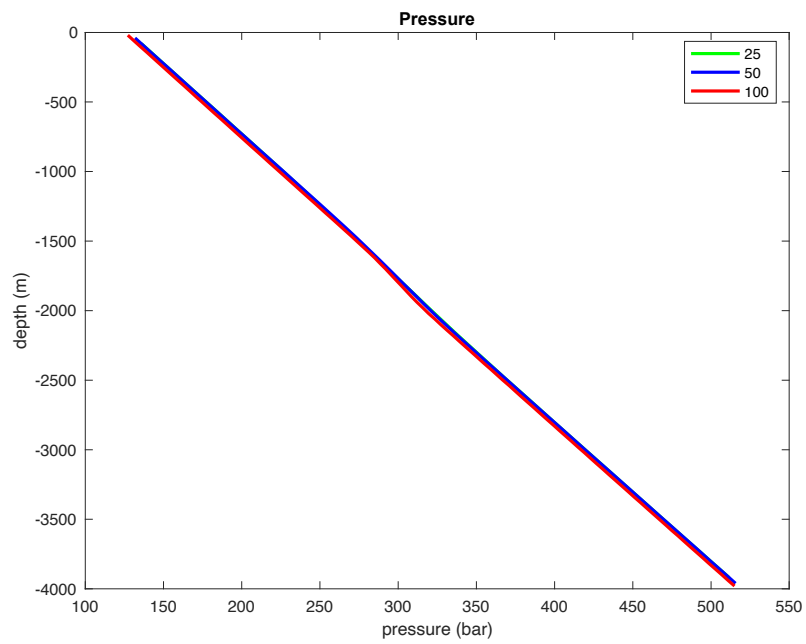
Figure 5.7 Pressure depth profile at 4 000 s for old model with varying grid refinement when slope limiters are copied
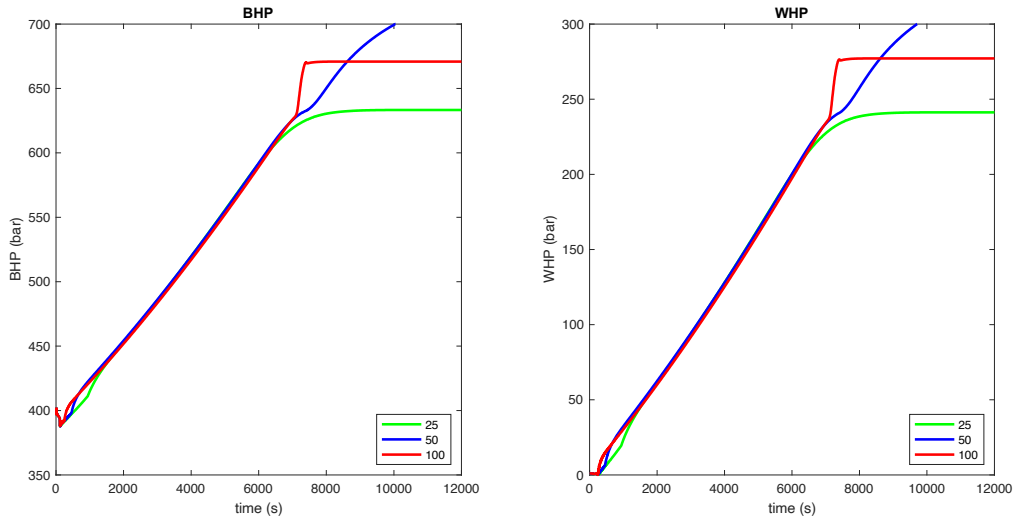
Figure 5.8 Pressure build up in well for old model with varying grid refinement when slope limiters are copied

The gas mass conservation problem was fixed by setting the slope limiter related to the gas volume fraction to zero in the inlet boundary cell [9], hereby called *the old fix*. However, the liquid mass conservation problem was still not omitted for grid refinements above 25 cells, as seen on the left-hand side of Figure 5.9. The liquid mass conservation problem occurs at the outlet boundary cell. Figure 5.10 shows the pressure development for this case.
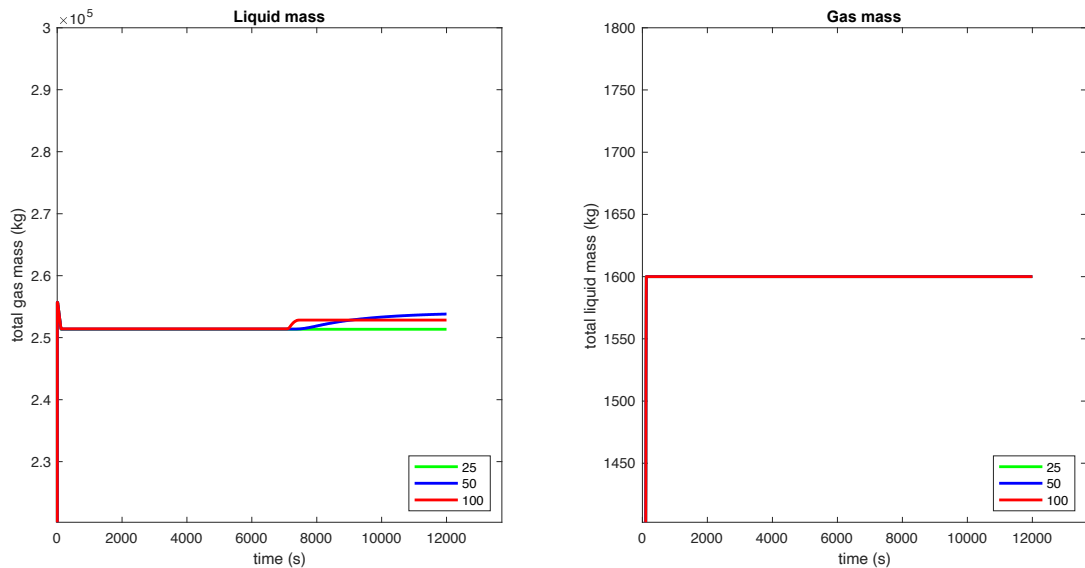
Figure 5.9 Mass of liquid and gas phase during the simulation of old model with varying grid refinement when slope limiters are copied using old fix
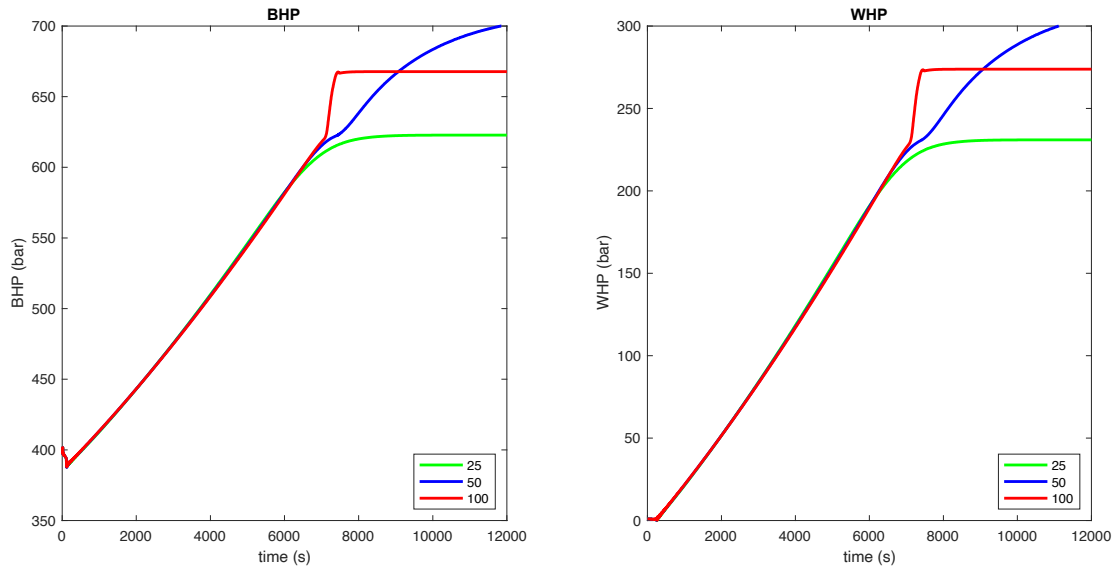
Figure 5.10 Pressure build up in well for old model with varying grid refinement when slope limiters are copied using old fix

To omit the liquid mass conservation problem, the slope limiter related to the gas volume fraction was set to zero also in the *outlet* boundary cell, hereby called *the new fix*. Figure 5.11 shows that the masses are conserved with the new fix. As a result, Figure 5.12 shows a more accurate pressure build up after the new fix is implemented. The pressures stabilize around 7 000 s to approximately 627 bars and 235 bars for BHP and WHP respectively.
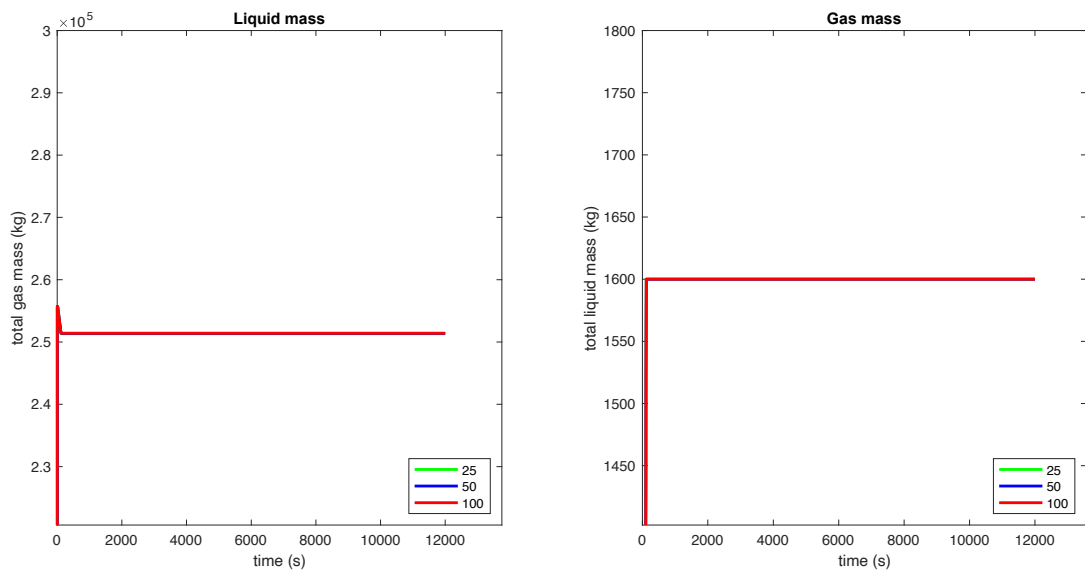
Figure 5.11 Mass of liquid and gas phase during the simulation of old model with varying grid refinement when slope limiters are copied using new fix

When comparing Figure 5.4 and Figure 5.12 it is seen that the difference in final pressures between a rough grid of 25 cells and the more refined grids of 50 and 100 has been reduced with the new fix.
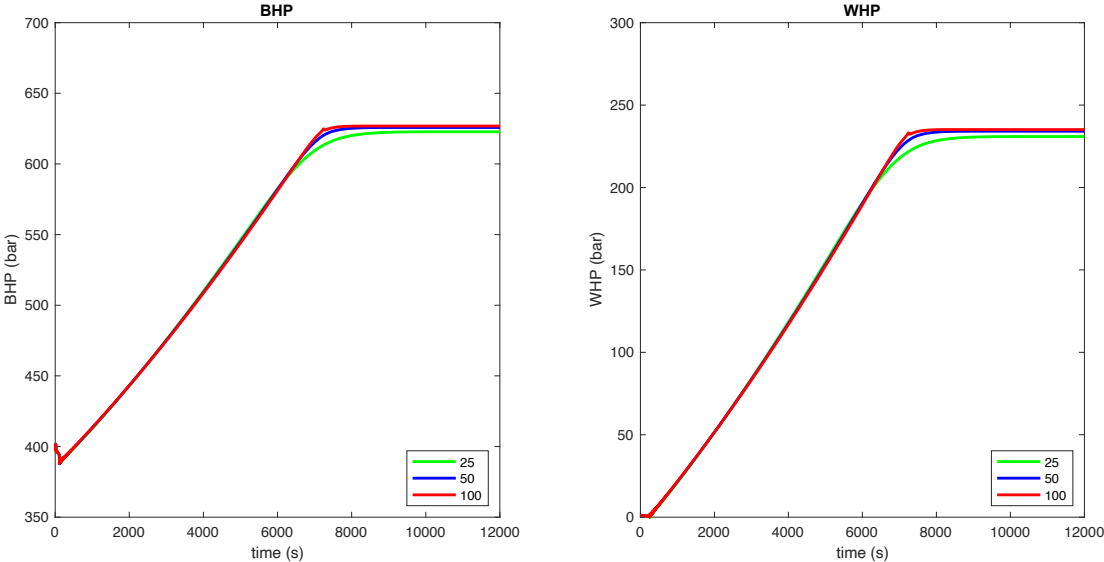
Figure 5.12 Pressure build up in well for old model with varying grid refinement when slope limiters are copied using new fix

For further simulations, i.e. in the new model, the slope limiter related to the gas volume fraction will be set to zero both in the inlet and outlet boundary cell. With the mass conservation issues resolved, the influence of different parameters on pressure build up can be discussed.

5.2. Case 2 – Grid Effects on New Model

In case 2, the influence of varying grid refinement on the pressure build up is considered. By varying the number of cells between 25, 50, and 100, the CFL criterion is kept constant at 0.1875 for timesteps of 0.02, 0.01, and 0.005 respectively. This is a modification of case 1 in [7], where the old model was used. The new model is used for the simulations, including varying flow regimes, suspension of 3%, and a gas volume transition interval of 2%, i.e. the gas volume is fully suspended for all gas fractions below 0.03, the suspended gas develop to bubble flow in the gas fraction interval [0.03, 0,05], and bubble flow is fully developed for gas fractions at 0.05. Simulations of 14 000 s length were sufficient so that the pressures could stabilize.

As shown in Figure 5.13, both liquid and gas mass are conserved for all grid refinements, which serves the new model satisfactory as a closed well is considered. This means that the liquid and gas masses are preserved throughout the simulations also for the new model.
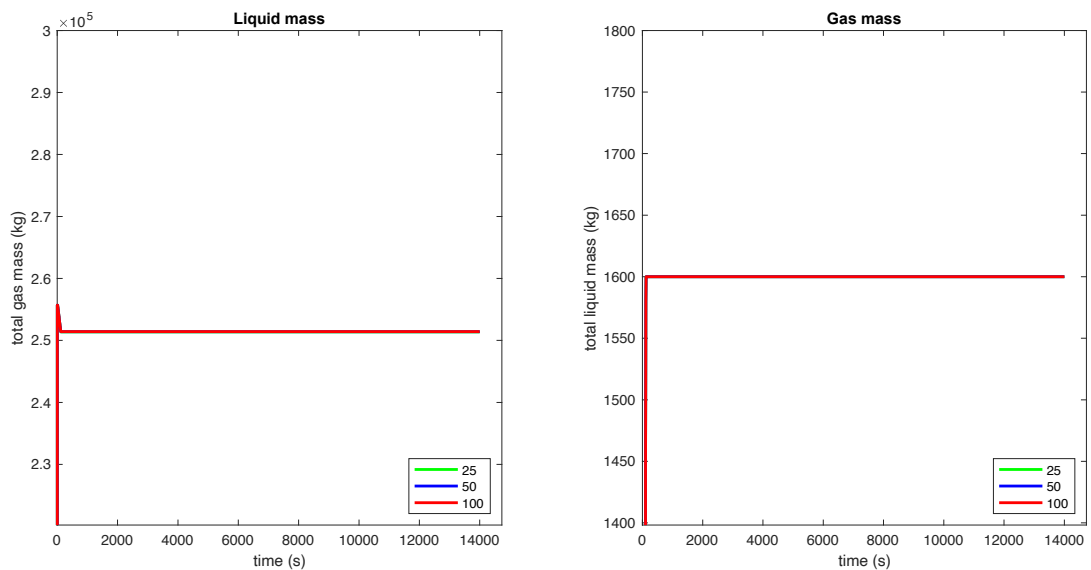
Figure 5.13 Mass of liquid and gas phase during the simulation of new model with varying grid refinement

A slight expansion of the gas kick will occur when the influx migrates upwards in the closed well. This is a result of compressible liquid. When the pressure increases, the liquid compresses slightly, giving room for some limited gas expansion. Figure 5.14 shows the gas volume vs time for the different grid refinements. The gas volume is slightly overestimated when simulating with 25 cells. By refining the grid to 50 cells and 100 cells, slightly less gas expansion is observed and both grid refinements give almost the same final value.
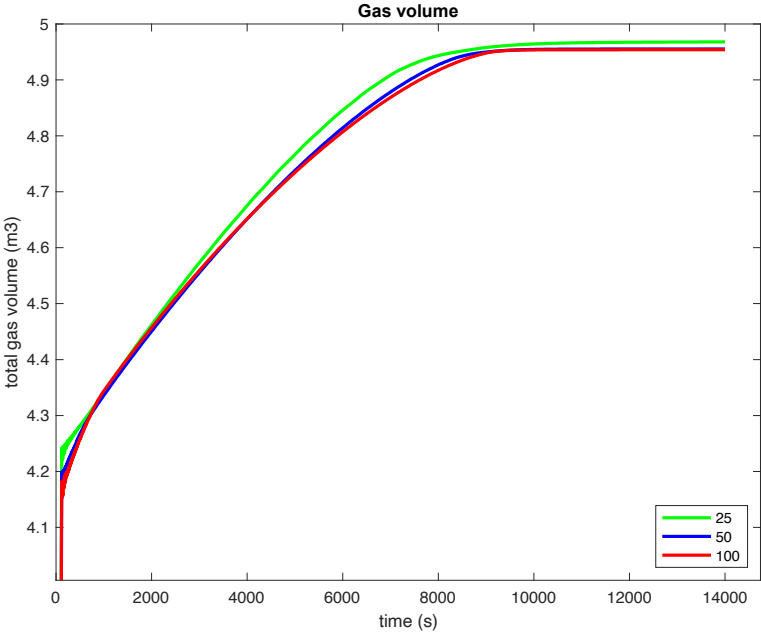
Figure 5.14 Gas volume when kick is migrating upwards in a closed well for new model with varying grid refinement

As seen in Figure 5.15, the pressure build up increases slightly when increasing the number of cells, which demonstrates that there is an effect when reducing the numerical diffusion. The pressure build up is lower with a rough grid of 25 cells, which seems to underestimate the actual pressure build up. A grid refinement of 50 cells demonstrates more accurate calculations than 25 cells, yet the pressure build up is not too far off the pressures of 100 cells. There is a larger effect of increasing the grid from 25 to 50 cells than when changing the grid from 50 to 100 cells. This is what to expect, since when continuing to refine the grid, the solution will converge to the exact solution when numerical diffusion is being reduced. Nevertheless, the gained improvement will be reduced for each time the grid is refined. Since the computational time multiplies by four for each grid refinement [7], simulations for future cases will be of 50 cells to save computational time. It seems to give sufficiently exact results to discuss other effects.
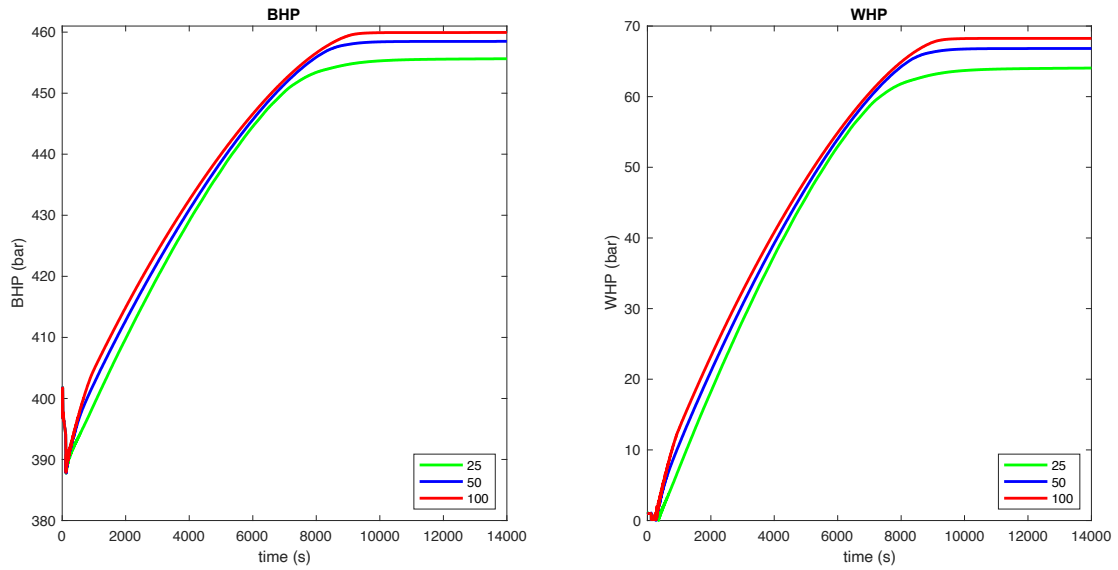
Figure 5.15 Pressure build up in well for new model with varying grid refinement

Also observed in Figure 5.15, both final BHPs and WHPs decrease when simulating with the new model compared with simulating with the old model shown in Figure 5.12. The pressures stabilize at 9 000 s for the case of 100 cells, where BHP=460 bars and WHP=68 bars. For rougher grids, the pressures stabilize at 8500 s and 8000 s for 50 and 25 cells respectively. The BHP is 458 bars for 50 cells and 456 bars for 25 cells, and the WHP is 67 bars for 50 cells and 64 bars for 25 cells. As seen from Figure 5.12, the old model predicts that the gas has reached further up in the well than the new model, since the pressures stabilize at 7 000 s. The reason for this is that the old model used only one gas slip model for all gas volume fractions, and it used typical slug flow values (K =1.2 m/s, S = 0.55 m/s). Since slugs move at higher velocities, the old model predicts that the gas has reached further up in the well. However, when using the new model, suspension effects are included as well as bubble flow. For suspended gas, there is no movement and when bubble flow is present, the gas will move slower than when having slug since S has a typical smaller value for bubble flow compared to slug flow.

Figure 5.16 shows the gas volume fraction depth profiles taken at 4 000 s. The transition between gas and liquid should show a sharp profile; however, this is not the case for a rough grid of 25 cells. By increasing the grid, sharper transition zones are achieved since numerical diffusion is reduced. Therefore, a grid of 50 cells will be used in the later simulations. Even more accurate results would have been obtained with 100 cells, but it will require much more simulation time.
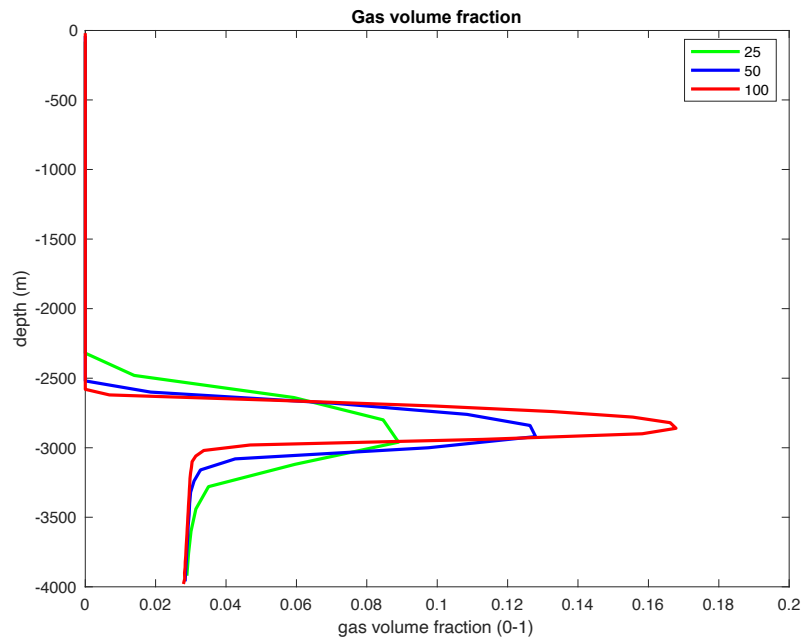
Figure 5.16 Gas volume fraction depth profile at 4 000 s for new model with varying grid refinement

Figure 5.17 shows the velocities of liquid and gas taken at 4 000 s. Although the liquid velocity should be close to 0 m/s, the increase in gas velocity results in a slightly negative liquid velocity since the gas forces the liquid downwards when migrating upwards. A grid of 100 cells would calculate the local variations more accurately, making the transient drift flux model able to describe this physical effect which is less noticeable when simulating with a rough grid, e.g. 25 cells. Further simulations will be run using 50 cells to save computational time.
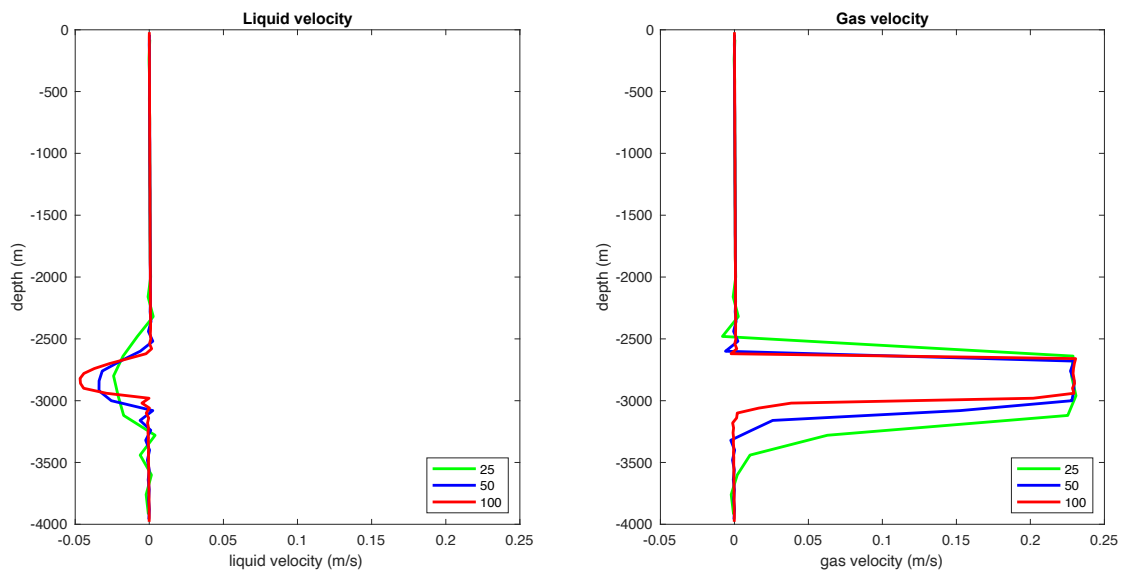
Figure 5.17 Liquid and gas velocity in well at 4 000 s for new model with varying grid refinement

36

5.3. Case 3 – A Comparison Between the Old Model and the New Model

The purpose of case 3 is to compare the old and the new model. To demonstrate the differences in pressure build up and gas migration velocities, the new model is simulated using 1% suspension limits in order for the kick volume to migrate to surface. Initially, the kick volume will be 4 m^3. Later, the kick size will be increased to 8 m^3 and 12 m^3 to demonstrate that different flow regimes can exist at different depths when using the new model. Average gas migration velocities will also be calculated. The simulations were run for 20 000 s in order for the pressures of the new model to stabilize.

4 m^3

Figure 5.18 shows the total gas volume for the two models for a 4 m^3 kick. Since the new model includes suspension effects, some of the initial kick volume will not be able to migrate, resulting in less gas migrating and less total gas volume compared to the old model (reduced by 0.55 m^3). This is because the gas volume is in full suspension for gas fractions lower than 0.01 and fully developed bubble flow occurs for gas fractions at 0.03. At 16 000 s, the gas stops migrating, and the pressures for the new model are expected to stabilize at this point. The old model does not include suspension effects; the whole kick volume is able to migrate. At around 7 500 s, the gas stops migrating. These differences will affect the pressure build up slopes, which will be shown.
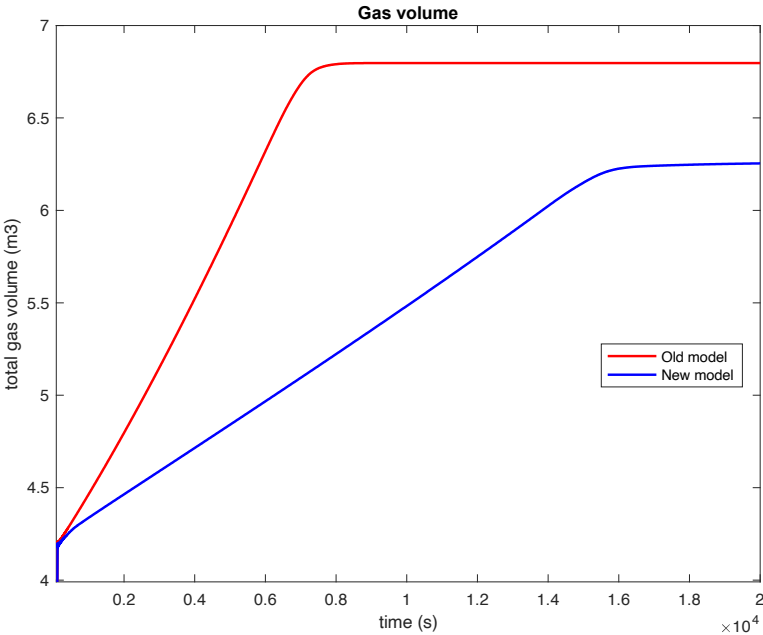
Figure 5.18 Gas volume when kick is migrating upwards in a closed well for old and new model with 1% suspension, 4 m^3 kick

As observed in Figure 5.19, which shows the BHPs and WHPs for the two models, the new model gives much lower final pressures. On the left-hand side, it is seen that the BHP stabilizes to approximately 577 bars for the new model. The old model stabilizes to 626 bars, which is a difference of 49 bars. The WHP stabilizes to 185 bars and 234 bars for the new model and old model respectively. The main reason for the differences in final pressures is suspension effects, which will be discussed in detail in chapter 5.4.

The lack of suspension effects and the high gas migration velocity of the old model enables it to predict that the gas has reached further up in the well compared to the new model. The old model only considers slug flow, and thus includes a constant gas migration velocity, i.e. S=0.55 m/s. Since the new model varies between suspension, bubble flow, and slug flow depending on the gas fraction, it will take longer time for the kick to reach surface since bubble flow has a lower S-value. This is why the pressures stabilize later for the new model. In the next section, the average gas migration velocities will be calculated based on simulated position of the kick bulks at different times.
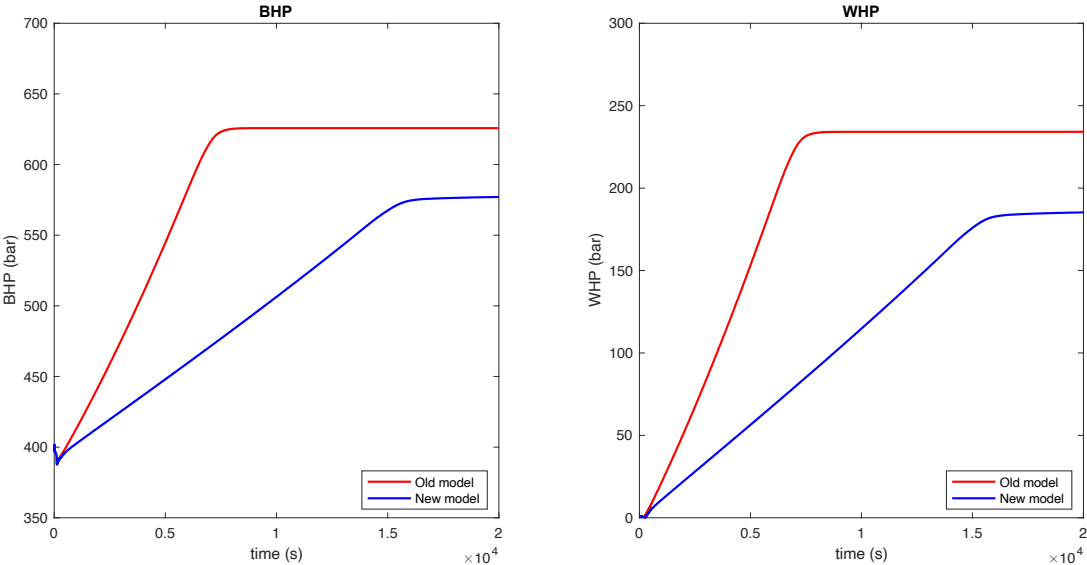
Figure 5.19 Pressure build up in well for old and new model, 4 m^3 kick

Figure 5.20 and Figure 5.21 show the gas volume fraction depth profiles for the two models taken at 2 000 s and 6 000 s respectively. It is seen on the figures that the kick is able to travel further for the old model. The old model has a constant flow regime, i.e. slug flow, which has a higher gas migration velocity, S-value, than bubble flow. As the flow regime varies in the new model, the average gas migration velocity will be lower compared to the old model. As seen from the gas volume fraction depth profiles, the new model will predict bubble flow at

both instances and the gas migration velocity will be lower than for the old model where slug flow was assumed all over. This is clearly demonstrated in Figure 5.22 and this is the main reason that the kick migrates much slower when using the new model. For the new model, 1% suspension is used, which will halt gas fractions under the minimum suspension limit from migrating. In Figure 5.21, one can observe a tail of suspended gas behind the gas bulk that is migrating.

While the old model does not include suspension effect, enabling the whole gas kick to migrate, the new model will reduce the gas volume that is able to migrate. In some cases, this can lead to an earlier transition from slug to bubble flow, which can also lead to that the new model will reduce the gas kick travel distance compared to the old model. For a 4 m^3 kick, the new model only predicts bubble flow throughout the simulation. If the kick volume is increased to sufficiently large gas fractions to form slugs, it will be seen that the new model is able to show that the flow regime changes at different locations in the well.
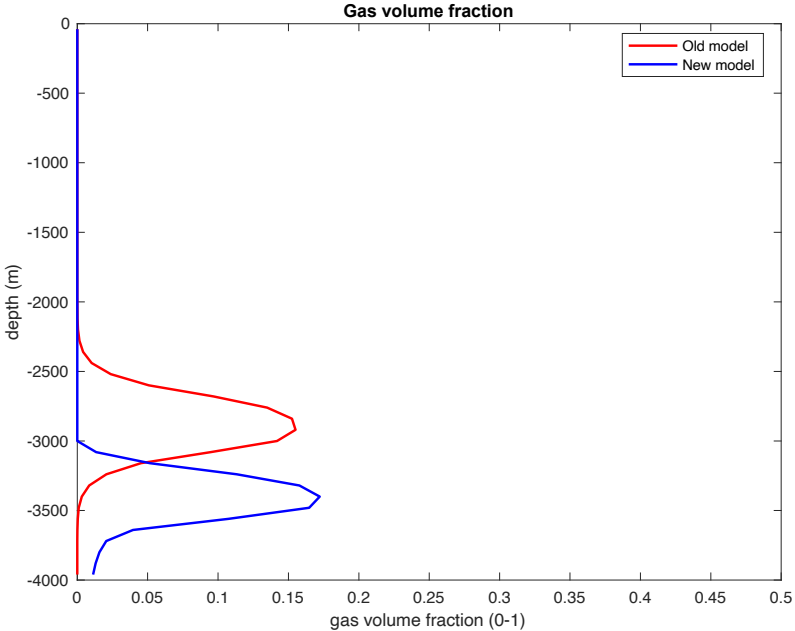
Figure 5.20 Gas volume fraction depth profile at 2 000 s for old and new model, 4 m^3 kick
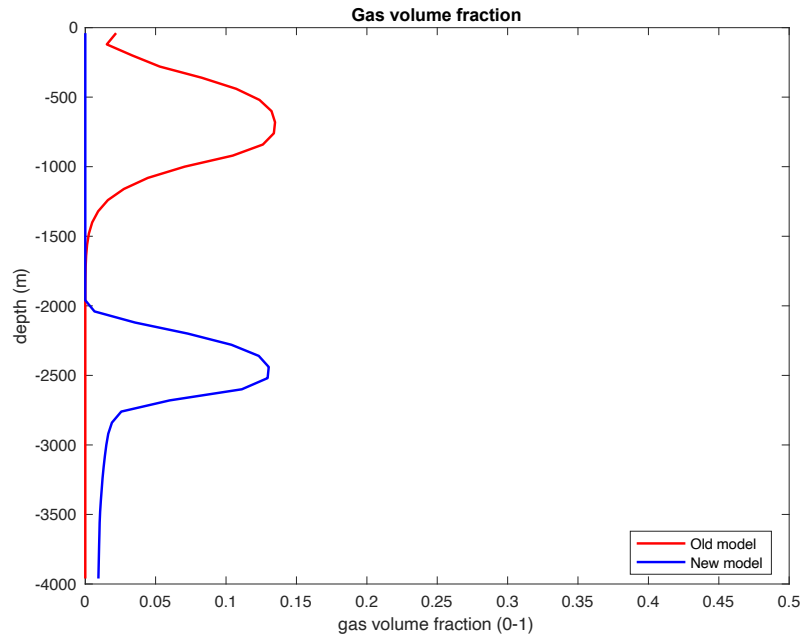
Figure 5.21 Gas volume fraction depth profile at 6 000 s for old and new model, 4 m³ kick

Figure 5.20 shows the locations of the kick bulks at 2 000 s. The gas bulk is located at 3 400 m for the new model. After 6 000 s, the bulk has moved to 2440 m, which means that it has traveled 960 m. The average gas migration velocity can be calculated by dividing the distance traveled by the time it took. The average gas migration velocity is therefore S_{avg}=0.24 m/s between 2 000 s and 6 000 s of simulation. For the old model, the bulk has moved from 2 920 m to 680 m, which gives it an average gas migration velocity of S_{avg}=0.56 m/s in the same time interval. This coincides quite well with the constant S-value of 0.55 m/s used in the old model. The difference in gas migration velocities between the two models explain why the old model predicts that the gas has reached further than the new model, as seen on both Figure 5.19 and Figure 5.21. For the 4 m³, the kick migrated in the bubble flow regime giving a lower S-value compared to the old model. In the new model, larger gas fractions are needed in order for the gas to migrate as there is a minimum suspension limit where the gas is in full suspension. Besides, since the old model does not consider suspension effects, the whole kick volume is able to migrate at a larger velocity than the new model.

The gas velocities taken at 2 000 s are shown in Figure 5.22. The plot shows that the new model is able to display different gas velocities depending on the gas fractions that are present. The blue curve shows that the 4 m³ gas kick is able to reach bubble flow at its maximum, where S=0.23 m/s. The red curve shows that the gas velocity for the old model is constant at S=0.55

m/s independent of gas fractions, which in turn will make the kick to migrate faster from the beginning and reach surface faster than the new model.
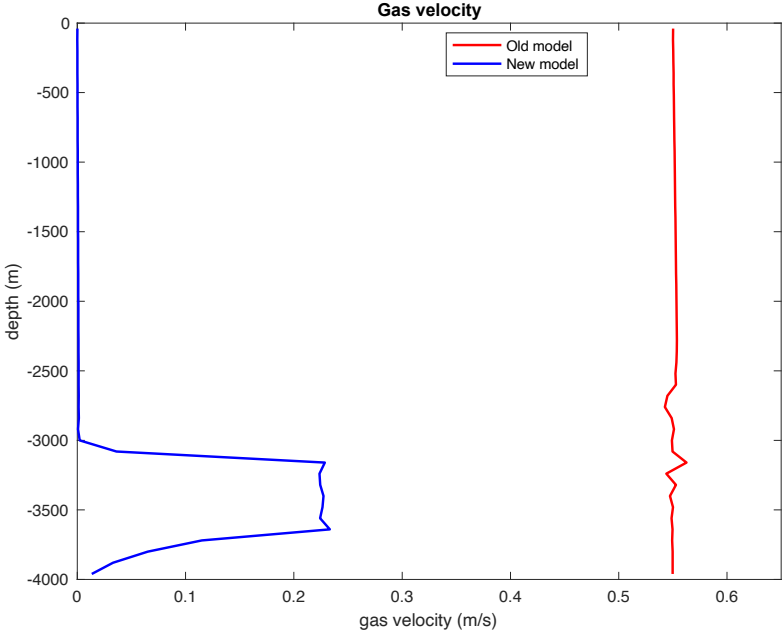
Figure 5.22 Liquid and gas velocity in well at 2 000 s for old and new model, 4 m³ kick

It has been demonstrated that the new model is able to display different gas migration velocities and different pressure build up. In the next section of this chapter, the kick volume is increased to 8 m³ to show that different flow patterns can exist at different locations in the well.

8 m³

Figure 5.23 shows the total gas volume for the two models for an 8 m³ kick. The final total gas volume of the new model is 0.32 m³ less than the old model. As the new model is affected by the suspension effects, some of the gas will be prevented from migrating. The new model predicts that the gas stops migrating at 15 000 s, while the old model predicts the gas kick to stop migrating at 7 500 s. It will be seen that the pressures stabilize when the respective gas volumes stop migrating.
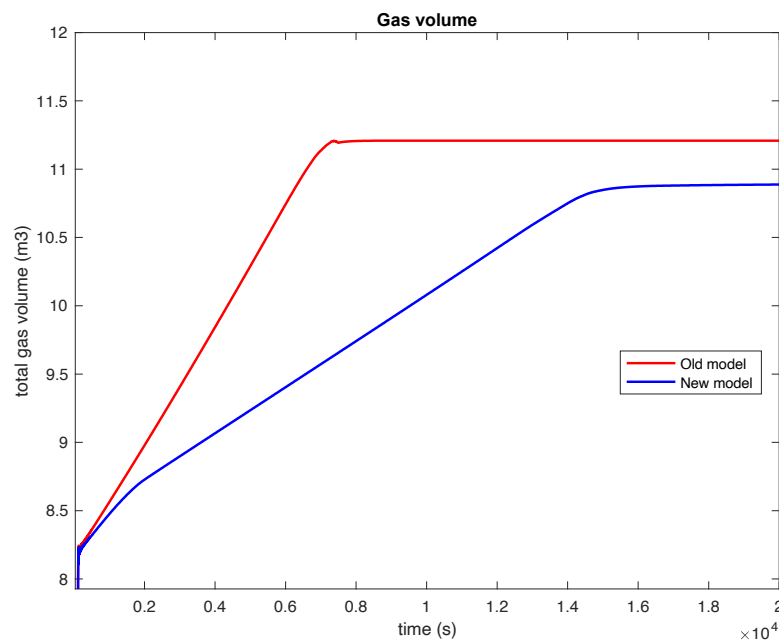
Figure 5.23 Gas volume when kick is migrating upwards in a closed well for old and new model, 8 m³ kick

Figure 5.24 shows the final BHPs and WHPs for the two models. The new model predicts that the BHP stabilizes to 631 bars while the old model predicts a higher final BHP of 659 bars, which gives a difference of 28 bars when including varying flow regimes and 1% suspension. The WHPs stabilize to 243 bars and 272 bars for the new model and old model respectively. Again, the new model stabilizes at later stages than the old model.

In addition, the new model is able to show when the transition from slug to bubble flow will occur. From Figure 5.24, it is observed that the curve for the new model is steeper the first 2 000 s compared to later stages. This indicates that the gas volume was close to the transition zone to slug flow. Figure 5.24
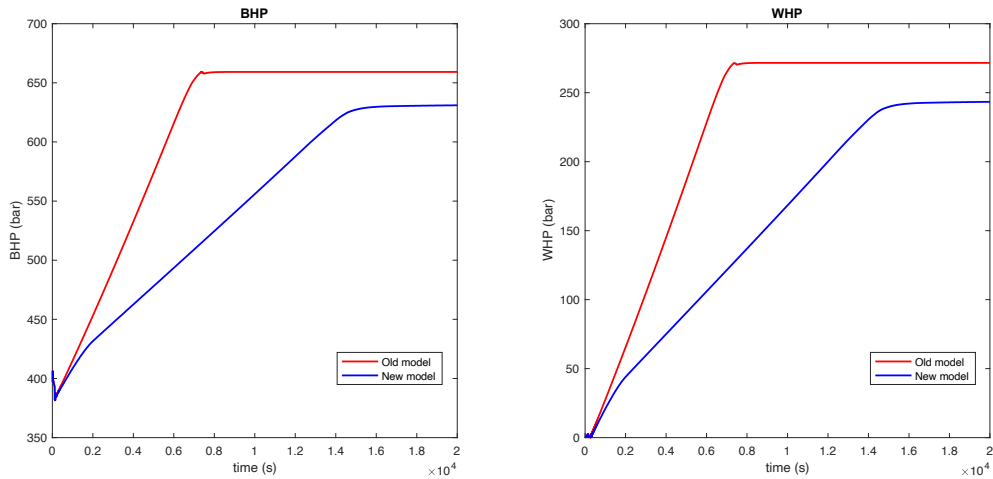
Figure 5.24 Pressure build up in well for old and new model, 8 m³ kick

The gas volume fraction depth profiles taken at 2 000 s are shown in Figure 5.25. The old model predicts that the gas has moved to 2 840 m, while the new model predicts 2 920 m. At 6 000 s (Figure 5.26), the same kick bulks have moved to 680 m and 2 100 m for old model and new model respectively. The average gas migration velocity for the old model is S_{avg}=0.54 m/s in this time interval, but for the new model S_{avg}=0.21 m/s. For the 8 m³ kick, both models predict bubble flow at 2 000 s with a slight transition to slug flow, which will be seen in the gas velocity plot (Figure 5.27).
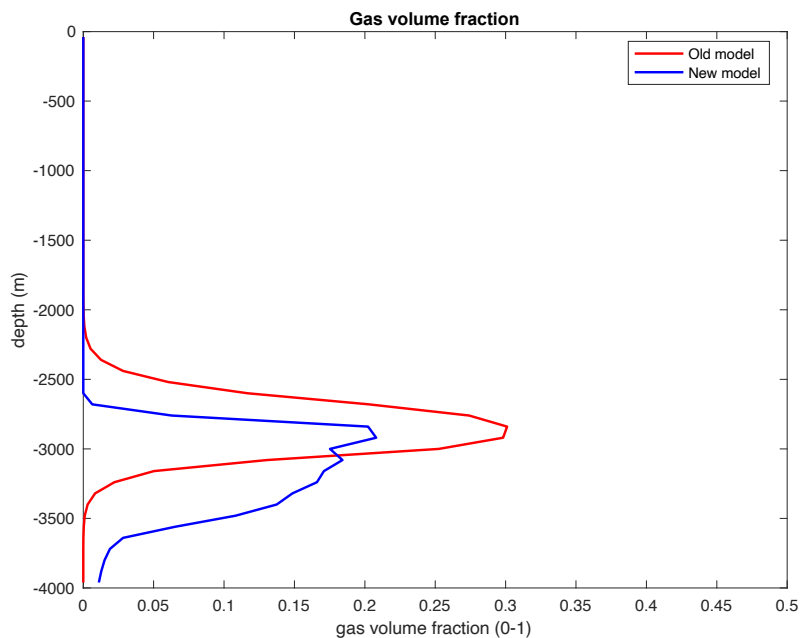
Figure 5.25 Gas volume fraction depth profile at 2 000 s for old and new model, 8 m³ kick
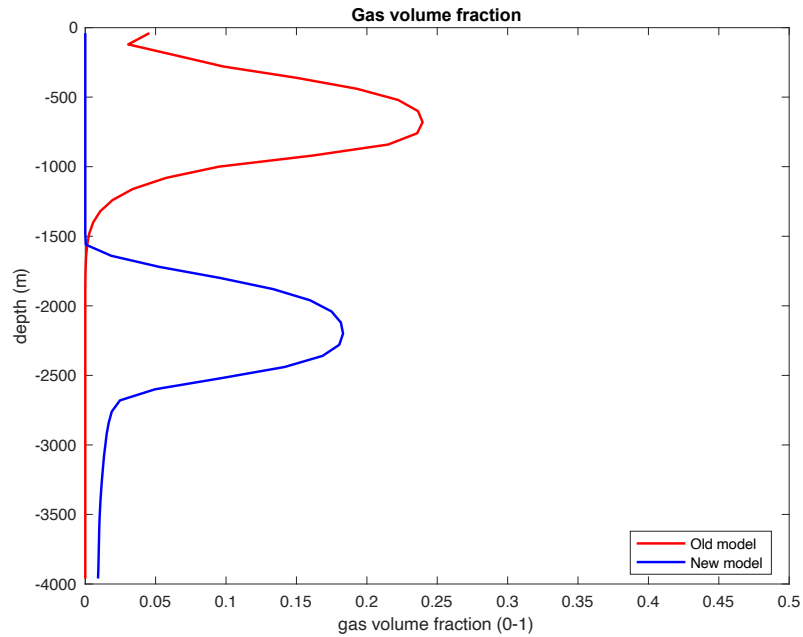
Figure 5.26 Gas volume fraction depth profile at 6 000 s for old and new model, 8 m³ kick

The gas velocities taken at 2 000 s are shown in Figure 5.27. As evident on the figure, the new model is able to predict different gas velocities at different depths. While the old model has a constant gas migration velocity of S=0.55 m/s, the new model predicts a gas migration velocity of S=0.23 m/s, which corresponds to bubble flow, but it is also able to show that the kick is close to the transition to slug flow at 2 920 m. If the kick size is increased to 12 m³, it would be clearly seen in the gas velocity plot that the gas migrates in the slug flow regime.
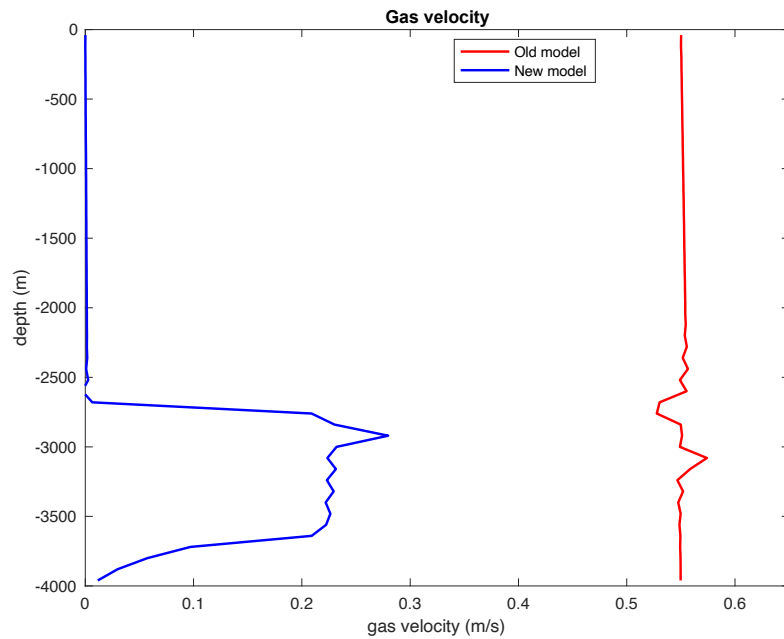
Figure 5.27 Gas velocity in well at 2 000 s for old and new model, 8 m³ kick

12 m³

To again demonstrate that the new model is able to predict the flow pattern transitions, a simulation was run for a 12 m³ kick. Figure 5.28 shows the pressure vs time plots for a 12 m³ kick. The final BHPs are 674 bars and 653 bars for the old model and the new model respectively, and the final WHPs are 291 bars and 270 bars for the corresponding models. For a 12 m³ kick, the slope of the new model changes sometime between 2 000 s and 6 000 s. In this interval, the transition from slug to bubble flow occurs, which the calculations in the next section will verify.
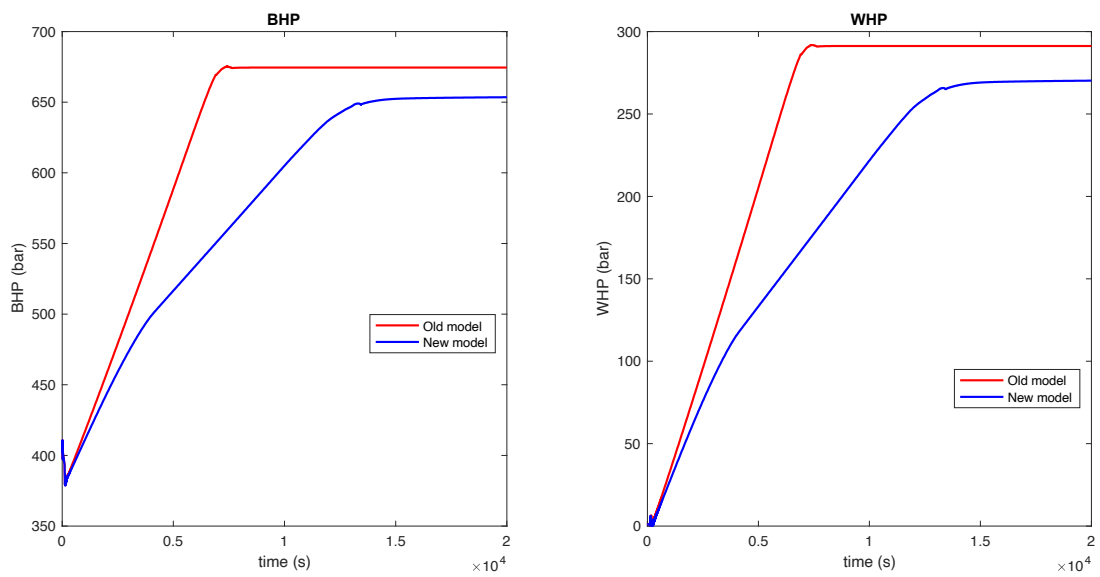
Figure 5.28 Pressure build up in well for old and new model, 12 m³ kick

Figure 5.29 shows that the gas kick bulk is located at the same depth as previously, 2 840 m, for both models and the gas volume fraction is 0.48, which means that slug flow exists.
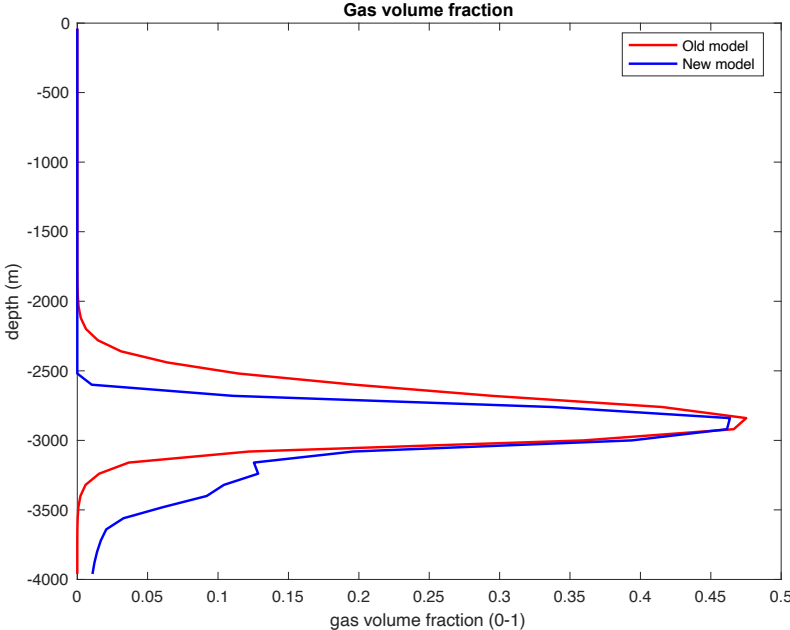
Figure 5.29 Gas volume fraction depth profile at 2 000 s for old and new model, 12 m³ kick

Figure 5.30 shows the gas volume fraction depth profiles for the two models taken at 6 000 s. The old model predicts that slug flow still exists, but the new model predicts that bubble flow is now present. The new model is able to show that slug flow has become bubble flow at 6 000 s since the suspension effects has reduced the gas fraction. The old model still predicts that $S_{avg}=0.54$ m/s, while the average gas migration velocity of the new model is $S_{avg}=0.34$ m/s since it has moved to 1 480 m during 4 000 s. The average gas migration velocity for the 12 m³ kick is a value in between bubble and slug flow.
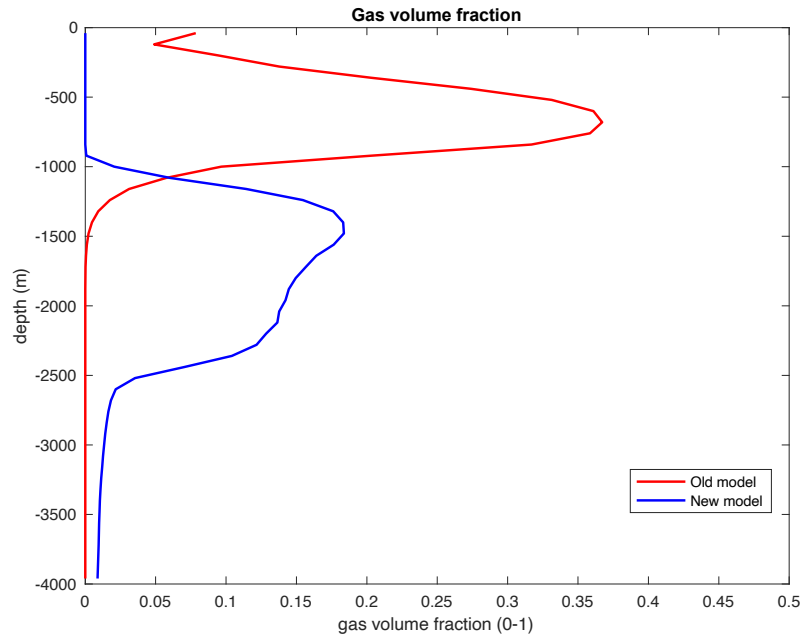
Figure 5.30 Gas volume fraction depth profile at 6 000 s for old and new model, 12 m³ kick

Figure 5.31 shows the gas velocities taken at 2 000 s for a 12 m³ kick. As observed, the new model is able to predict that the gas velocity goes from S=0.23 m/s to S=0.55 m/s at 2 000 s, which corresponds to the transition from bubble to slug flow. This also demonstrates that for a fixed time, different parts of the kick can move with different velocities. At 6 000 s (Figure 5.32), the gas velocity is S=0.23 m/s. This confirms that the transition from slug to bubble flow occurs between 2 000 s and 6 000 s, which was seen in the pressure plots.

For an 8 m³ kick, it was seen that the kick was mainly in the bubble flow regime at 2 000 s, but with a small part of the kick being in the transition interval between slug and bubble flow. Hence, it was in the bubble flow regime at both 2 000 s and 6 000 s, ending up in an average gas migration velocity of S_{avg}=0.23 m/s in this time interval.

In the next chapter, the new model will be used to show how the pressures and gas migration velocities are affected by suspension effects.
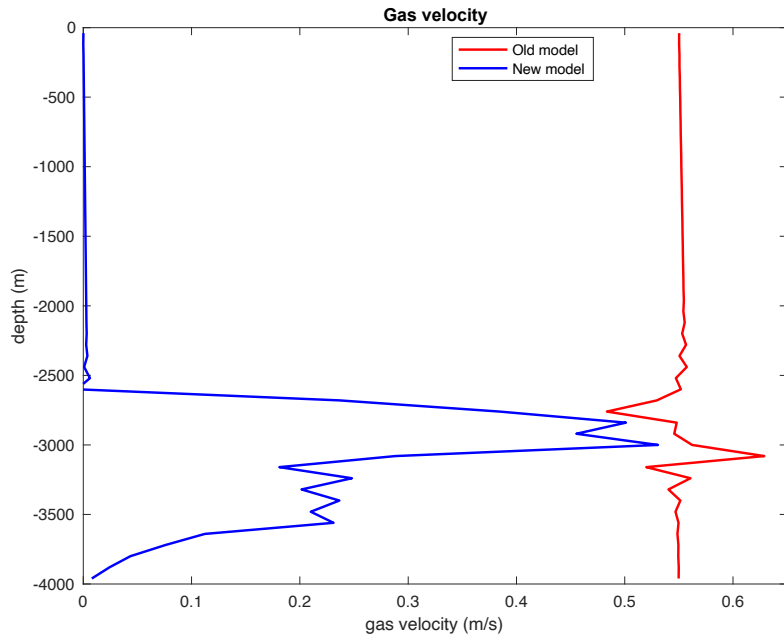
Figure 5.31 Gas velocity in well at 2 000 s for old and new model, 12 m³ kick
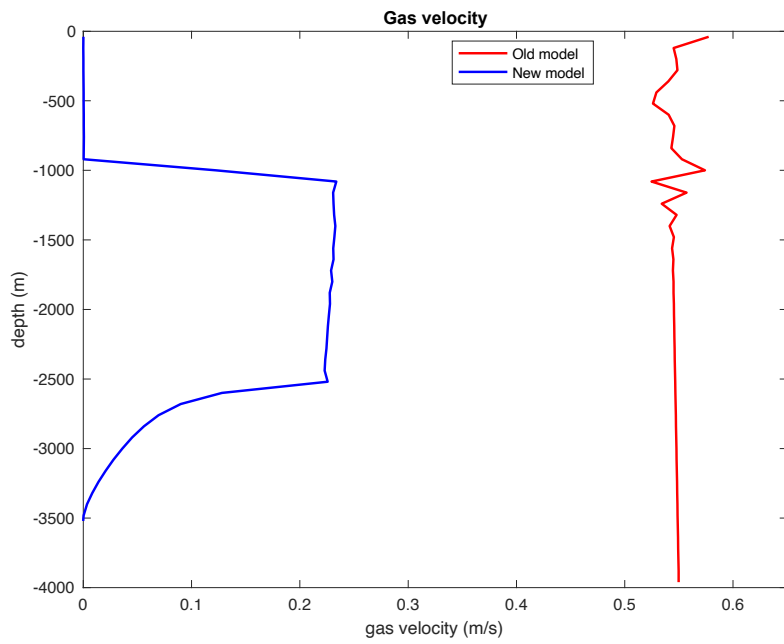
Figure 5.32 Gas velocity in well at 6 000 s for old and new model, 12 m³ kick

5.4. Case 4 – Effect of Different Suspension Limits

4 m³

In case 4, the effect of different suspension limits on pressure build up is demonstrated. It was decided to use a 2% gas volume transition interval for the suspended gas to bubble flow transition. For gas fractions below the minimum suspension limit, the gas volume is fully suspended. In the gas fraction interval of width 0.02, the gas volume in suspension is transforming to bubble flow, and bubble flow is fully developed for gas fractions taking place at the maximum suspension limit. The suspension limits of 0% (no suspension) represent the case of Newtonian drilling fluids, and the remaining cases represent Non-Newtonian drilling fluids. The suspension limits are summarized in Table 5.1.

Suspension limits [%]	Minimum suspension limit [gas fraction]	Maximum suspension limit [gas fraction]
0	0.00	0.00
1	0.01	0.03
3	0.03	0.05
5	0.05	0.07
7	0.07	0.09

Table 5.1 Suspension limits for case 4

Figure 5.33 shows the total gas volume vs time for varying suspension limits. The black curve shows that if no suspension effects are considered, the gas volume will expand significantly with time as a result of the drilling mud being compressible and gas fully migrating before it stops just after 17 000 s. The final gas volume stabilizes at 16 000 s and decreases by 0.5 m³ for as little as 1% suspension. For 3% and 5% suspension, the gas volume expands slightly during the first 8 000 and 4 000 s respectively, before the gas expansion halts. The physical effect can be described as less of the initial gas kick volume being able to migrate for increasing suspension. For an introduced gas volume of 4 m³, the extreme case of suspension would occur at 7%, where it is observed that the gas volume is not able to expand notably and halts at 2 000 s. In the latter case, the gas is suspended quickly.

Figure 5.33 Gas volume when kick is migrating upwards in a closed well for varying suspension limits, 4 m³ kick

Figure 5.34 shows the final BHPs and WHPs for varying suspension limits. The pressure curves shown in Figure 5.34 reflect the gas volume that is able to migrate and expand, shown in Figure 5.33. As long as the gas is able to migrate, the pressures will increase. When the gas stops migrating, the pressures stabilize. If the suspension limit is low, almost all of the initial kick volume is able to travel to the BOP, resulting in high final pressures. When considering suspension effects, some of the gas is left in the well, and the final pressures become much lower compared to the case with no suspension. The final pressure reduction is more significant for higher suspension limits. It also seems like the pressures stabilize significantly faster for high suspension limits, indicating that the gas volume stops migrating at earlier stages, as seen in Figure 5.33. It will be seen that these kicks are fully suspended.
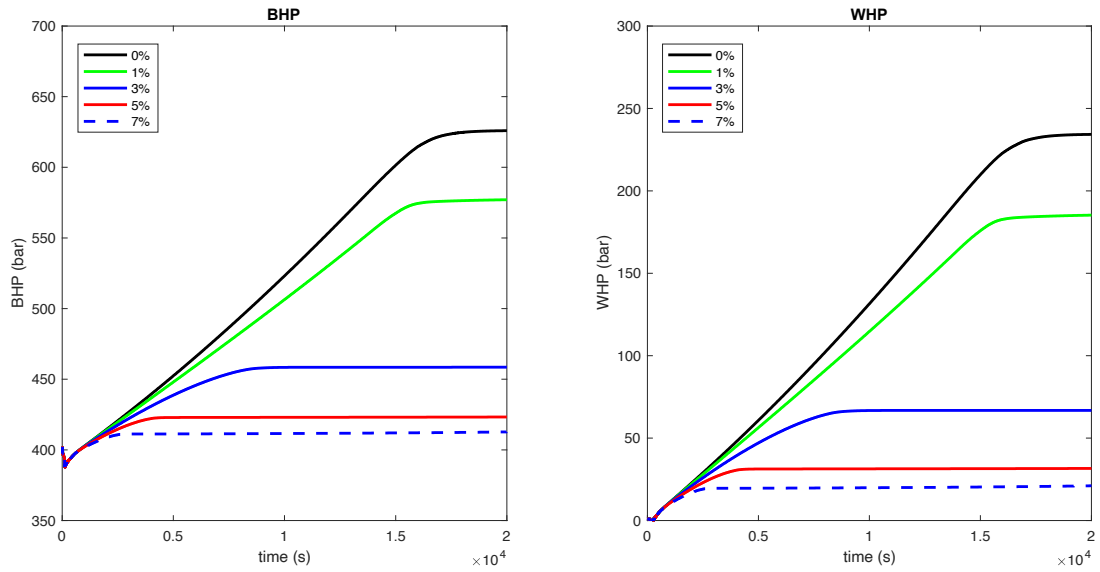
Figure 5.34 Pressure build up in well for varying suspension limits, 4 m³ kick

Table 5.2 summarizes the simulation results from the pressure plots. An important remark is that, by including only 1% suspension, the final BHP and WHP drop by 49 bars compared to the case with 0% suspension despite the fact that the kick has reached surface in both cases at around the same velocity, which calculations will reveal.

Suspension limits [%]	Final BHP [bars]	Final WHP [bars]	Stabilization time [s]
0	626	234	17 000
1	577	185	16 000
3	459	67	8 000
5	423	32	4 000
7	413	21	2 000

Table 5.2 Suspension limits, final BHP, final WHP, and pressure stabilization time, 4 m³ kick

Figure 5.35 on pp. 53 shows the gas volume fraction depth profiles taken at 4 000 s. For lower suspension limits, e.g. 0% and 1%, it is observed long sharp kick fronts with a higher gas volume fraction below, indicating that the gas volume migrates more freely. For high suspension limits, e.g. 3% and 5%, more of the initial kick volume is being suspended, resulting in a shorter kick front with a reduced gas volume fraction below. The extreme case of 7% suspension results in a blunt kick front, where the initial kick volume is not able to migrate, as evident from Figure 5.36, which shows the gas volume fraction depth profiles taken at 14 000

s. In this case, the kick has the same position at both time instances and has not moved any further.

Also seen in Figure 5.35 and Figure 5.36, some of the initial kick volume is left behind when considering suspension effects. The black curve in Figure 5.36 shows that there is no gas volume left at the bottom after 14 000 s for the case of no suspension. However, for the cases where suspension is included, a tail of suspended gas which reaches to the bottom of the well can be seen. For high suspension limits, the gas volume fraction tails below the kick are shifted to the right, indicating that that a higher gas fraction has been suspended in the well.

Figure 5.35 also shows that the front of the kick is located at the same position after 4 000 s independent of suspension limits. This can be due to the short distance traveled; the gas has not had enough time to be completely left as a trail of bubbles in the well [10]; the gas fraction is still sufficiently high and a large amount of the initial gas kick is migrating. For the simulation considered here, where only bubble flow is considered as long as the gas is migrating, the S-value will be independent of the suspension limits as long as the gas is migrating. This is clearly seen in Figure 5.36, where the gas bulk of 0% and 1% suspension are still at around the same location after 14 000 s. The S-value is here determined from the bubble flow model since the local gas fraction is below 0.2. However, it is not completely right to say that the S-value is independent of the suspension limit. The major difference in S-value is seen when going from slug to bubble flow, which will be shown when the kick size is increased. A larger suspension limit will reduce the gas fraction of the bulk of the kick earlier and provoke an earlier transition to bubble flow. So, if a larger kick volume is taken, one might observe this phenomenon where the kick starts migrating with an S-value determined from the slug flow model and then an earlier transition to bubble flow is seen. In this case, bubble flow exists throughout the simulation, as seen in the gas volume fraction depth profiles. The average gas migration velocities will be calculated in the next section.

Figure 5.35 Gas volume fraction depth profiles at 4 000 s for varying suspension limits, 4 m³ kick
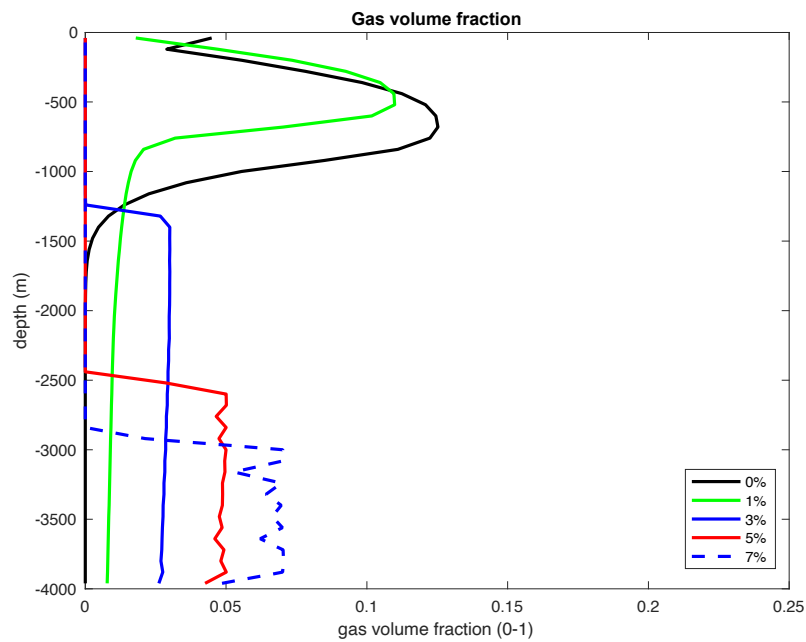
Figure 5.36 Gas volume fraction depth profiles at 14 000 s for varying suspension limits, 4 m³ kick

When being able to illustrate the gas volume fraction depth profiles at different times, the average gas migration velocity, S_{avg}, can be calculated. For 0% and 1% suspension, the kick bulks can be clearly located in the well. At 4 000 s, the kick bulks are located at around 3 000 m. After 14 000 s of simulation, the same two kick bulks have moved to around 680 m, i.e. the kick bulks have moved 2320 m. In these cases, the average is S_{avg}=0.23 m/s in the time interval between 4 000 s and 14 000 s, which is typically the value for bubble flow. For 3% suspension,

the gas has stopped migrating sometime before 14 000 since all the gas is spread out in a tail at this time. From Figure 5.34, it was seen that the pressure for the 3% kick with suspension stabilized at 8 000 s, which was 8 000 s earlier than the case with 1% suspension. This confirms that a significant reduction in the time before the pressure stabilizes can indicate that the gas has been suspended. For higher suspension values, it seems that the kicks have not migrated between 4 000 s and 14 000 s. This indicates that the gas has been fully suspended. In these cases, the S-value cannot be approximated. It is worth mentioning again that the cases of 0% and 1% suspension limits showed a difference of 49 bars in the final BHP and WHP although the gas migration velocities were approximately the same.

One can actually from Figure 5.36 see that the kick with 1 % suspension limit moves very slightly faster than for the case with 0 % suspension. This is actually related to the difference in pressure build up. For the 1 % suspension case, the pressure is lower and that will lead to a lower gas density. This will increase the S-value slightly when looking at equation 3.5 since the density difference between liquid and gas will increase. This is just an example that shows how parameters are related. Such dependencies can only be captured by a transient flow model.

Figure 5.37 shows the gas velocity profiles for the different suspension limits. As the suspension limit increases, it is observed that the gas velocities are first increasing further up in the well. This is caused by the fact that the tail of suspended gas is longer. For a 7% suspension limit, the gas is not able to move, indicating that the initial kick volume is trapped. In this case, circulation is needed.

The gas velocity figure shows that the more suspension, the shorter is the section of gas that is actually moving; the cases with higher suspension limits have a shorter section where the gas velocity is greater than S=0 m/s. The gas velocity is around S=0.23 m/s for all suspension limits except from 7% suspension. As long as the kick bulks migrate and the gas volume fractions are such that the kicks are in the same flow regime, they will migrate at the same velocity.
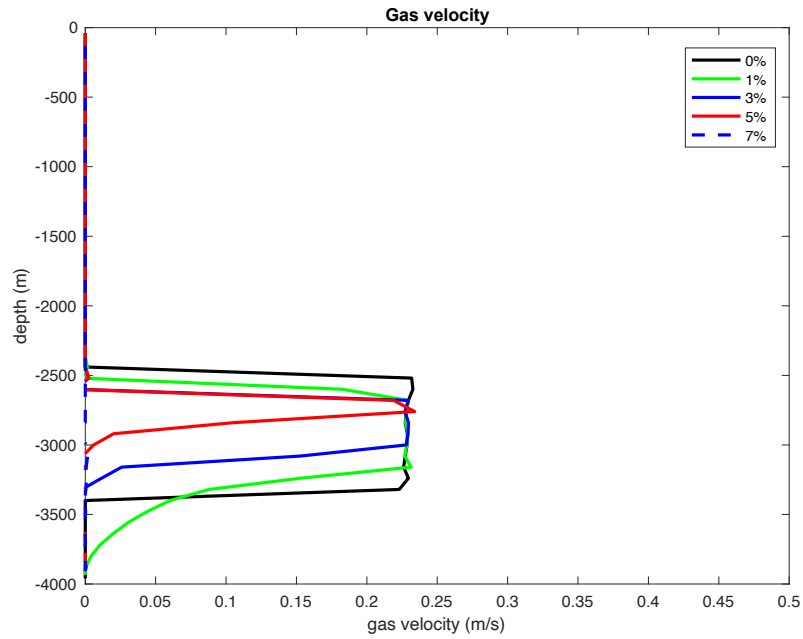
Figure 5.37 Gas velocity in well at 4 000 s for varying suspension limits, 4 m³ kick

In this section, it was seen that the 4 m³ kick was only able to migrate to the BOP for suspension limits below 3%. Therefore, the kick size will now be increased to 8 m³ to show that the kick with 3% suspension is now able to migrate to the BOP, and it is essentially migrating at a higher velocity for higher gas fractions.

8 m³

It was decided to also introduce an 8 m³ kick to the system. Figure 5.38 shows the total gas volume vs time for an 8 m³ kick. As seen on the figure, the difference in final gas volumes between 0% suspension (no suspension) and 1% suspension is 0.31 m³, which is slightly less than for the 4 m³ kick. For the kick with 0% suspension, the gas stops migrating sometime around 16 000 s, while the case of 1% suspension stops just after 14 000 s. The 3% suspension curve stabilizes at 14 000 s. The 5% and 7% suspension curves stabilize at 9 000 s and 5 000 s respectively. As in previous cases, the pressures are expected to stabilize at these stages.
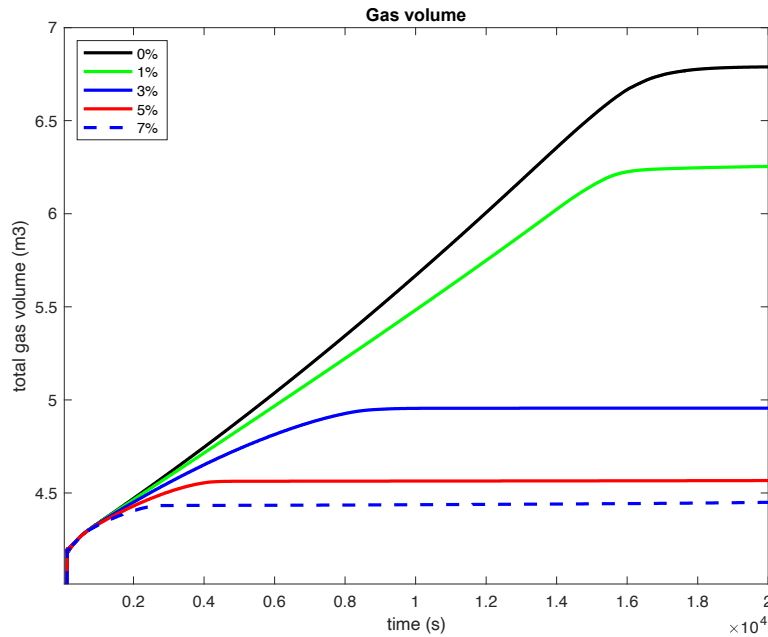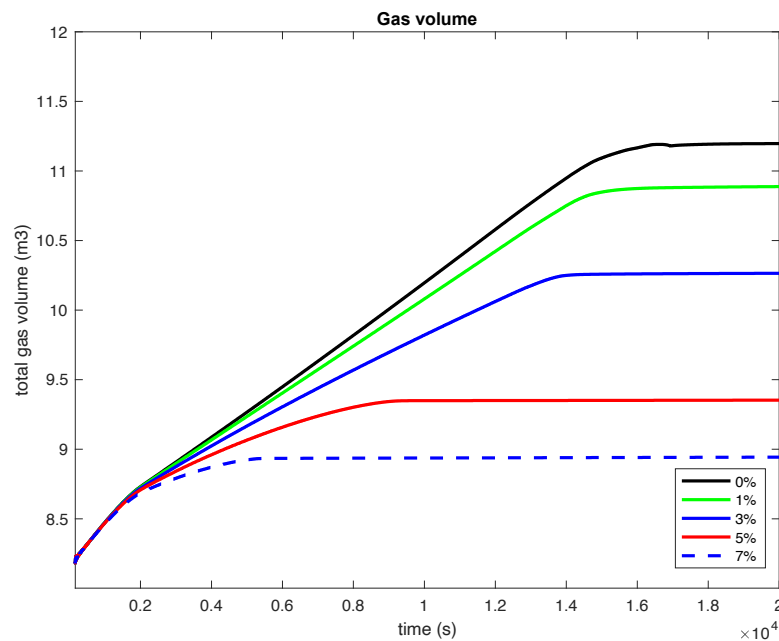

Figure 5.38 Gas volume when kick is migrating upwards in a closed well for varying suspension limits, 8 m³ kick

Figure 5.39 shows the pressure development for the 8 m³ kick for varying suspension limits, and Table 5.3 summarizes the relevant simulation results.
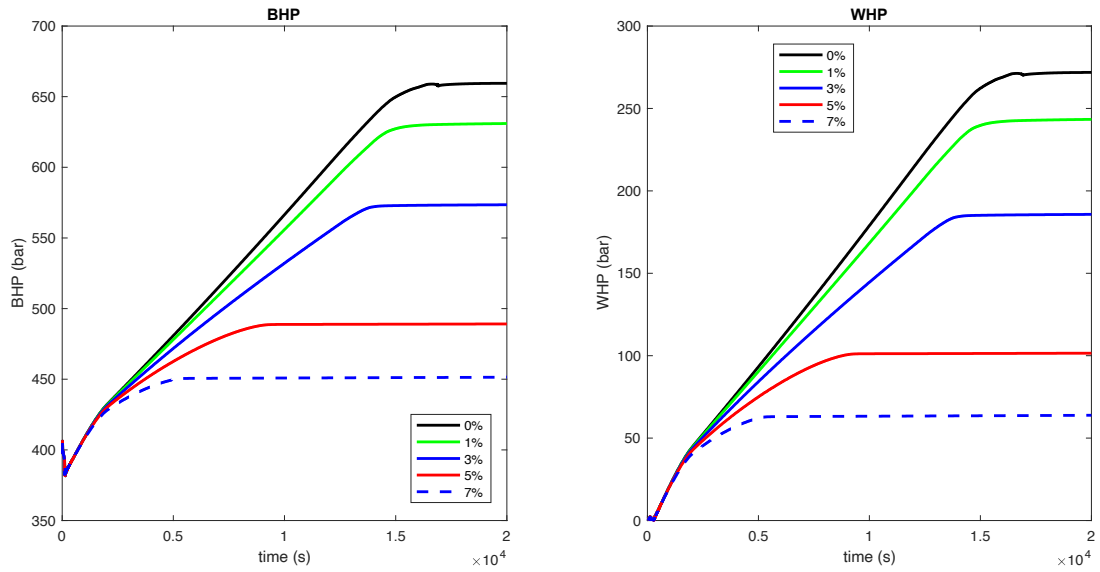
Figure 5.39 Pressure build up in well for varying suspension limits, 8 m³ kick

Suspension limits [%]	Final BHP [bars]	Final WHP [bars]	Stabilization time [s]
0	669	272	17 000
1	631	243	15 000
3	573	186	14 000
5	480	101	9 000
7	451	64	5 000

Table 5.3 Suspension limits, final BHP, final WHP, and pressure stabilization time, 8 m³ kick

For a 4 m³ kick, the final WHP was 234 bars (Figure 5.34) for the Newtonian case (no suspension). If the kick volume is doubled, the final WHP becomes 272 bars for the Newtonian case. However, according to Boyle's law, the final WHPs should be the same under the assumption that the liquid is incompressible. Furthermore, the pressure drop from the Newtonian to the Non-Newtonian case (1% suspension) was 49 bars for the 4 m³ kick, but when increasing the kick size to 8 m³, the pressure drop is only 29 bars. A possible explanation to this inconsistency could be that the liquid is not able to occupy as much of the well for the larger kick size. The relative compressibility of the liquid is decreased, and the 8 m³ kick is not able to expand as much as the 4 m³ kick. Hence, in comparison with the 4 m³ kick, the final well pressures were not reduced as much for increasing suspension limits when considering an 8 m³ kick, but there were still significant differences for various suspension limits.

The pressures stabilize at much earlier stages for the 5% and 7% suspension curves. Previously, the kicks starting from and above 3% suspension stabilized quite early for a 4 m³ kick compared to the cases with less suspension, and it turned out that the kicks were fully suspended. In this case, where an 8 m³ kick is considered, the kick with 3% suspension stabilizes at around the same stages as the 1% suspension kick (15 000 s), but the kick with 5% suspension stabilizes at 9 000 s. This may indicate that the 3% suspension case is able to migrate to the BOP, while the kicks with 5% and 7% suspension are suspended.

Figure 5.40 shows the gas volume fraction depth profiles for an 8 m³ kick taken at 4 000 s. At 4 000 s, the kick bulks are located at around the same depth of 2 600 m. In Figure 5.40, the gas fraction is around 0.18, which means that bubble flow exists. It will be seen that bubble flow exists throughout the simulation for the cases where the kick is still migrating. This is shown in Figure 5.41, which shows the gas volume fraction depth profile at 10 000 s.
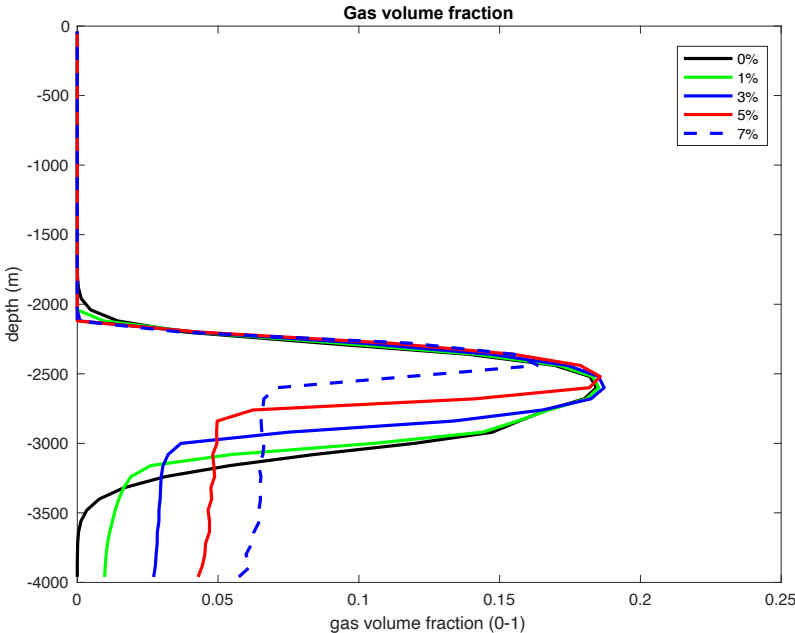
Figure 5.40 Gas volume fraction depth profile at 4 000 s for varying suspension limits, 8 m³ kick
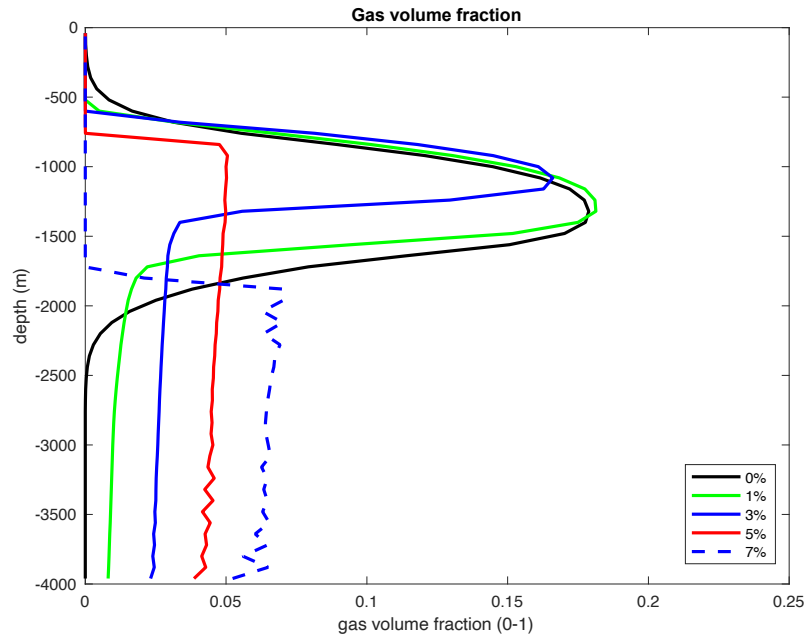
Figure 5.41 Gas volume fraction depth profile at 10 000 s for varying suspension limits, 8 m³ kick

At 4 000 s, the kick bulks are located at 2 600 m. The kick bulks with 0% and 1% suspension have moved to around 1 320 m at 10 000 s. The average gas migration velocity is therefore S_{avg}=0.21 m/s in this time interval for these cases. From Figure 5.41, it is seen that the kick with 3% suspension has also been able to migrate to this depth, but it has actually reached even further. S_{avg}=0.25 m/s for the latter case since it has moved to 1 080 m. The kick with 3% suspension is essentially able to move slightly faster than 0% and 1% suspension. The pressure for the case of 3% suspension is lower, which will give a lower gas density, and in turn it will increase the S-value since the difference in liquid and gas densities will increase. Thus, there is actually a case where a higher suspension value will give a slightly higher average gas migration velocity. The dependencies between suspension effects, gas migration velocities, and final pressures are again captured by the transient flow model. The kicks with 5% and 7% suspension are fully suspended at 10 000 s, which the pressure plots also indicated, and the average gas migration velocities cannot be calculated.

Figure 5.42 shows the gas velocities taken at 4 000 s for an 8 m³ kick. From the gas velocity figure, it is seen that a suspension limit of 7% is not sufficient to keep the gas from migrating. Although Figure 5.41 showed that the bulk will stop migrating sometime before 10 000 s, the kick is essentially able to migrate at 4 000 s. The suspension effects are not able to keep the gas from migrating since the kick volume is sufficiently large at 4 000 s. The gas migration velocity for this kick size is still S=0.23 m/s, which corresponds to bubble flow. The kick volume will

59

be increased even more, to 12 m^3, to show that the transient flow model is able to describe the transition from slug to bubble flow, and how this affects the gas migration velocities when also considering varying suspension limits.
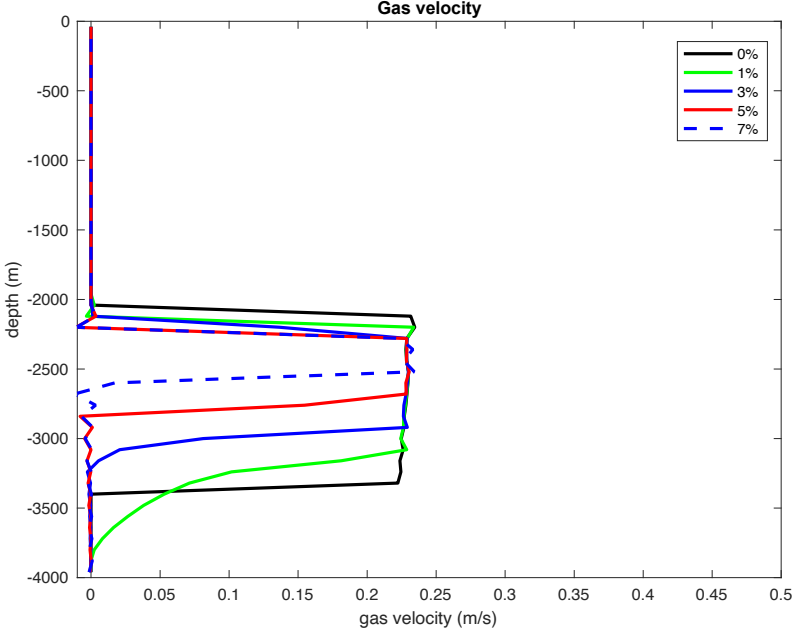
Figure 5.42 Gas velocity in well at 4 000 s for varying suspension limits, 8 m^3 kick

12 m³

The kick volume was increased to 12 m³ in attempt to demonstrate a case where slug flow is reduced towards bubble flow, and how the gas migration velocities are affected for varying suspension limits. Figure 5.43 shows the development of the pressures for a 12 m³ kick. The simulation results from the pressure plots are summarized in Table 5.4.
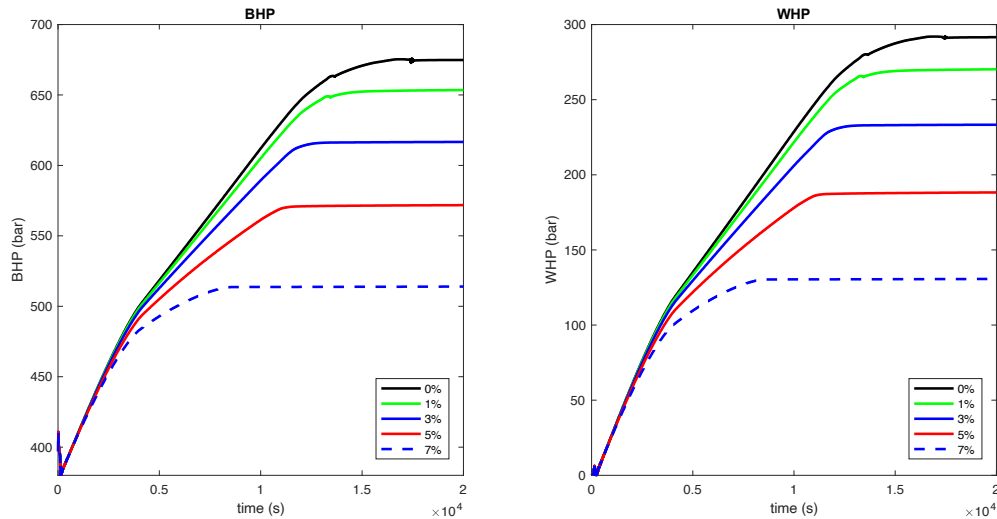
Figure 5.43 Pressure build up in well for varying suspension limits, 12 m³ kick

Suspension limits [%]	Final BHP [bars]	Final WHP [bars]	Stabilization time [s]
0	675	291	17 000
1	653	270	13 000
3	617	233	12 000
5	572	188	11 000
7	514	131	8 000

Table 5.4 Suspension limits, final BHP, final WHP, and pressure stabilization time, 12 m³ kick

Figure 5.44 shows the gas volume fraction depth profiles for a 12 m³ kick taken at 4 000 s. At this point, the kick is able to reach slug flow although bubble flow is observed at greater depths. This transition was also captured in Figure 5.43.
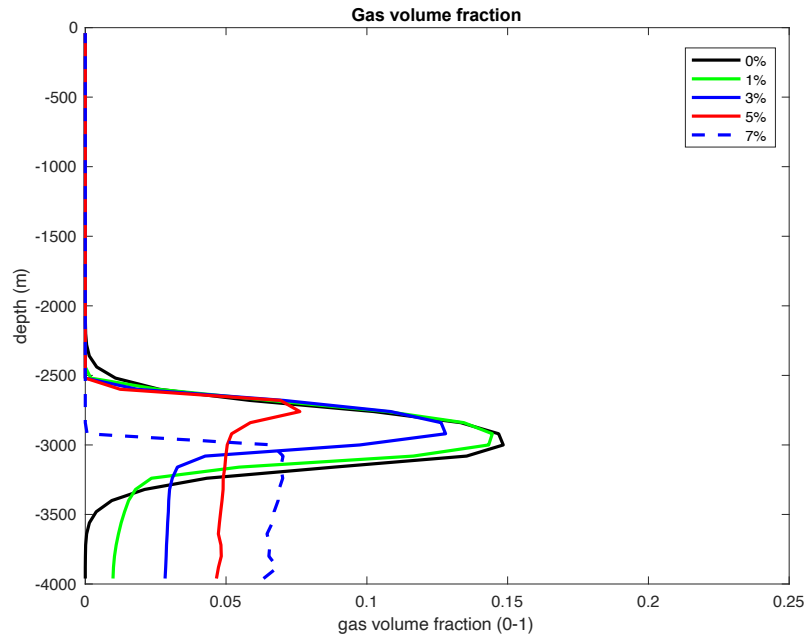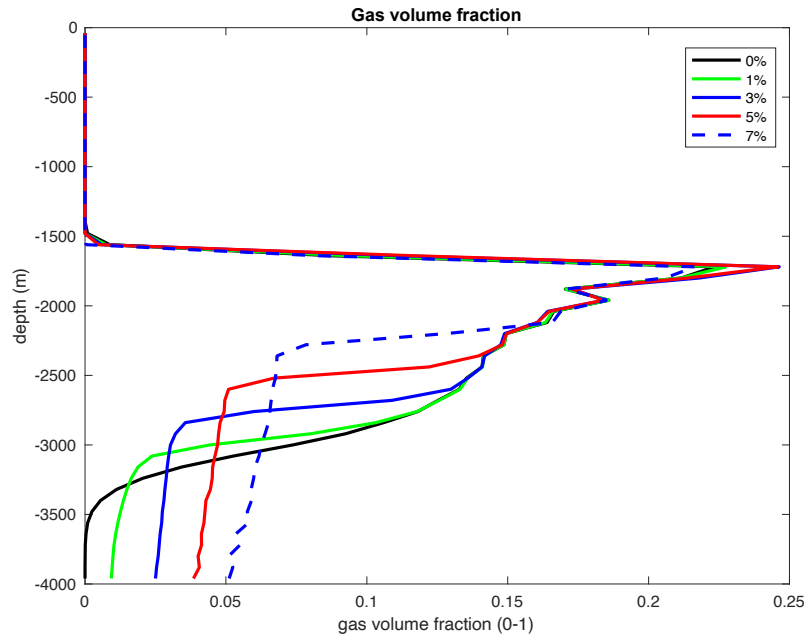
Figure 5.44 Gas volume fraction depth profile at 4 000 s for varying suspension limits, 12 m³ kick

Figure 5.45 shows the gas volume fraction depth profile at 10 000 s. At this stage, it is seen that the gas kick with 7% suspension has been suspended while the other gas bulks have been able to migrate to around 600 m.
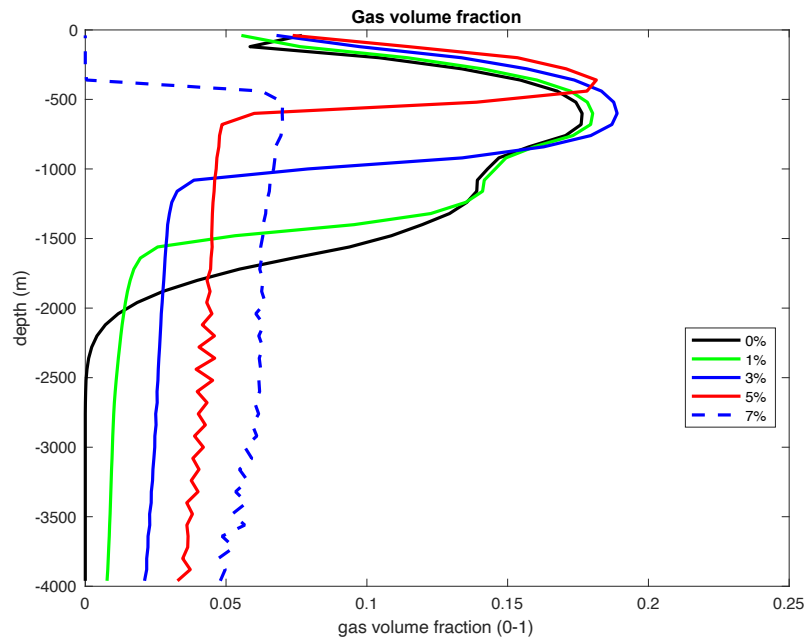
Figure 5.45 Gas volume fraction depth profile at 10 000 s for varying suspension limits, 12 m³ kick

The gas kick bulks for all cases are located at 1 720 m at 4 000 s. After 10 000 s, for the cases of 0%, 1%, and 3%, the kicks have moved to 600 m, while the kick with 5% suspension has actually moved to 360 m. At this point, the kick with 7% suspension has already stopped

migrating. The average gas migration velocity for the three first cases is S_{avg}=0.19 m/s. For the latter case, S_{avg}=0.23 m/s. Again, it is observed that a kick with high suspension limit is able to achieve a slightly higher average gas migration velocity. An important observation is that all three kick volumes showed a decrease in final pressures with increasing suspension effects; however, the gas volume fraction depth profiles and calculations gave quite similar gas migration velocities; furthermore, Figure 5.45 and calculations revealed a slightly higher average gas migration velocity for the kick with 5% suspension limit even though the final pressures were the lowest of the four migrating kicks, as seen in Figure 5.43.

For a 12 m³ kick, the gas velocity changes as the kick migrates. Figure 5.46 shows that bubble flow exists for the lower part of the kicks at 4 000 s. The gas velocity is mainly S=0.23 m/s, but at for the upper part of the kicks, it becomes S=0.46 m/s, which means that it approaches slug flow, where S=0.55 m/s. Higher gas fractions are achieved with a larger kick volume, which enables the kick to transform to slug flow.
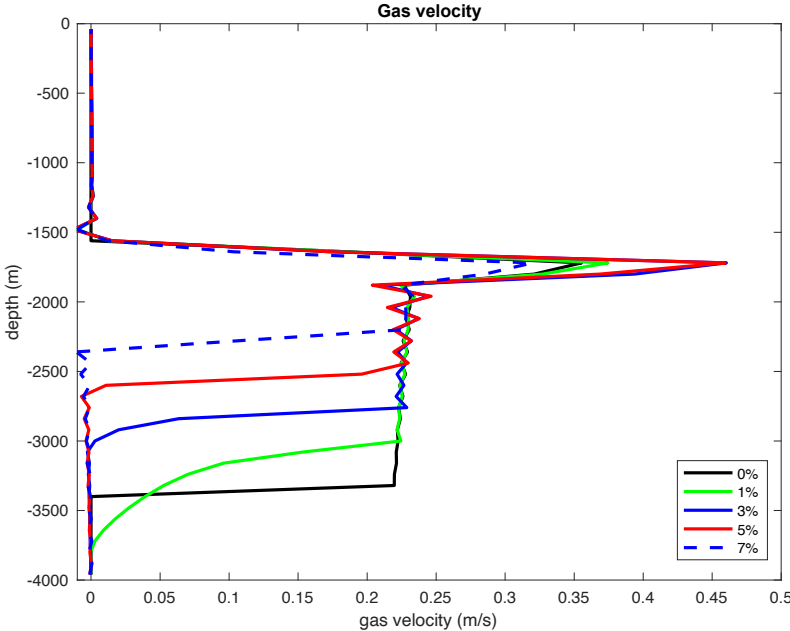
Figure 5.46 Gas velocity in well at 4 000 s for varying suspension limits, 12 m³ kick

Using the transient flow model, the dependencies between the different parameters can be shown. It would be beneficial to run simulations to develop a table for each specific well to predict how the kick behaves. The table can aid the rig crew in developing contingency procedures for handling situations where kick is involved. An example of a table developed using the new model is provided below. Using the table, one can predict if the kick has been

fully suspended, especially when looking at the final WHP and the time it takes for the pressures to stabilize.

Kick volume [m³]	Suspension limits [%]	Able to reach surface? [Yes/No]	S_avg [m/s] (4 000 s- 14 000 s)	Final WHP [bars]	Pressure stabilization time [s]
4	0	Yes	0.23	234	17 000
4	1	Yes	0.23	185	16 000
4	3	No	-	67	8 000
4	5	No	-	32	4 000
4	7	No	-	21	2 000
8	0	Yes	0.21	272	16 000
8	1	Yes	0.21	243	14 000
8	3	Yes	0.25	186	14 500
8	5	No	-	101	9 000
8	7	No	-	64	5 000
12	0	Yes	0.19	291	17 000
12	1	Yes	0.19	270	13 000
12	3	Yes	0.19	233	12 000
12	5	Yes	0.23	188	11 000
12	7	No	-	131	8 000

Table 5.5 Kick volume, suspension limits, ability to reach surface, and average gas migration velocity for a specific time interval, and final WHP and pressure stabilization time

As a final note to case 4, Table 5.6 shows a summary of some simulation results of varying kick volumes and suspension limits, and how this affects the average gas migration velocities depending on the time interval that is considered. Based on the gas volume fraction depth profiles one is able to calculate S_{avg}, and the results can give an indication of at which conditions and at what time interval the transition from slug to bubble flow occurs. S_{avg} is calculated in two different time intervals to show that the locations of the sensors certainly will have an impact on the gas migration velocities.

Kick volume [m³]	Suspension limits [%]	S_{avg} [m/s] (500 s-4 000 s)	S_{avg} [m/s] (4 000 s-10 000 s)
4	0	0.21	0.24
4	1	0.21	0.24
4	3	0.23	N/A
4	5	0.27	N/A
4	7	N/A	N/A
8	0	0.32	0.21
8	1	0.32	0.21
8	3	0.32	0.25
8	5	0.32	N/A
8	7	0.32	N/A
12	0	0.57	0.19
12	1	0.57	0.19
12	3	0.57	0.19
12	5	0.57	0.23
12	7	0.57	N/A

Table 5.6 Simulation results of kick volume, suspension limits, and average gas migration velocities for different time intervals

The table shows that the gas migration velocity changes depending on what time interval that is considered. For example, for a 4 m³ kick with 3% suspension, the gas kick migrates at an average around the bubble flow velocity between 500 and 4 000 s. Then, it becomes fully suspended sometime in the time interval of 4 000 s and 10 000 s. In this case, it is not expedient to know the gas migration velocity in the early time interval as the kick will be suspended later on. Furthermore, if only the early time interval is considered, one would make assumptions on when to expect the gas volume at surface, but in reality, the gas will become fully suspended. Another example is the 12 m³ kick with 1% suspension. At the early time interval, the average gas migration velocity corresponds to the slug flow velocity. After 4 000 s, the transition from slug to bubble flow occurs, and the average gas migration velocity is reduced towards the one for bubble flow, which one would not expect if only considering the early time interval. This highlights the importance of placing several sensors at different depths along the well for measuring accurate velocities. Besides, if gas migration velocities are deduced using pressure build up slopes only at early stages, flow pattern transitions after these stages would not be taken into account.

5.5. Case 5 – Effect of Different Transition Intervals from Full Suspension to Fully Developed Bubble Flow

It was decided to mainly use a transition interval of 2% for the transition between fully suspended gas to fully developed bubble flow in the simulations for this thesis. In case 5, the effect of different transition intervals will be studied by making the interval longer, to 4%. To take into account suspension effects, the suspension value will be fixed at 3%. This means that for gas fractions below 0.03, the gas volume is in full suspension. The suspended gas transforms into bubble flow in the interval [0.03, 0.05] and [0.03, 0.07] for 2% and 4% transition intervals respectively, meaning that bubble flow is fully developed at a gas fraction of 0.05 for 2 % transition interval and at 0.07 for 4% transition interval. Fully suspended gas will therefore take place at a fixed value in these simulations. For a 4 m^3 kick volume, it will in both cases stop before it reaches the BOP.

4 m^3

Since fully suspended gas will take place at a fixed value, there will be a transition interval from fully suspended gas to fully developed bubble flow. If this interval is made wider, the gas will move more slowly for gas volume fractions just above the fixed suspension limit. Figure 5.47 shows the gas volume vs time for the two different transition intervals for a 4 m^3 kick volume. A 2% transition interval results in a slightly greater final gas volume than a 4% transition interval. For a 4% transition interval, the gas moves more slowly upwards before it is fully suspended. More of the initial kick volume will still be in the transition interval in comparison with a 2% transition interval, resulting in less gas migrating as fully developed bubble flow. The gas stops migrating at around 9 000 s and 14 000 s for the 2% and 4% transition intervals respectively, as seen from Figure 5.47. At these time stages, the pressures will also stabilize.

66
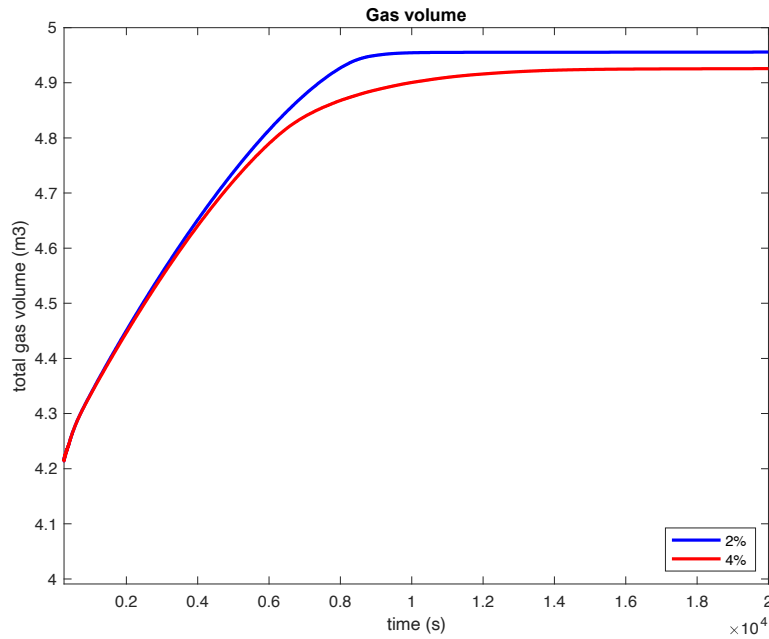
Figure 5.47 Gas volume when kick is migrating upwards in a closed well for varying transition intervals, 4 m³ kick

Figure 5.48 shows the final BHPs and WHPs for varying transition intervals. For a transition interval of 2%, the BHP stabilize at 459 bars, while for a transition interval of 4%, the BHP stabilize at 456 bars, a marginal difference of 3 bars. The final WHPs are 69 bars for a 2% transition interval and 64 bars for a 4% transition interval. The pressures for the low transition interval stabilize significantly earlier than the high transition interval, at 9 000 s. For the high transition zone, the pressures stabilize around 14 000 s. Such a delay indicates that the gas migration velocity of the wider interval is generally lower.
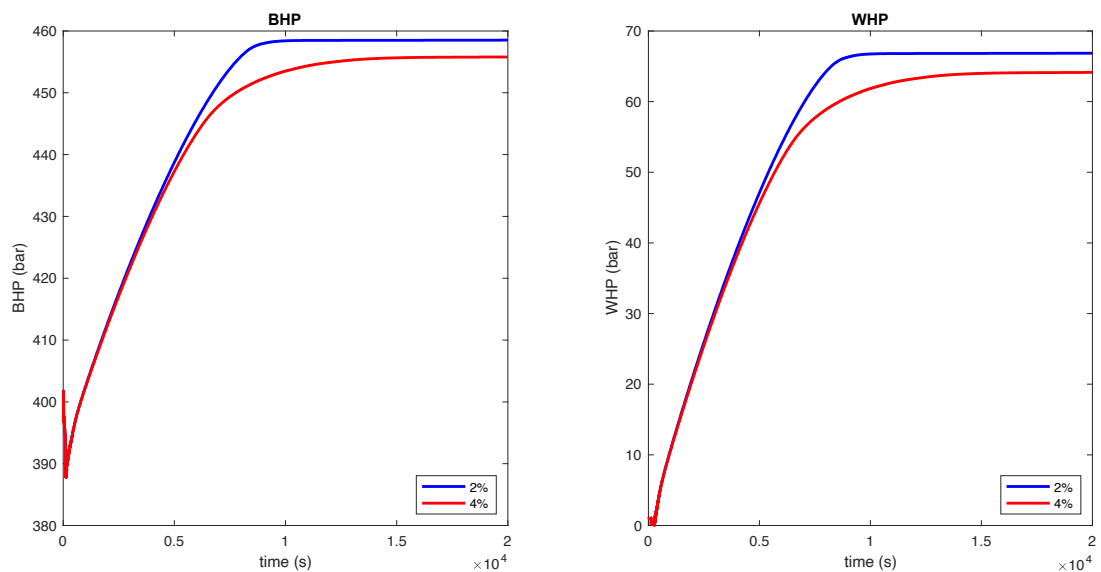
Figure 5.48 Pressure build up in well for varying transition intervals, 4 m³ kick

Figure 5.49 shows the gas volume fraction depth profiles for the two transition intervals taken at 4 000 s. The gas volume fraction depth profiles do not vary considerably when using two different intervals. However, the 2% transition interval has a longer tail where the gas is in suspension. For a 4% transition interval, there is a transition between the gas bulk and the tail of fully suspended gas (around 3 700 m to 3 000 m). In this depth interval, there is a more gradual transition for the gas volume fraction between the minimum suspension limit and the maximum gas fraction of the kick bulk. The gas located in this transition zone will more very slowly.
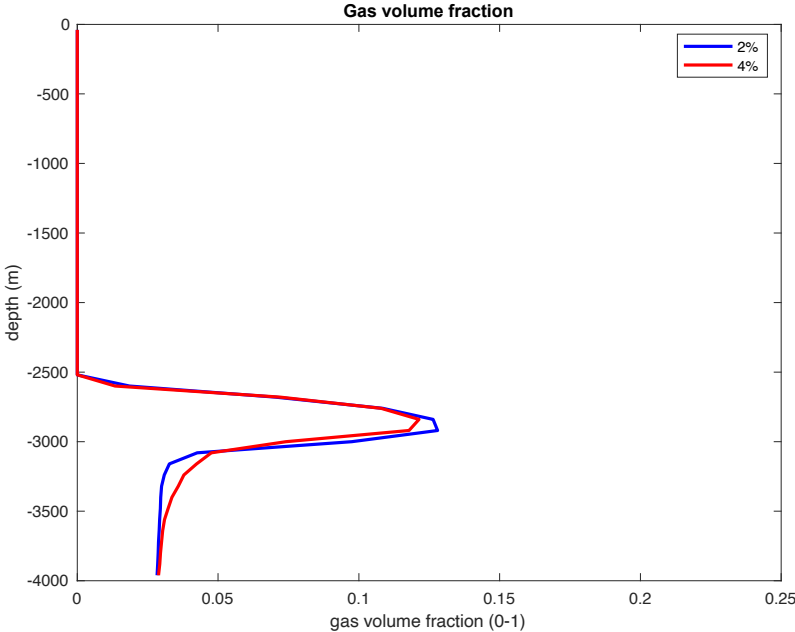
Figure 5.49 Gas volume fraction depth profiles at 4 000 s for varying transition intervals, 4 m³ kick

From chapter 5.4, it was seen that the 4 m³ gas kick is fully suspended when considering 3% suspension. The gas volume fraction depth profiles were therefore also taken at 9 000 s. Figure 5.50 shows that the gas volume fraction for a wider transition interval is higher than the shorter transition interval at this stage, and the bulk is located at a greater depth. The gas migration velocity of the wider transition interval is generally lower, and it would take longer time before it stops migrating. Also seen in Figure 5.50, the gas volume fraction of the shorter transition interval is already approaching the minimum suspension limit, i.e. the gas fraction of 0.03. From Figure 5.49, it was observed that some gas existed behind the kick bulk for the wide transition interval and the gas fraction was slightly higher for the short transition interval. In Figure 5.50, the gas volume fraction of the wide transition interval is slightly higher than for the short transition interval, which indicates that the gas that was previously in the transition

interval has now been able to migrate while the gas fraction of the short transition interval has been reduced.
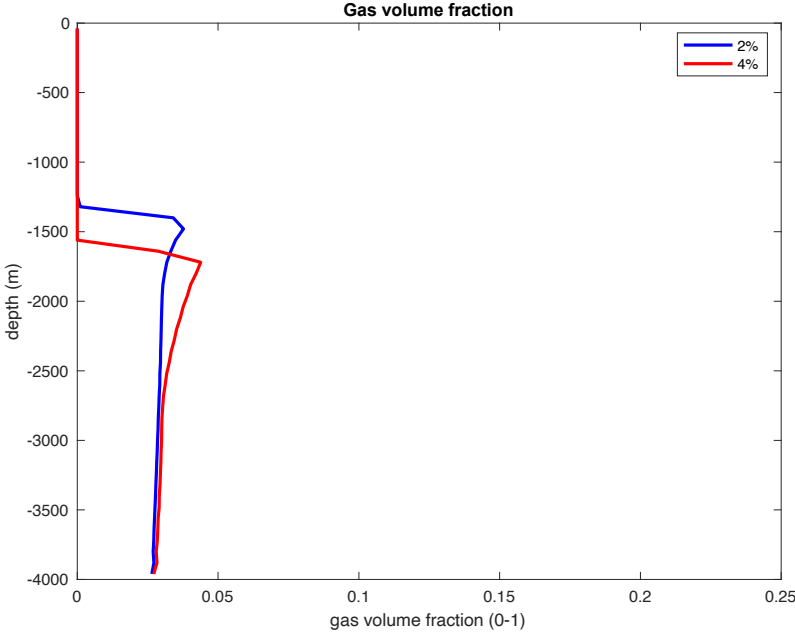
Figure 5.50 Gas volume fraction depth profiles at 9 000 s for varying transition intervals, 4 m³ kick

The difference of using a 2 % and 4 % gas volume interpolation interval is also shown in Figure 5.51, which shows the gas volume fraction depth profiles at 14 000 s, but the differences here are rather small. For the short interval, where fully bubble flow was reached for a smaller gas volume fraction, the end result was that the kick reached a bit further up in the well before it was fully stopped. But in both cases the kick stops almost at the same location in the well. A wide interval is slightly more affected by the suspension effect, and when looking at the pressure build up slopes, the differences are more visible. Hence, the main difference was that the interval to a large extent had impact on when the whole kick would stop but to a much lower extent at which location it will stop.
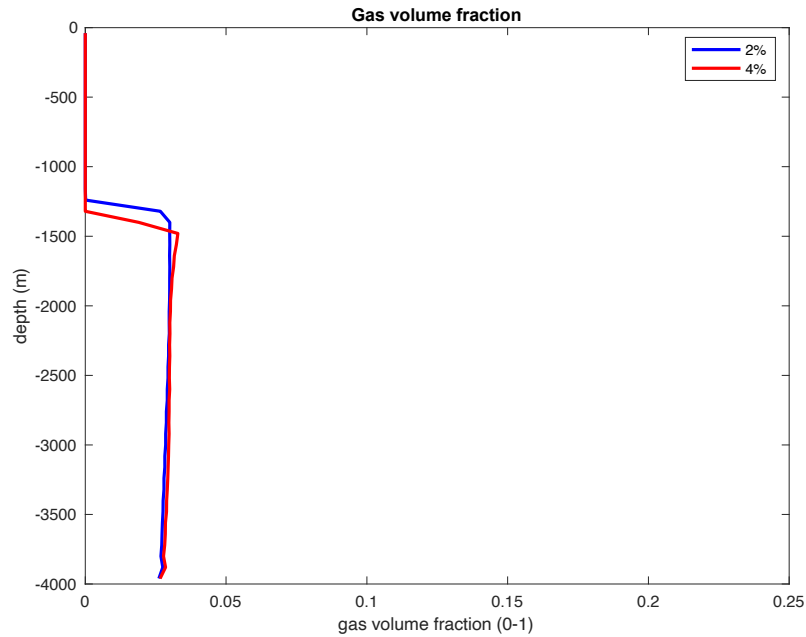
Figure 5.51 Gas volume fraction depth profiles at 14 000 s for varying transition intervals, 4 m³ kick

By looking at the gas volume fraction depth profiles, it is useful to calculate the average gas migration velocity if the kick is able to reach surface. From Figure 5.47 and Figure 5.48, the gas volume for a 4% transition interval seemed to migrate at a lower velocity. At 14 000 s (Figure 5.51) both kicks have actually stopped migrating sometime earlier. In chapter 5.4, the S-value was calculated from the plots taken at 4 000 s and 14 000 s for low suspension limits; on the other hand, the kick will not reach surface in the case of 3% suspension, and gas volume fraction depth profiles cannot be used for the same purpose.

If the gas volume fraction depth profiles were *only* taken at 14 000 s, there would not be any information of when the gas volume stopped migrating, and hence, is would not be possible to use the gas volume fraction depth profiles to estimate the S-values after all since there is no information about when the kick stopped nor at which location it stopped. In fact, neither the gas volume fraction depth profiles at 14 000 s nor the pressure build up slopes at can be used to approximate the S-value. The gas volume will not reach surface without circulation; therefore, using pressure slopes to estimate S would be misleading. The ideal solution would be to use reliable simulators that are able to show the gas bulk at different times, but it would not be expedient to estimate S (for example by taking the gas volume fractions at 4 000 s and 9 000 s) in this case since it does not reach surface without circulation. Instead, simulators can be used to estimate where the gas kick has stopped to design required contingency procedures.

Figure 5.52 shows the gas velocities for varying transition intervals taken at 4 000 s. For a 4% transition interval, there is again a transition between the gas bulk and the tail of fully suspended gas (around 3 700 m to 3 000 m), which was also seen in Figure 5.49. The gas will migrate slower in this interval; hence, it will take longer time before the kick is fully suspended when the transition interval is made wider.
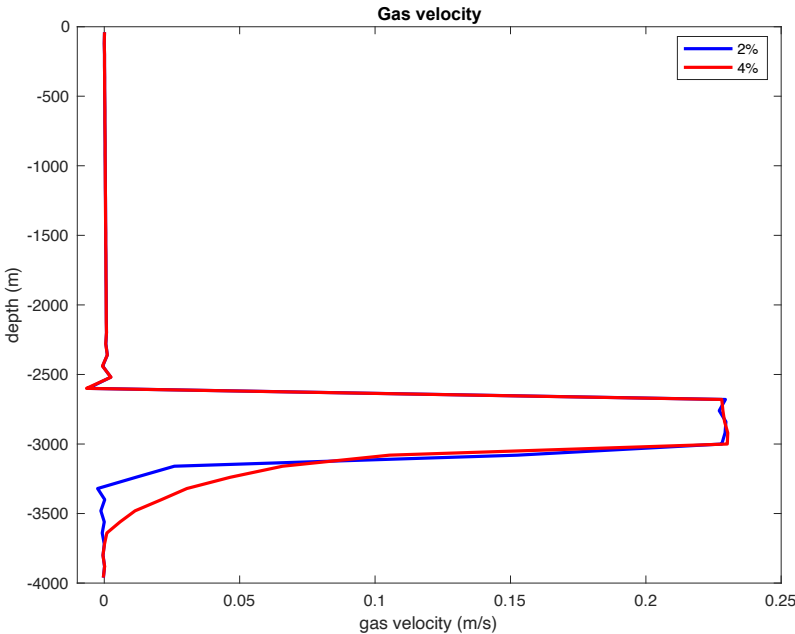
Figure 5.52 Gas velocity in well at 4 000 s for varying transition intervals, 4 m³ kick

In the next section, the kick volume is increased to 8 m^3 in order for the gas to migrate to surface. Then, the average gas migration velocities will be calculated.

8 m³

To study the transition interval from fully suspended gas to fully developed bubble flow even further, simulations were run for an 8 m³ kick volume. The kick of this size is able to reach surface for suspension limits of 3% according to the summary in chapter 5.4. This means that the average gas migration velocities can be calculated using gas volume fraction depth profiles.

Figure 5.53 shows the total gas volume vs time for the two transition intervals for an 8 m³ kick. The gas volume stabilizes at around 14 000 s both transition intervals.
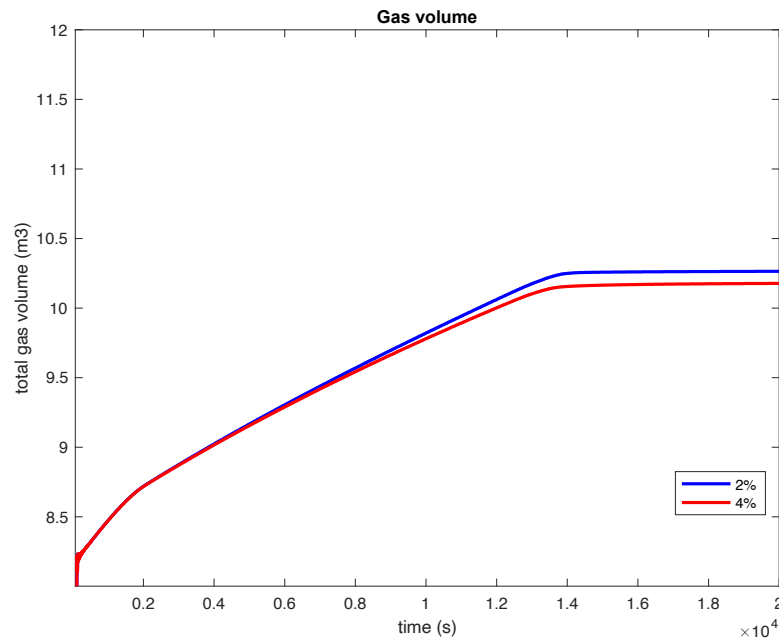
Figure 5.53 Gas volume when kick is migrating upwards in a closed well for varying transition intervals, 8 m³ kick

Figure 5.54 shows the pressure evolution for the two transition intervals. The final BHP for the shorter transition interval stabilizes at 573 bars, while it stabilizes at 565 bars for the wider transition interval. The final WHPs stabilize to 186 bars and 178 bars for the corresponding transition intervals. The difference of 8 bars for both pressures is due to the fact that for the wider interval, there is still some gas in suspension although the kick has reached surface.
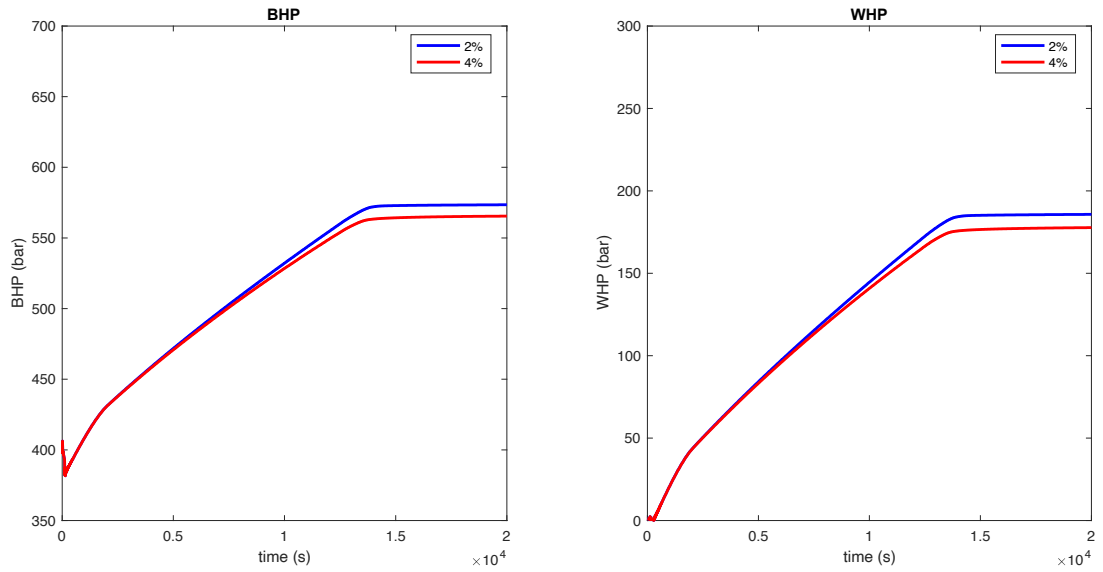
Figure 5.54 Pressure build up in well for varying transition intervals, 8 m³ kick

The gas volume fraction depth profiles taken at 4 000 s are shown in Figure 5.55. Bubble flow exists for both transition intervals, but the value of the gas volume fraction show that the kicks are close to the bubble-slug transition zone.

As for the case where a 4 m³ kick was considered, there is a transition from full suspension to fully developed bubble flow for the 4% transition interval also for this kick size. At a depth interval from around 3 500 m to 3 000 m, the kick volume will migrate slower for the wider transition interval. Looking at Figure 5.55, which shows the gas volume fraction depth profiles at 4 000 s, the gas fractions are 0.18 for both kicks, and bubble flow exists. At 9 000 s (Figure 5.56) the gas fraction of the main bulk (2% transition interval) of the kick has a slightly higher value compared to the case with a wider interval. This is due to the fact that for the wider interval, more gas is located below the main bulk of the kick where it is either fully suspended or moving very slowly. Hence, there is less gas left in the main bulk of the kick.

73
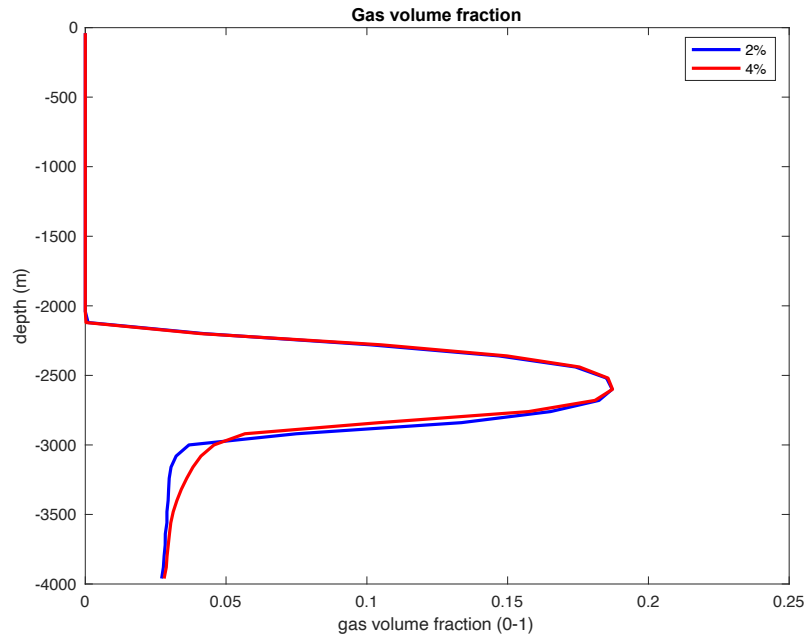
Figure 5.55 Gas volume fraction depth profiles at 4 000 s for varying transition intervals, 8 m³ kick

At 4 000 s, the kick bulks were located at 2 500 m. After 9 000 s, they have moved to 1 300 m, and S_{avg}=0.24 m/s in this time interval. Figure 5.57 shows that both kick bulks are able to reach surface at 14 000 s.
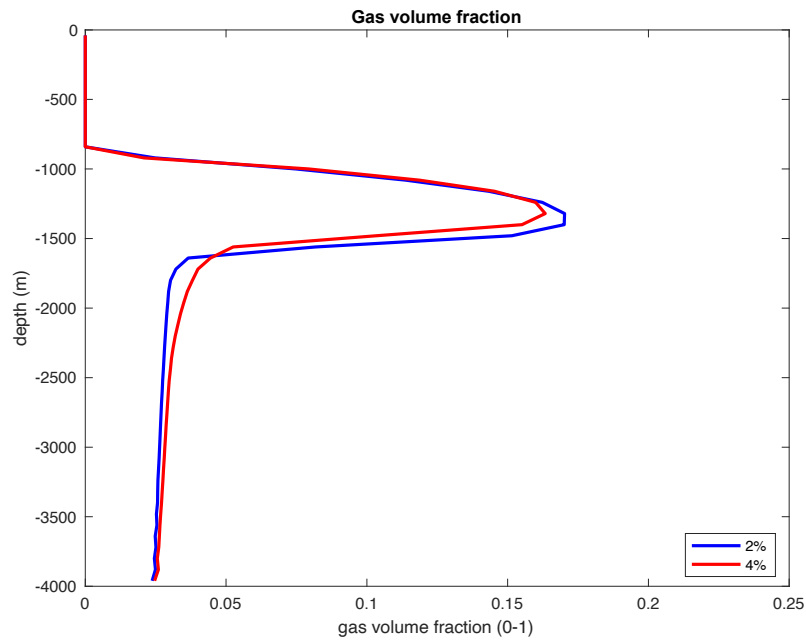
Figure 5.56 Gas volume fraction depth profiles at 9 000 s for varying transition intervals, 8 m³ kick
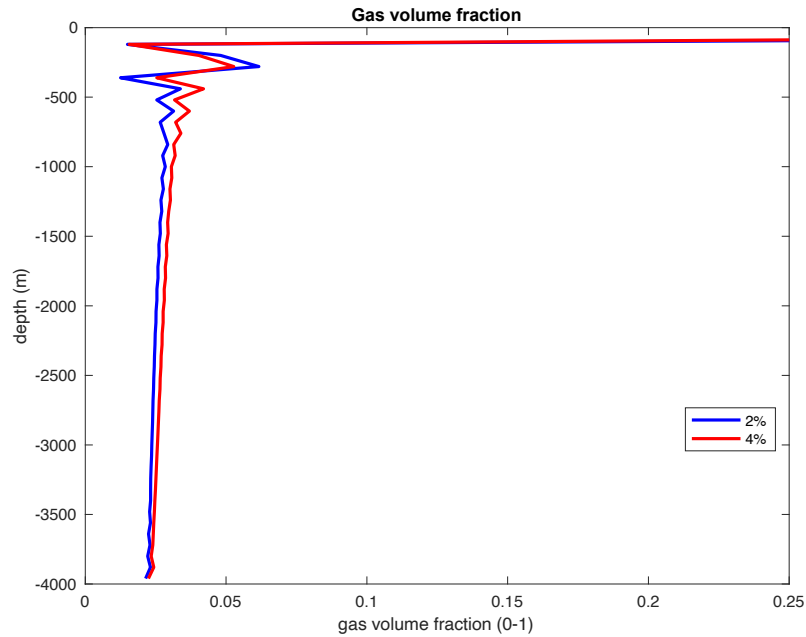
Figure 5.57 Gas volume fraction depth profiles at 14 000 s for varying transition intervals, 8 m³ kick

The gas velocities are S=0.23 m/s (Figure 5.58), which are typically the value for bubble flow. There is a transition from fully suspended flow to bubble flow for the wider transition interval. In this transition interval, the gas moves slowly. In comparison with a 4 m³ kick, the section of gas that is actually moving is larger. For the 8 m³ kick, the bulk of the kick that is moving at fully developed bubble flow extends from 3 000 m to 2 250 m at 4 000 s. For the 4 m³ kick, it extended from 3 250 m to 2 625 m. This is clearly because the initial kick volume is doubled. Also, the front of the 8 m³ kick is at shallower depth than for a 4 m³ kick (Figure 5.52) at this stage. If the gas volume fractions are taken at quite early stages, e.g. 500 s (Figure 5.59), it is observed that the gas kick bulks migrated in the slug flow regime, which explains why the kick bulks has reached further than for a 4 m³ kick at 4 000 s, where only bubble flow existed.
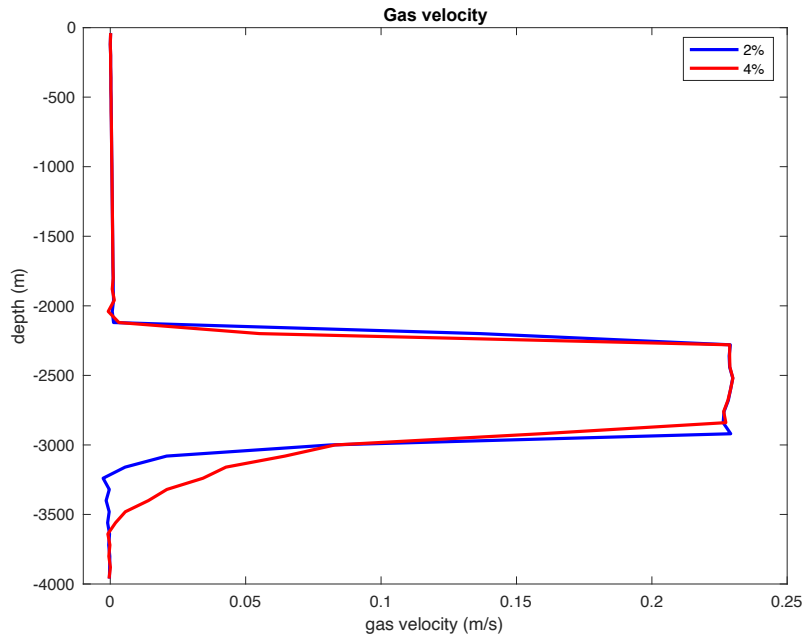
Figure 5.58 Gas velocity in well at 4 000 s for varying transition intervals, 8 m³ kick
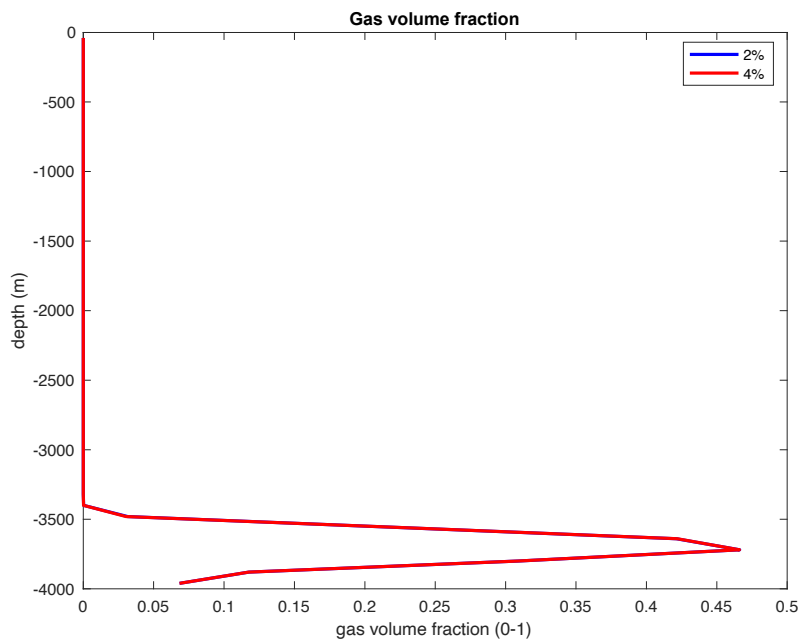
Figure 5.59 Gas volume fraction depth profiles at 500 s for varying transition intervals, 8 m³ kick

In case 5, simulations were not run for a 12 m³ kick since the gas migration velocities would be more affected by the fact that slug flow existed rather than the width of the transition interval. For the two kick volumes considered, there will be mobile gas behind the kick bulk for the wider transition interval, and the gas behind the kick bulk will migrate slowly. The pressure build up will therefore be steeper for a low transition interval before it stabilizes. The location where the gas kicks stop migrating and the time it takes for them to reach surface is not affected by the transition interval.

5.6. Case 6 – Transition Zone from Bubble to Slug Flow

Since the model used in the simulations assume a Newtonian drilling fluid, the transition from bubble to slug flow has been implemented for gas fractions from 20-25%. However, in [10] and [34], it was suggested to use a lower transition zone for Non-Newtonian drilling fluids, meaning that slug already forms from gas fractions of 10%. In case 6, the effect of lowering the transition zone from bubble to slug flow on pressure build up will be demonstrated. To study the effect of different transition zones solely, fully developed bubble flow will take place from gas fractions of 0 and suspension limits will not be considered initially. In addition, the suspension limits will later be fixed at 1% and 3% and the transition interval to fully developed bubble flow will be fixed at 2%.

4 m^3

Figure 5.60 shows the gas volume vs time during the simulation of the two transition zones without considering suspension effects. The final gas volume is the same after 20 000 s of simulations. However, the gas volume migrates and stabilizes faster for the lower transition zone, at 16 000 s. For the higher transition zone, the gas volume stops migrating at 17 000 s. This affects the pressure build up, as shown in Figure 5.61.
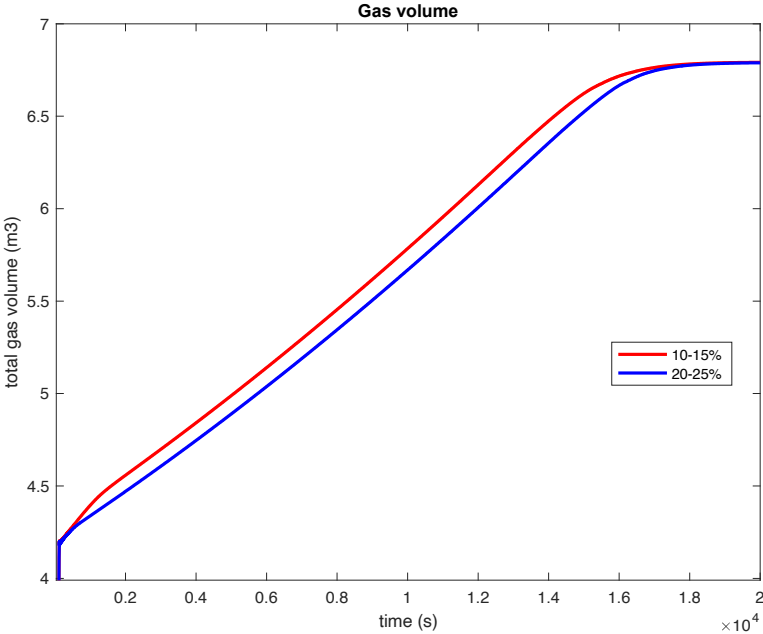
Figure 5.60 Gas volume when kick is migrating upwards in a closed well for varying transition zones, 4 m^3 kick

An important remark is that the varying transition zones result in the same final pressures of 626 bars and 234 bars for BHP and WHP respectively, yet they affect the pressure build up differently. The phase shift is evident in the pressure plots (Figure 5.61) because slug flow takes place at smaller gas volumes when considering a low transition zone. The S-value for slug flow is larger than for bubble flow, enabling the kick to reach surface faster for a low transition zone. It can be noted that the pressure build for the case with lower transition zone has a steeper slope until around 1 500 s before both pressure build up slopes are the same. This indicates that slug flow or transition from bubble to slug flow was present initially for the case with lower transition zone before this also became bubble flow. Thus, the major difference in gas migration velocities was in the early part of the simulation.
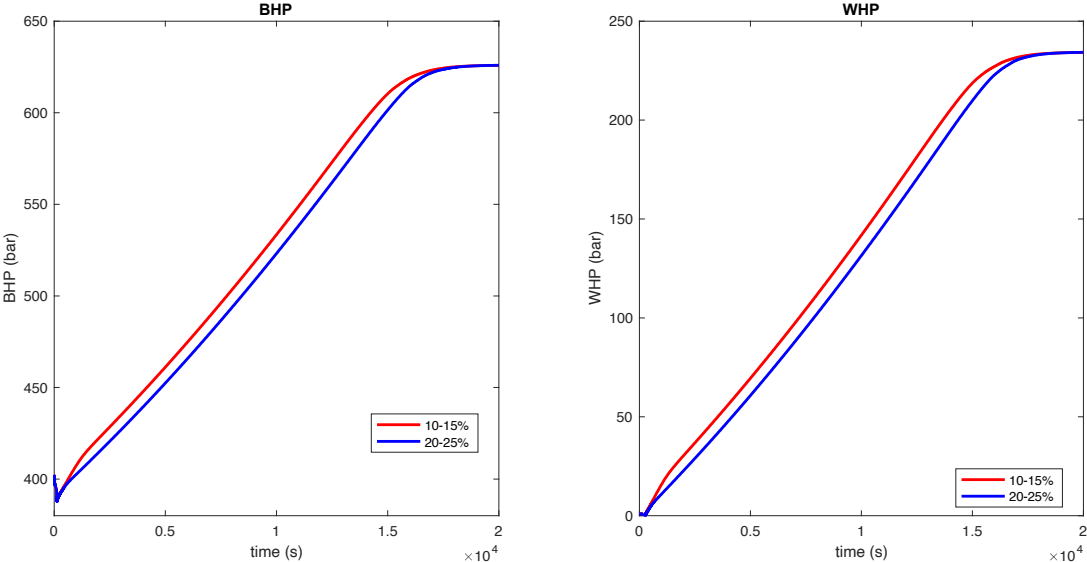
Figure 5.61 Pressure build up in well for varying transition zones, 4 m³ kick

Also, since the final BHP and WHP curves for the two transition zones coincide, it means that the gas kick has reached the BOP in both cases, and an average S_{avg} can be approximated using the gas volume fraction depth profiles, which will be shown later. This would correspond to placing several sensors in the well to measure the *time of flight* [10]. The S_{avg}-value will be an average obtained by the presence of having different flow patterns in the well at different times and locations. Figure 5.62 shows that the gas volume fraction at 600 s is approximately at the same position in both cases. But from Figure 5.63, it is seen that for the lower transition zone, the kick will move with slightly different velocities. The top part of the kick moved with S-values close to slug, while the lower part of the kick moves with S-values from the bubble flow regime. Hence, when the gas volume fraction is considered at 2 000 s, the gas kick for the low

transition zone has been spread more out and the maximum gas volume fraction in the bulk of the kick has been reduced.

By looking at the pressure plots, it is seen that the phase shift occurs early during the simulations due to different slopes. The gas volume fraction depth profiles for the varying transition zones were therefore taken at 600 s. It is not logical to wait until the kick is at the BOP and then calculate what the kick migration velocity has been. One should definitively avoid letting a kick migrate to the BOP in a closed well since it will cause excessive pressures that at some point will break down the formation. In reality, the safest approach would be to place several sensors at greater depths that can measure the gas migration velocity. This way, the personnel could estimate when to expect the kick at surface. An alternative would be to use reliable simulators that can be used for the same purpose. For the simulation considered here, the locations of the gas kicks are taken at 600 s and 2 000 s to calculate the average S-values.

Figure 5.62 Gas volume fraction depth profiles at 600 s for varying transition zones, 4 m³ kick
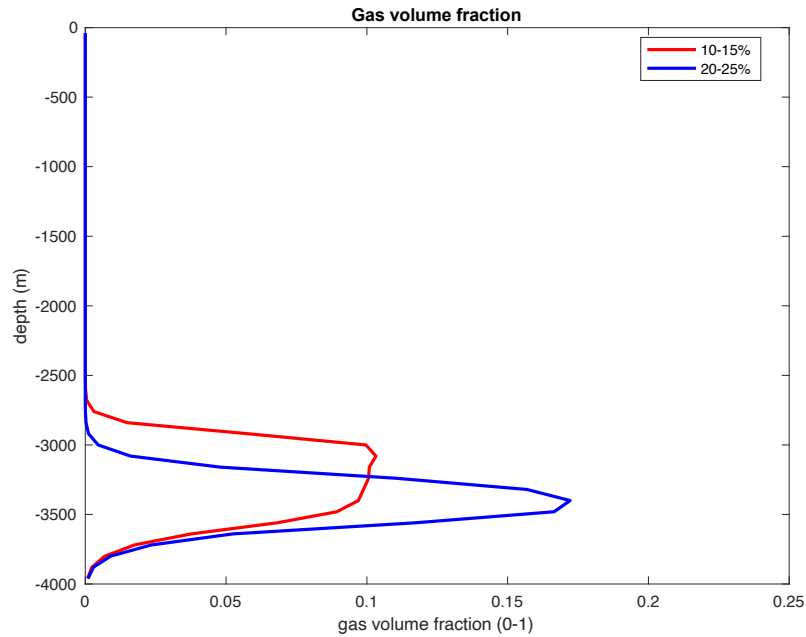
Figure 5.63 Gas volume fraction depth profiles at 2 000 s for varying transition zones, 4 m³ kick

The average S-value for the high transition zone is S_{avg}=0.17 m/s since the bulk has moved from 3 640 m to around 3 400 m in the time interval. S_{avg}=0.40 m/s for the low transition zone since it has moved from 3 640 m to 3 080 m. In this time interval, there is a larger difference in the average S-values for the different transition zones, and the pressure build up are different in this time interval. The difference is caused by the fact the for the low transition zone, slightly more gas is moving as slug flow and reaches surface faster.

Figure 5.64 shows the gas velocities taken at 1 000 s of simulation. With a high transition zone, larger gas fractions are needed to form slugs. Since slugs move faster, a low transition zone will give higher gas velocities. Figure 5.64 also shows that for the case with a low transition zone, the top part of the kick moves as slug flow while the lower part moves as bubble flow. However, for the high transition zone, the whole kick is migrating in the bubble flow regime.
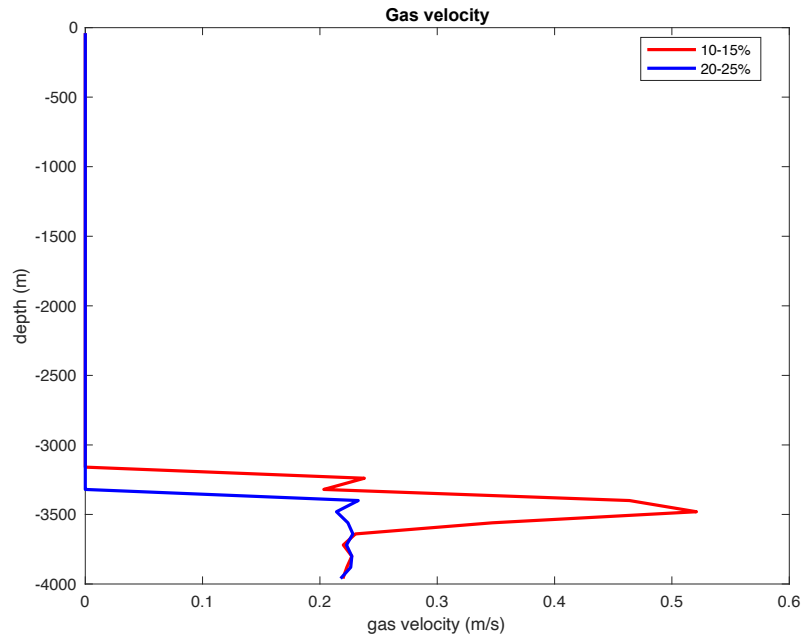
Gas velocity

Figure 5.64 Gas velocity in well at 1 000 s for varying transition zones, 4 m³ kick

Figure 5.65 shows the gas velocities taken at 2 000 s. Now the gas velocities approach the same value. The kick of the low transition zone has migrated faster at an earlier stage and reached further up in the well. But at 2 000 s, both kicks are in the bubble flow regime. Since the gas fraction was reduced due to the spreading of the kick, the transition to bubble flow has taken place also for the low transition zone at 2 000 s; the gas fraction is reduced more significantly for the low transition zone, which in turn will initiate the transition from slug to bubble flow, where S=0.23 m/s.
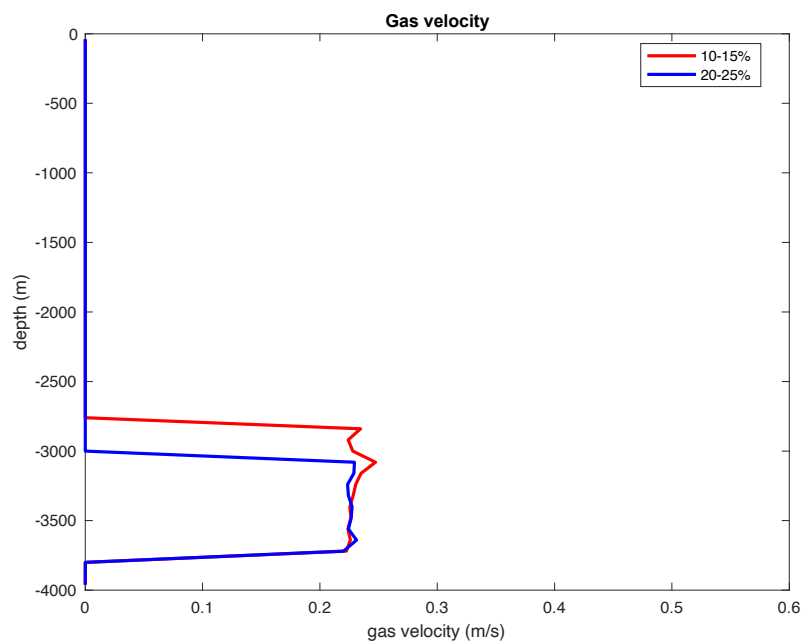
Gas velocity

Figure 5.65 Gas velocity in well at 2 000 s for varying transition zones, 4 m³ kick

81

The effect of lowering the transition zone from bubble to slug flow will now be studied including suspension effects. As previously shown, it is possible to approximate an average S-value for the kick migration when the gas kick has reached the BOP by using the surface pressure simulation results. This is only possible since no suspension effect is considered, and the kick migrates fully to surface. The only difference between a high transition zone and a low transition zone would be when the gas volumes and pressures stabilize reflecting that the kick moved slightly faster for the low transition zone. However, in a real operation it would not be done like this since one would be interested in predicting the gas migration velocity at an early stage of the operation. The major difference in gas migration velocity took place early in the simulation when the slopes of the pressure build up curves were different. The final gas volume, BHP, and WHP would still be the same.

In the following discussion, the effect of suspension will be included when studying the varying transition zones. The transition interval from suspended flow to fully developed bubble flow will be fixed at 2%. Now it is demonstrated that it would be more complex to estimate the S-value accurately from pressure slopes. Table 5.7 shows the suspension limits used in the simulations.

Suspension limits [%]	Minimum suspension limit [gas fraction]	Maximum suspension limit [gas fraction]
0	0.00	0.00
1	0.01	0.03
3	0.03	0.05

Table 5.7 Suspension limits for case 5

Figure 5.66 shows the BHPs and WHPs for the two transition zones for varying suspension limits. Table 5.8 summarizes the simulation results from the pressure plots. Note that these values are the same as the ones obtained in case 4 considering suspension effects, and the figures are shown again to highlight that the final pressures are much affected by suspension effects. If the transition zone from bubble to slug flow is changed to a lower interval, a phase shift to the left is observed, which can be seen in Figure 5.66 (dashed curves). The phase shift occurs early during the simulation, which at these stages would make the slopes of the low transition zone steeper.
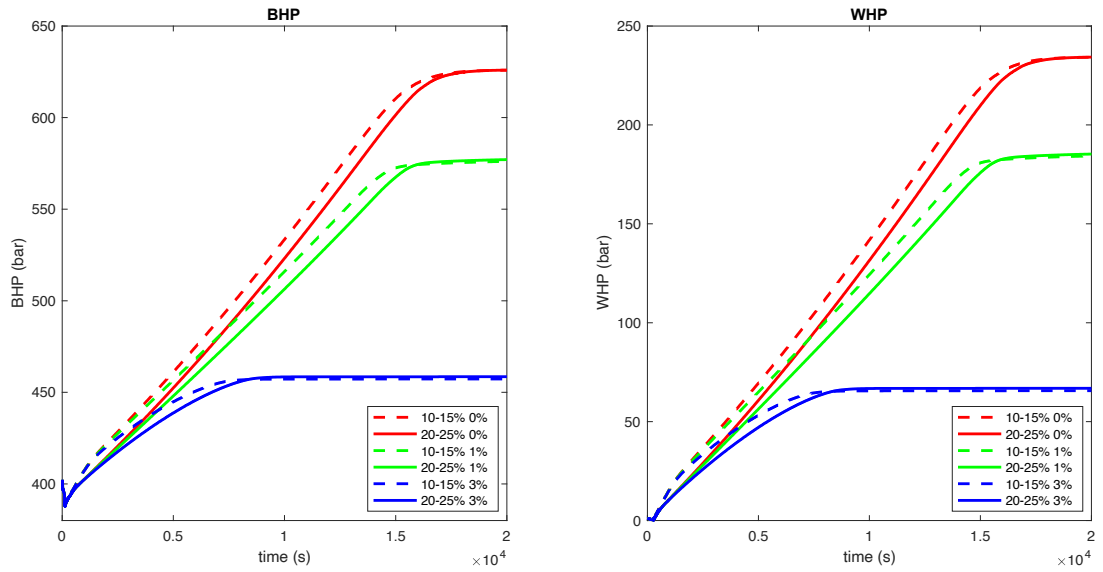
Figure 5.66 Pressure build up in well for varying transition zones and varying suspension limits, 4 m³ kick

Suspension limits [%]	Final BHP [bars]	Final WHP [bars]	Stabilization time [s]
0	626	234	17 000
1	577	185	16 000
3	459	67	8 000

Table 5.8 Suspension limits, final BHP, final WHP, and pressure stabilization time, 4 m³ kick

Figure 5.67 shows the gas volume fraction depth profiles for the two transition zones and varying suspension limits taken at 4 000 s. Again, the kick is located approximately at the same depth independent of suspension limits, but the front of the kick migrates faster for a low transition zone. Table 5.9 summarizes the locations of the kick bulks for the different situations at 4 000 s. The position is where the gas volume fraction is at its maximum.
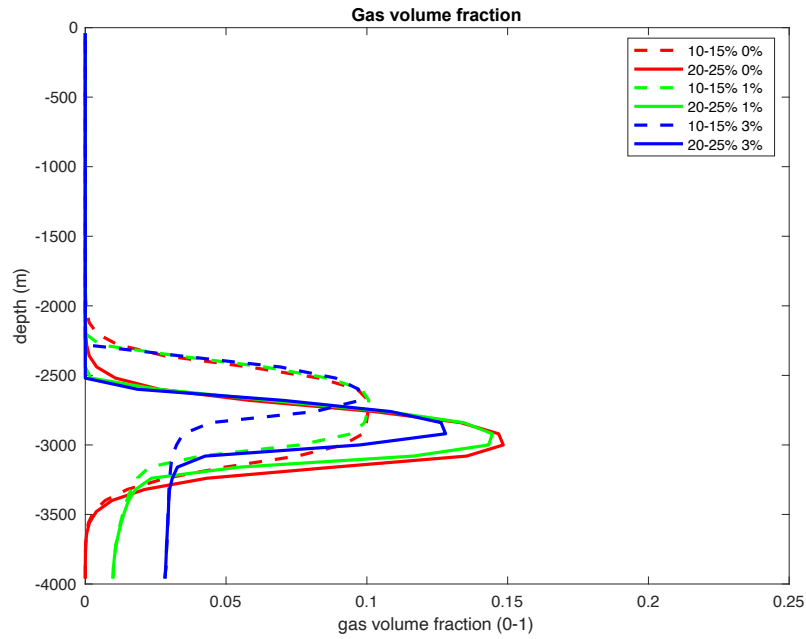
Figure 5.67 Gas volume fraction depth profiles at 4 000 s for varying transition zones, 4 m³ kick

Transition interval [%]	Suspension limits [%]	Depth [m]
10-15	0	2 760
10-15	1	2 760
10-15	3	2 760
20-25	0	3 000
20-25	1	3 000
20-25	3	3 000

Table 5.9 Transition interval, suspension limits, and location of gas bulk, 4 m³ kick

Figure 5.68 shows the gas volume fraction depth profiles taken at 10 000 s. The locations of the kick bulks are summarized in Table 5.10. Both Figure 5.67 and Figure 5.68 show that bubble flow exists throughout the simulations. The distance traveled and the S-values can be calculated for 0% and 1% suspension as the kick is able to travel to surface.
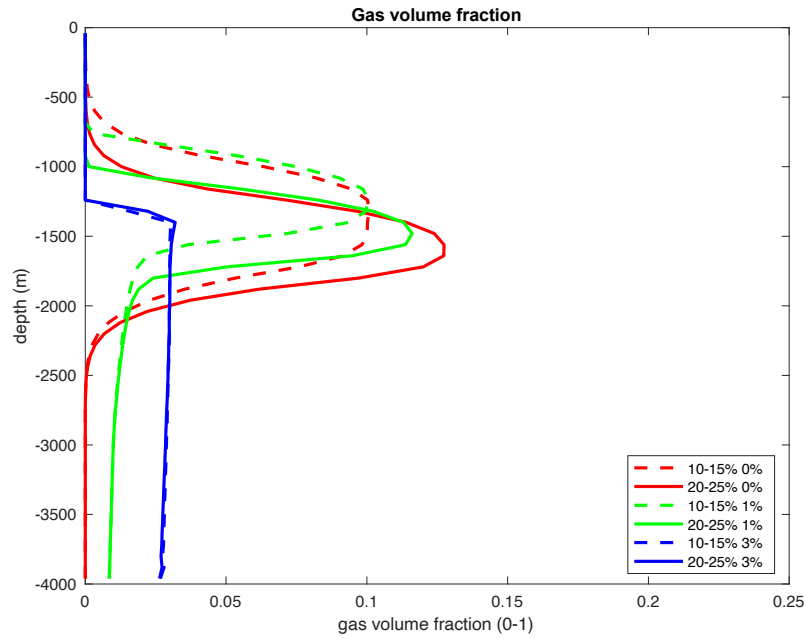
Figure 5.68 Gas volume fraction depth profiles at 10 000 s for varying transition zones and varying suspension limits, 4 m³ kick

Transition interval [%]	Suspension limits [%]	Depth [m]	ΔD [m]	S_{avg} [m/s]
10-15	0	1 320	1 440	0.24
10-15	1	1 320	1 440	0.24
10-15	3	N/A	N/A	N/A
20-25	0	1 560	1 440	0.24
20-25	1	1 560	1 440	0.24
20-25	3	N/A	N/A	N/A

Table 5.10 Transition interval, suspension limits, location of gas bulk, and average gas migration velocity, 4 m³ kick

Since only bubble flow exists (Figure 5.67 and Figure 5.68), it is expected that the S_{avg}-values are the same as long as the kicks migrate. If one approximates the gas migration velocities by using the slope of the pressure build up curves, it would give different results. A different set of values would be obtained since the slopes also change in time due to transition between slug and bubble, but most of all due to the effect of suspension and what the suspension limit is. Thus, using pressure build up slopes to approximate gas migration velocities can be misleading. In fact, it would be impossible to predict a unique gas migration velocity from measuring the slope of the pressure build up. The method where the gas volume fraction depth profiles at different time intervals are used would be the method that shows the most correct S_{avg}-values.

Furthermore, only the gas volume fraction depth profiles could show that the case of 3% suspension was suspended. For 3% suspension, the gas migration velocity cannot be calculated in the same manner as the kicks are suspended before the 10 000 s of simulation, as seen in Figure 5.68. For both transition zones, the kick stops migrating at around the same depth with a marginal difference in the pressure build up. In this case, the suspension effects dominated and led to a halt in the kick migration.

8 m³

In continuation of case 6, the kick volume was increased to 8 m³. Before considering suspension effects, the gas migration velocities will be calculated in the interval where the low transition zone gives higher pressure slopes than the high transition zone, i.e. the average gas migration velocities will be calculated in the time interval of 600 s and 2 000 s.

Figure 5.69 shows the gas volume vs time for an 8 m³ kick for the two transition zones without considering suspension effects. As seen in the figure, the phase shift by reducing the transition zone is more prominent than for a 4 m³ kick. The gas volume stabilizes at around 16 000 s for both transition zones, but slightly later for the high transition zone.
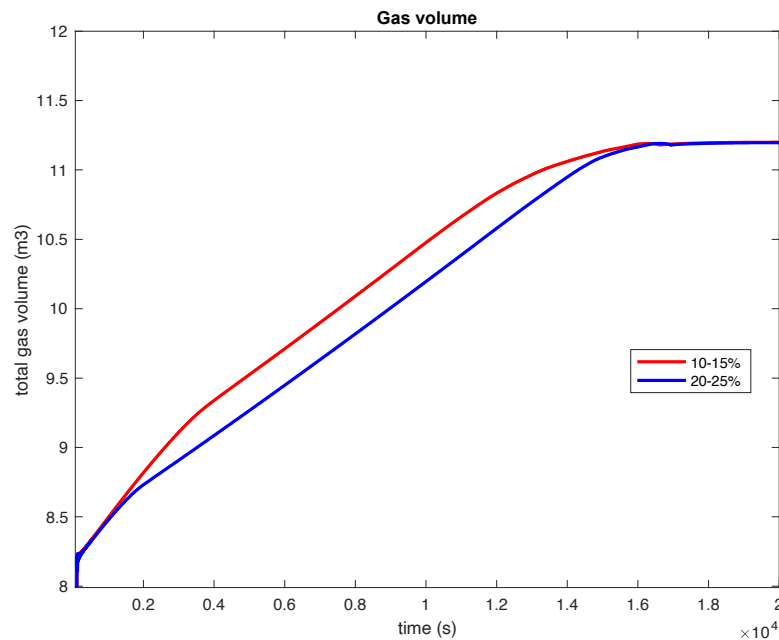
Figure 5.69 Gas volume when kick is migrating upwards in a closed well for varying transition zones, 8 m³ kick

The pressure plots are shown in Figure 5.70. This time, the phase shift is more prominent for a low transition zone compared to the smaller kick volume. The final BHPs and WHPs are 659 bars and 270 bars respectively for both transition zones. However, the pressures stabilize slightly faster for a low transition zone.

In addition, Figure 5.70 shows that the pressure build up slope is the largest at early stages for both transition zones. This indicates faster gas migration velocities due to the presence of slug flow in both cases. But for the high transition zone, the slope reduces earlier at around 2 000 s indicating a slower gas migration velocity caused by a transition to bubble flow. In the next

section, it is shown that the average gas migration velocities differ in this interval when considering the two different transition zones from slug to bubble flow.
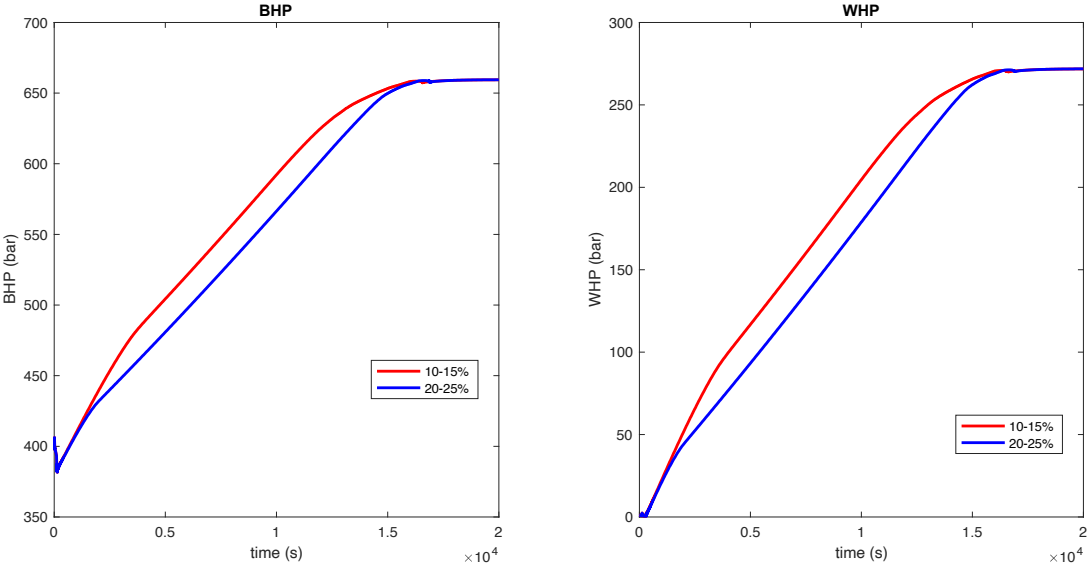
Figure 5.70 Pressure build up in well for varying transition zones, 8 m³ kick

The gas volume fraction depth profiles were taken at 600 s and 2 000 s. These are the stages where the gas kick of the low transition zone migrates at higher velocity than the high transition zone and gives a larger pressure build up slope, as observed in Figure 5.70. The gas kicks are located at 3 640 m at 600 s (Figure 5.71), and they are at 2 920 m at 2 000 s (Figure 5.72). The average gas migration velocity is S_{avg}=0.51 m/s in this time interval. Also seen in Figure 5.71 is that both gas kicks are in the slug flow regime. The kick of the high transition zone is in the bubble flow regime at 2 000 s (Figure 5.72) since the gas volume fraction is below 0.2. For the low transition zone, the gas volume fraction indicates that the upper part of the kick is in slug flow while the lower part is in bubble flow.
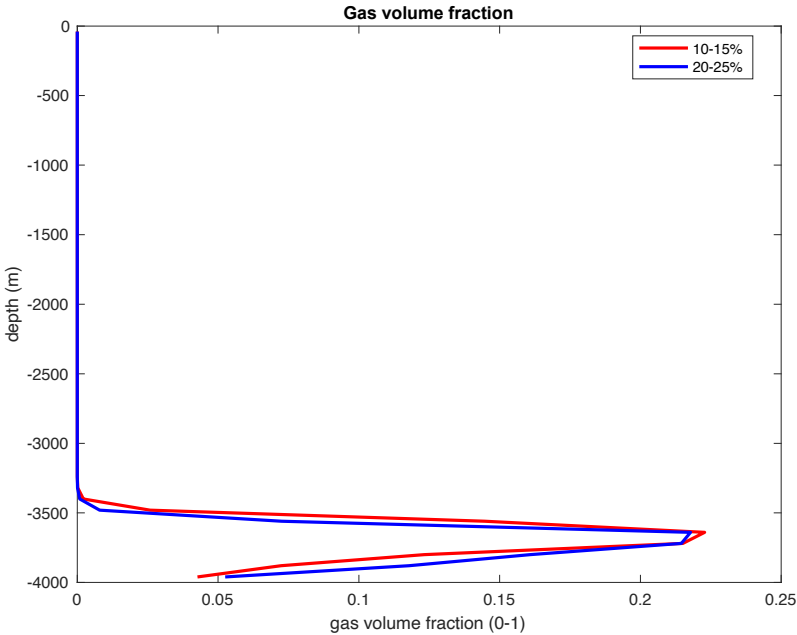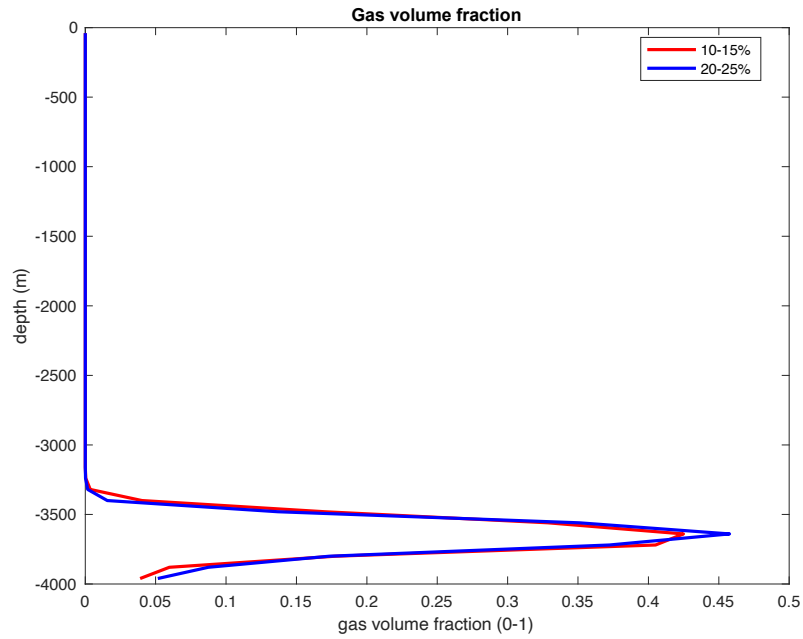
Figure 5.71 Gas volume fraction depth profiles at 600 s for varying transition zones, 8 m³ kick
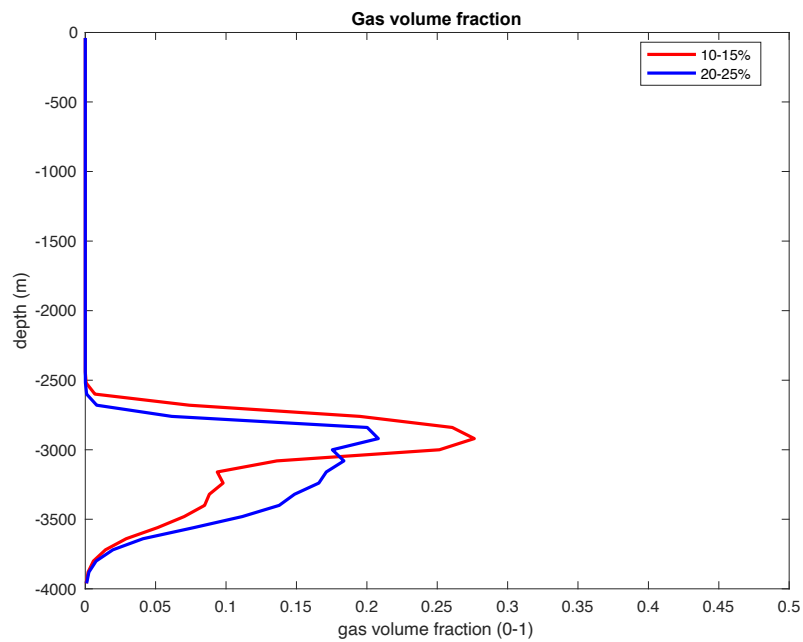
Figure 5.72 Gas volume fraction depth profiles at 2 000 s for varying transition zones, 8 m³ kick

The gas velocity figure (Figure 5.73) shows that both gas kicks exist in the slug flow regime at 1 000 s. The pressure build up shown in Figure 5.70 showed that they indeed migrated at the same velocities since the pressure build up slope is the same, but at 2 000 s, the pressure build up slopes are different.
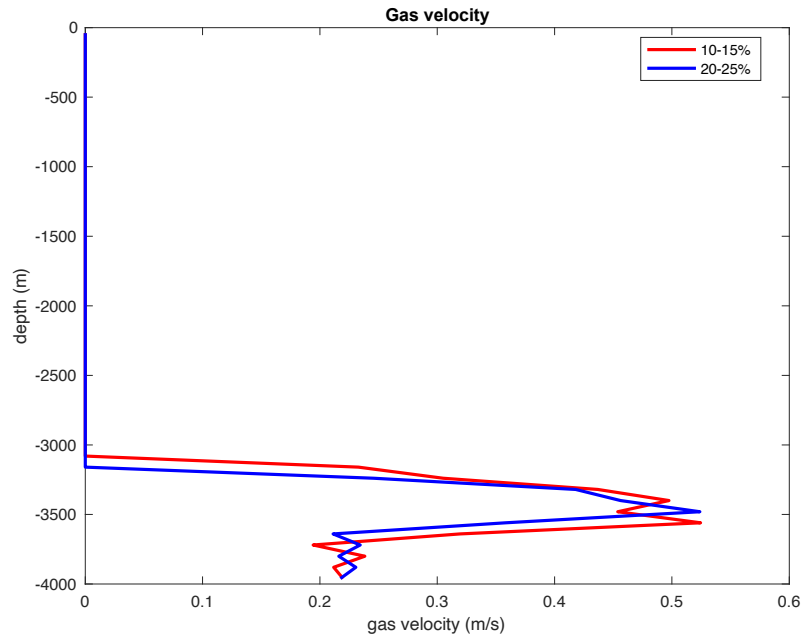
Figure 5.73 Gas velocity in well at 1 000 s for varying transition zones, 8 m³ kick

Figure 5.74 shows that the gas velocity of the kick with the low transition interval still moves as slugs at 2 000 s, while the kick with the high transition zone is mainly in the bubble flow regime with a very small section entering the transition zone between bubble and slug flow. This manifested in the small spike in the gas velocity. Since smaller gas fractions are needed to form slugs and slugs move at higher velocities than bubbles, the kick with the low transition zone is moving faster.
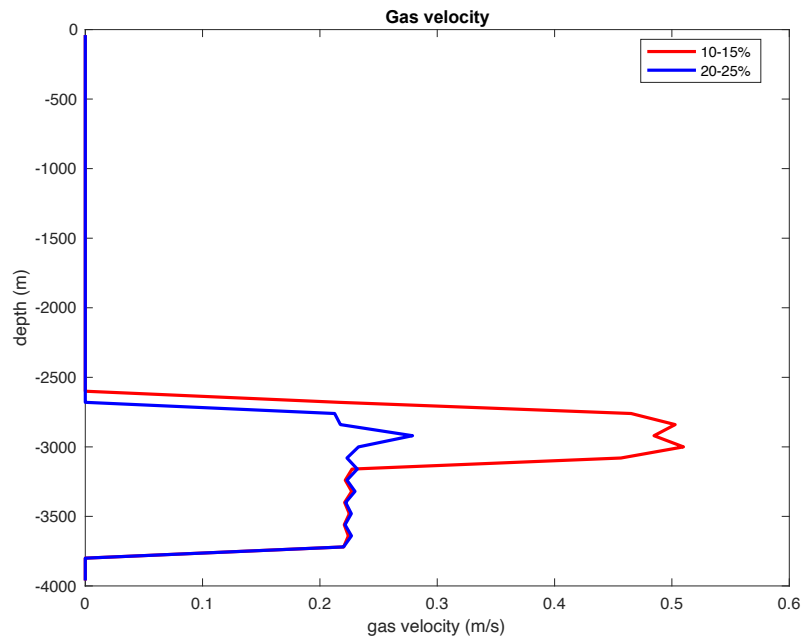
Figure 5.74 Gas velocity in well at 2 000 s for varying transition zones, 8 m³ kick

However, with a higher gas migration velocity, the gas fraction is also reduced faster since the kick is stretched out. Figure 5.75 shows that the gas velocity of the low transition zone is reduced towards the same value as the high transition zone at 4 000 s. At this stage, it was shown in Figure 5.70 that the pressure gradients were basically the same. Now the kicks are migrating with the same velocity and they will remain in the bubble flow regime until they reach surface. In the end, the pressures will stabilize at the same levels, but the kick with the low transition zone will reach surface first since slug flow was present for a longer time in the early part of the simulation.
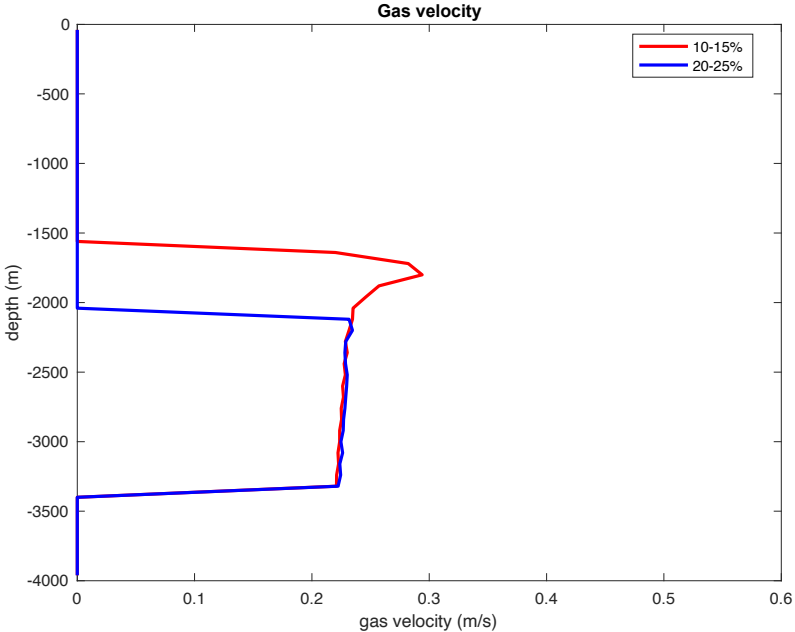
Figure 5.75 Gas velocity in well at 4 000 s for varying transition zones, 8 m³ kick

If suspension effects were considered, the pressure curves would look like the ones in Figure 5.76. In these simulations, all kicks reached the BOP. Although they stabilize to the same values almost independent of bubble-slug transition zone, the pressure build up curves for the low transition intervals stabilizes first indicating earlier kick arrival at the BOP. Table 5.11 summarizes some of the simulations results.
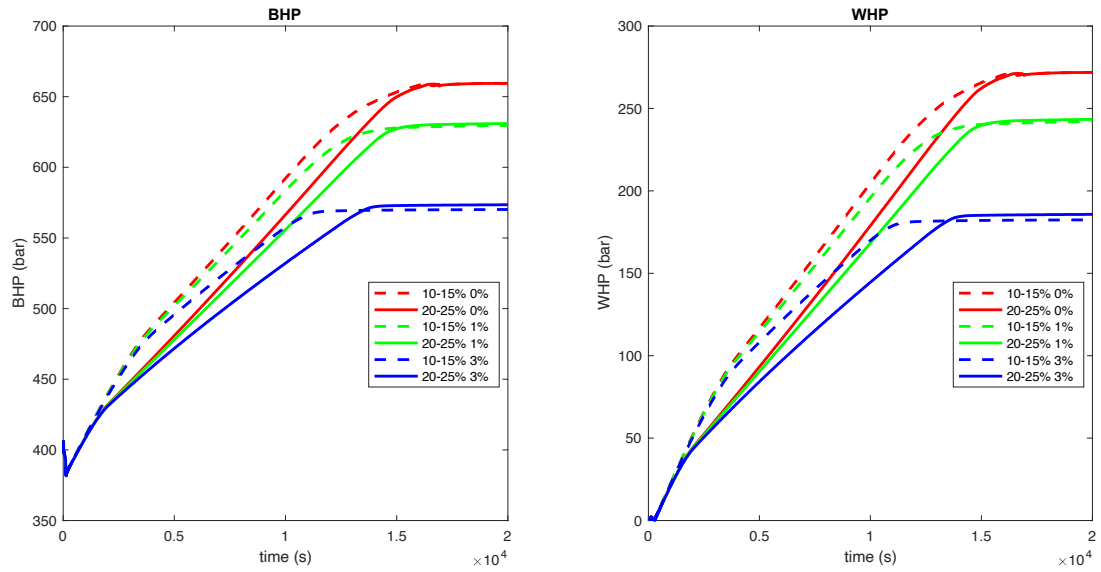
Figure 5.76 Pressure build up in well for varying transition zones and varying suspension limits, 8 m³ kick

Transition zone [%]	Suspension limits [%]	Final BHP [bars]	Final WHP [bars]	Stabilization time [s]
10-15	0	659	272	17 000
10-15	1	631	243	15 000
10-15	3	573	186	14 000
20-25	0	659	272	16 000
20-25	1	631	243	14 000
20-25	3	573	186	11 000

Table 5.11 Transition zones, suspension limits, final BHP, final WHP, and pressure stabilization time, 8 m³ kick

Figure 5.77 and Figure 5.78 show the gas volume fractions taken at 4 000 s and 10 000 s. The kick of the high transition zone migrates from 2 600 m to 1 320 m, i.e. S_{avg}=0.21 m/s in this time interval. The kick of the low transition zone moves from 1 720 m to roughly 500 m, and S_{avg}=0.20 m/s. In this time interval, both kick bulks are in the bubble flow regime, also shown in Figure 5.77 and Figure 5.78. However, if the pressure slopes (Figure 5.76) are used to estimate the gas migration velocities in this interval, the S_{avg}-values would not be the same, as the slopes are affected by suspension. The pressure build up slopes are highly reduced for the cases where suspension effects are considered.
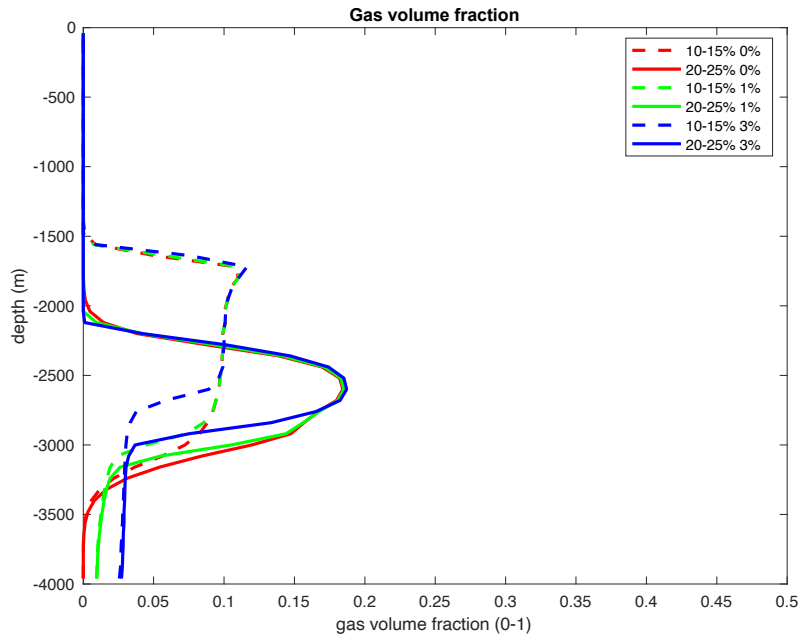
Figure 5.77 Gas volume fraction depth profiles at 4 000 s for varying transition zones and varying suspension limits, 8 m³ kick
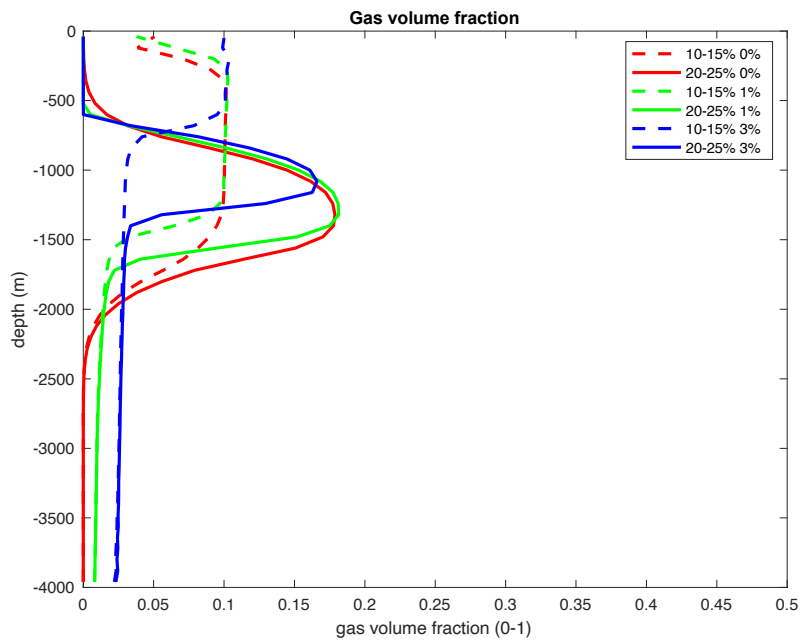
Figure 5.78 Gas volume fraction depth profiles at 10 000 s for varying transition zones and varying suspension limits, 8 m³ kick

In case 6, it has been shown that average gas migration velocities can be calculated using gas volume fraction depth profiles at relevant time stages. Here, one can note that the result can depend on which time stages (indirectly kick position) that are chosen since there can be transition from one flow regime to another in that interval. An important discovery was that if the gas migration velocity is based on information about the slope of the pressure build up, the

93

calculated gas migration velocities would be incorrect as the pressure slopes are highly affected by suspension effects. In some cases, e.g. 3% suspension for a 4 m^3 kick volume, the pressure curve gave no indications that the gas became fully suspended and that the kick migration stopped. However, the simulated gas volume fraction depth profiles confirmed this (Figure 5.68). It was seen that estimating gas migration velocities can be complicated as they are dependent on several parameters. The transient flow model is able to capture these dependencies and describe the behavior of the gas volume.

5.7.   Case 7 – Interpolation from Slug Flow to One-phase Gas

In case 7, the effect of varying the interpolation limits from slug flow to one-phase gas on pressure build up is studied. The interpolation limits are implemented in order for the drift flux model to be mathematically applicable to the gas slip relation. The gas fraction where slug flow approaches one-phase gas is obtained by rewriting the gas slip equation as below

$$v_g = \frac{Kv_l\alpha_l + S}{(1 - K\alpha_g)}$$

The gas slip relation cannot be calculated for K=1.2 and gas fractions around 0.83 since the equation would be undefined when dividing by zero. The numerical scheme interpolates towards one-phase gas before reaching this value, which returns a no slip condition where K=1.0 and S=0 m/s. In [7], K was interpolated to 1.0 m/s in the interval [0.7,0.8] and S was interpolated to 0 m/s in the interval [0.9,1.0], hereby called *case 1*. K will also be interpolated in the interval [0.6,0.8] and S in the interval [0.6,1.0], hereby called *case 2*. Furthermore, a 3% suspension value will be used, and slug flow starts from gas fractions of 20-25%, i.e. Newtonian drilling fluids are considered.

Since the length of the well is assumed 4 000 m, the outer diameter is 12 ¼", and the inner diameter is 5", the well volume is 253 m^3. In this case, the initial gas volume of 4 m^3 was too small to demonstrate any effect on pressure build up since the gas fraction initially was far below the transition zone under evaluation. With a small kick volume, the pressure plots showed no difference between case 1 and case 2. As seen on the previous gas volume fraction depth profiles taken at 4 000 s, the gas bulk is between 0.10 to 0.15, which is far below the gas fraction of 0.83. The gas expansion is also very low in a closed, static well. The only time one will obtain gas volume fraction close to 1 is when the gas starts to accumulate in the upper cells. So, to study the effects of interpolation to one-phase gas on pressure build up, a larger kick volume must be introduced to introduce a larger gas fraction initially that touches the interpolation borders. In case 7, the gas rate was increased to 46 kg/s to introduce 12 m^3 of gas to the system.

95

The simulation results are shown below. The differences are not large. If Figure 5.79 is inspected, it can look like the kick in case 2 has moved slightly less in the initial part of the simulation when the gas volume fraction is large. The slip parameters used in case 2 will cause an earlier transition to one-phase gas for high gas volume fraction and this will reduce the speed of the gas kick slightly.
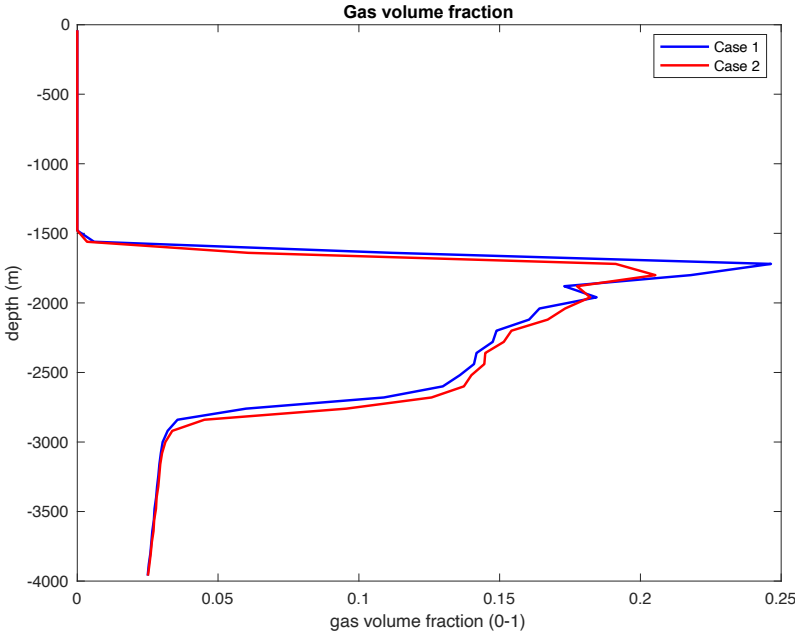
Figure 5.79 Gas volume fraction depth profiles at 4 000 s for varying interpolation limits,12 m^3 kick

This initial slight difference in velocities can also have led to a change in gas distribution later (4 000 s) such that the transition from slug to bubble flow will not happen at the identical same time. Hence, a small phase shift will occur from approximately 4 000 s as seen in Figure 5.80. But the main result seems to be that the kick for case 1 will reach the surface slightly faster than for case 2 (Figure 5.81). This is reasonable since case 1 represents the situation where slug flow persist longer for higher gas volume fractions and the S-value is largest for pure slug flow, which is seen in Figure 5.82.
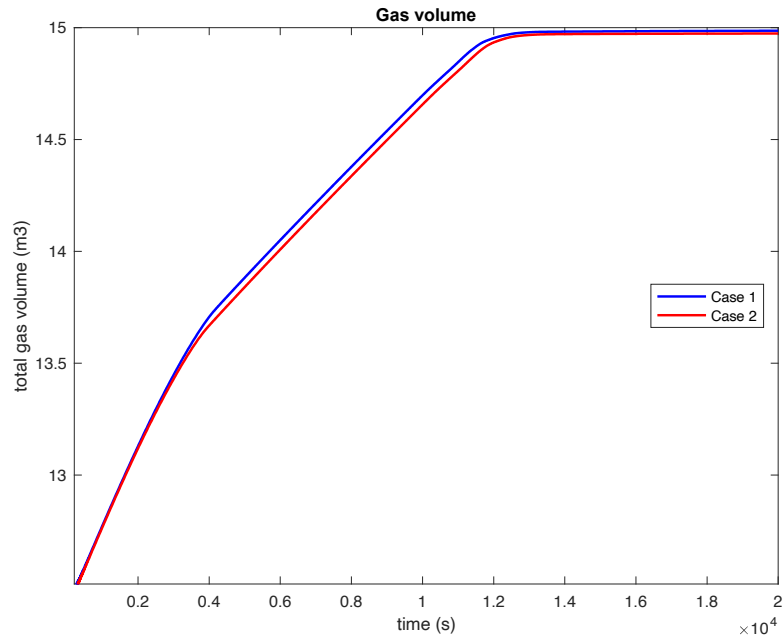
Figure 5.80 Gas volume when kick is migrating upwards in a closed well for varying interpolation limits,12 m³ kick
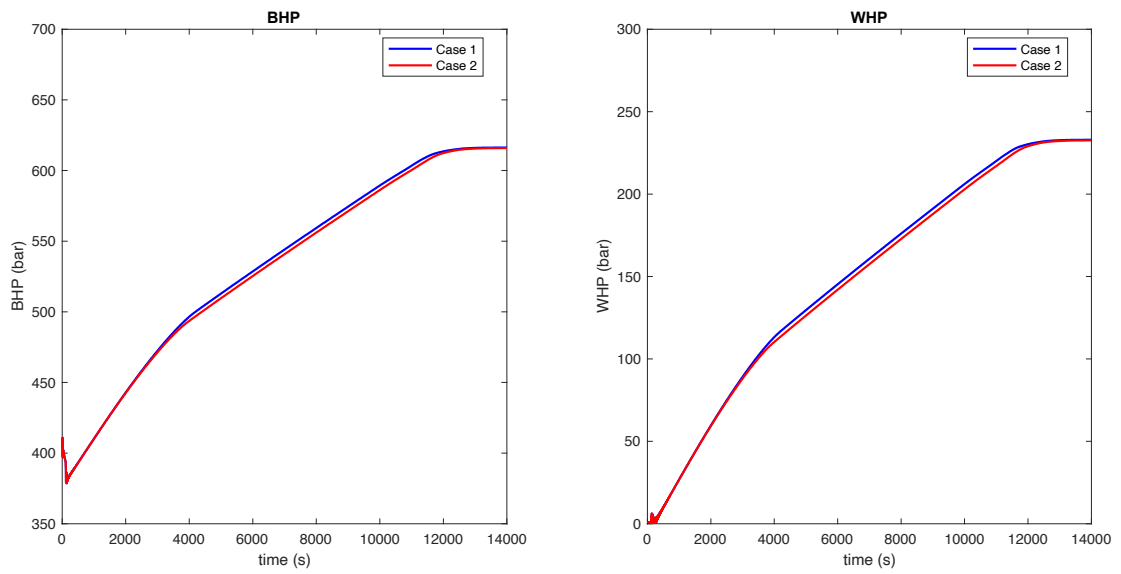
Figure 5.81 Pressure build up in well for varying interpolation limits,12 m³ kick

The small difference in pressure stabilization times between interpolating using case 1 and case 2 is clearly shown in Figure 5.82, which shows the gas velocity at 4 000 s. At around 1 750 m, the gas velocity is S=0.45 m/s for case 1, which is a value between bubble and slug flow. However, the gas velocity of case 2 is approximately S=0.23 m/s, which is the gas velocity for bubble flow; hence, the kick of case 1 will reach surface faster. For a short interpolation interval, i.e. case 1, the gas migration velocity is higher as slug flow persists longer.
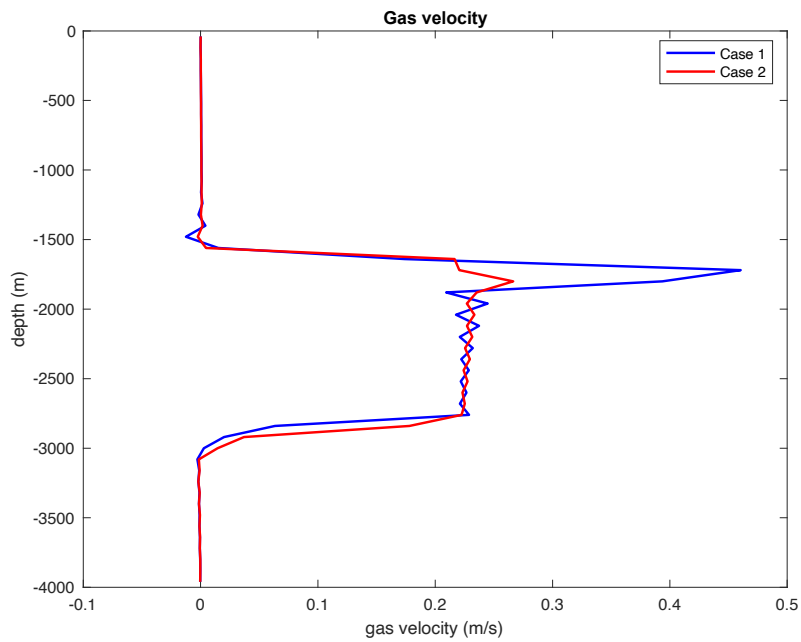
Figure 5.82 Gas velocity in well at 4 000 s for varying interpolation limits, 12 m³ kick

6. Conclusion and Future Work

6.1. Conclusion

A new model has been used to study kick migration in a closed well. The model incorporates a gas slip model taking into account both suspension effects, bubble flow, and slug flow. Modelling assumptions, numerical approximations, and kick sizes have been varied to study the pressure buildup for a migrating kick.

Although the effect of different parameters on pressure buildup was studied by varying the parameters separately, it was seen that the pressure buildup is dependent on several parameters simultaneously. The transient flow model is able to capture these dependencies. Simulation results showed that the pressures are affected by both modelling assumptions, numerical approximations, and what physical effect that is causing the measured effects related to the pressures, i.e. how fast the pressures increase, when the final pressures are reached, and at what final pressure levels they will stabilize.

In case 1, different techniques of handling the slope limiters in the boundary cells were studied. They cannot be calculated in the same way as for the interior numerical cells. Simulation results showed that the pressure vs depth profiles were more accurate when the slope limiters were copied from the closest neighbor cell rather than set to zero, but mass conservation problems were encountered in the boundary cells. This is a fundamental flaw. Previously, it was found that a gas mass conservation problem was omitted by setting the slope limiter related to the gas volume fraction to zero in the outlet boundary cell [9]. It was shown in case 1 that the liquid mass conservation problem was omitted when the slope limiter for gas volume fraction also was set to zero in the inlet boundary cell. It is recommended to copy the slope limiters from the closest neighbour cells for most accurate results, but the slope limiters in the boundary cells related to the gas volume fraction should both be set to zero to avoid mass conservation problems.

To ensure that the new model would provide the optimal results, numerical diffusion was studied in case 2. It was seen that the numerical diffusion was reduced when increasing the number of cells from 25 to 50, and even more accurate results were obtained when increasing the number of cells from 50 to 100 cells. However, the computational time was significantly increased as the grid was refined; thus, it was recommended to simulate using a grid of 50 cells

as the simulation results converged towards an acceptable solution. Numerical diffusion was still observed throughout the simulation study, e.g. locating the kick front accurately for the calculation of average gas migration velocities was challenging. Despite this, a grid of 50 cells was sufficient for the purpose of this thesis, which was to identify the influence of different modelling assumptions, numerical approximations, and physical effects on pressure build up. For even more accurate results, one might consider using a grid of 100 cells despite the increased computational time.

In case 3, the old model and the new model were compared to show that the new model is able to display different gas velocities for different flow regimes. The old model was based on using constant slip parameters in the gas slip relation; K and S had values typical for slug flow. In the new model, different flow regimes were included, i.e. suspended flow, bubble flow, and slug flow. Using three different gas kick sizes, it was shown that the new model is able to predict flow pattern transitions based on the pressure build up slopes, i.e. when the pressure build up changed abruptly, the flow pattern transition occurred. For the larger kick sizes, this was quite evident. The kick started migrating in slug flow with a steeper pressure build up slope. Then, it transitioned to bubble flow with a less steep pressure build up slope. In general, the new model estimated that it would take longer time for the gas kicks to reach surface than what was seen with the old model. This was due to presence of different flow patterns, and the prevailing flow regime in the kick migration simulations was the bubble flow regime. The gas migrates slower in bubble flow compared to slug flow.

It was shown in case 4 that using the slope of the pressure build up to estimate gas migration velocities was an unreliable approach. Simulation results disclosed that suspension effects would reduce the slopes of the pressure build up. The value of the final pressure after stabilization also became lower for increasing suspension limits. In cases where substantial suspension effects were considered, it was seen that the pressure stabilized at quite early stages to relatively low final pressures. Two implications from the simulation results could indicate that the gas kick had become fully suspended and stopped migrating in the well: a significant drop in the WHP compared to lower suspension limits and earlier pressure stabilization time (Table 5.5). Gas volume fraction depth profiles taken at relevant stages could reveal that the gas kick was fully suspended in the well in these cases. For the cases where the gas kicks were able to migrate, the gas kick bulks migrated at the same velocity if they were in the same flow regime despite the varying degree of suspension which affected the slope of the pressure build

up. In fact, Table 5.6 showed that the gas migration velocity varied depending on what time interval was considered. This is caused by flow regime transitions. The importance of sensor locations for accurate prediction of gas migration velocities was highlighted. It is reasonable to conclude that it is impossible to approximate a unique gas migration velocity from different pressure build up slopes.

The transition interval from full suspension to fully developed bubble flow was studied in case 5. For the wider transition interval, mobile gas was observed behind the gas kick bulk. In this transition interval, the gas migrated more slowly, resulting in slightly reduced pressure build up slopes compared to a low transition interval. The transition interval neither affected the location where the kick eventually became fully suspended nor the time it took for the gas kicks to reach surface.

In case 6, where the transition zone from bubble to slug flow was studied, a steeper pressure build up slope was seen for a low transition zone at early stages. This was because more slug flow was present when lowering the transition interval. Hence, a phase shift in the pressure build up curves occurred quite early in the simulation when comparing the two transition intervals. For the remaining stages of the simulation, the slope of the pressure build up was the same as the one for a high transition zone, indicating that the gas volume fraction of the kick with low transition zone was reduced such that transition to bubble flow took place. The gas volume fraction was reduced since the kick was stretched out with different parts of the kick moving with different velocities. Calculations based on the gas volume fractions taken at early stages revealed a higher gas migration velocity for a low transition zone than for a high transition zone. Hence, the kick moved longer up in the well in the initial stage of the simulation compared to the case where a high transition zone was considered. Following these stages, the gas migration velocities of the gas kicks that still migrated were the same for both transition zones. But the kicks using the low transition zone reached the surface slightly faster due to the initial differences in gas migration. This case also emphasized that the location where sensors are placed are quite important in predicting accurate gas migration velocities.

For the last case, where the interpolation interval from slug flow to one-phase gas was studied, it was seen that the pressure build up in a closed well was not significantly affected by using a wider interval. The main difference was that for the kick with the shorter interpolation interval, i.e. case 1, slug flow persisted for a longer time, enabling it to migrate slightly faster to surface

compared to the wider interpolation interval, i.e. case 2. However, the difference was only present for a large kick size. For a closed well, the difference in pressure build up between using a short interpolation interval and a wider interpolation interval was marginal, but as seen in the gas velocity plot (Figure 5.82), the shorter interpolation interval (case 1) would estimate the variations in the gas velocity more accurately.

In general, it was demonstrated that there is no contradiction between field measurements and simulation results, but it all depends on what one actually measures and what physical effect that is causing the measured effects.

6.2.   Future Work

For the simulation work conducted in this thesis, a closed vertical well of constant geometry was considered for simplicity. The main goal of this thesis was to isolate the different effects in order to study their influence on pressure build up slopes. For further studies, it would be beneficial to repeat the simulation work also considering different well geometries in order to extend the numerical scheme towards real-scale situations. For example, the gas slip model can become more advanced by taking into account corrections for annular geometry and inclination effects, as described in [16]. The corrections are implemented in the code given in Appendix B, but they were not used for the simulation work in this thesis. There is potential that further simulation work using the new model and considering different annular geometries and inclination effects can disclose less inconsistency between field measurements and simulation results.

References

[1]   T. Azwell *et al.*, "The Macondo Blowout Environmental Report," University of California, Berkeley, Jan. 2011.

[2]   H. Jones, "Crude Oil and Produced Water Leak Into Lake Texoma," *NBCDFW*, Aug. 11, 2019. https://www.nbcdfw.com/news/local/crude-oil-and-produced-water-leak-into-lake-texoma/2111678/. (Accessed Mar. 26th, 2020).

[3]   T. Jacobs, "Early Kick Detection: Testing New Concepts," *J. Pet. Technol.*, vol. 67, no. 08, Jan. 2015, [Online]. Available: https://pubs.spe.org/en/jpt/jpt-article-detail/?art=1159.

[4]   K. K. Fjelde and S. Evje, "The AUSMV Scheme - A Simple but Robust Model for Analyzing Two-Phase Flow." University of Stavanger, 2010.

[5]   S. Ekrann and R. Rommetveit, "A Simulator for Gas Kicks in Oil-Based Drilling Muds," in *SPE Annual Technical Conference and Exhibition*, Las Vegas, Nevada, 1985, doi: 10.2118/14182-MS.

[6]   H. Shi *et al.*, "Drift-Flux Modeling of Two-Phase Flow in Wellbores," *SPE J.*, vol. 10, no. 01, pp. 24–33, Mar. 2005, doi: 10.2118/84228-PA.

[7]   K. K. Fjelde, J. Frøyen, and A. A. Ghauri, "A Numerical Study of Gas Kick Migration Velocities and Uncertainty," in *SPE Bergen One Day Seminar*, Grieghallen, Bergen, Norway, 2016, doi: 10.2118/180053-MS.

[8]   D. Gomes, K. S. Bjørkevoll, K. K. Fjelde, and J. Frøyen, "Numerical Modelling and Sensitivity Analysis of Gas Kick Migration and Unloading of Riser," in *Volume 8: Polar and Arctic Sciences and Technology; Petroleum Technology*, Glasgow, Scotland, UK, Jun. 2019, p. V008T11A033, doi: 10.1115/OMAE2019-95214.

[9]   K. Roxman, "Boundary Condition Treatment in a Transient Flow Model," M.S. thesis, Dept. Petroleum Eng., University of Stavanger, Norway, 2019.

[10]   A. Johnson, I. Rezmer-Cooper, T. Bailey, and D. McCann, "Gas Migration: Fast, Slow or Stopped," presented at the SPE/IADC Drilling Conference, Jan. 1995, doi: 10.2118/29342-MS.

[11]   A. B. Johnson and J. A. Tarvin, "Field calculations underestimate gas migration velocities," presented at the IADC European Well Control Conference, 1993.

[12]   R. Gonzalez, J. Shaughnessy, and W. D. Grindle, "Industry leaders shed light on drilling riser gas effects," *OGJ*, vol. 98, no. 29, pp. 42–46, July 17th, 2000.

[13]   D. W. Rader, A. T. Bourgoyne, and R. H. Ward, "Factors Affecting Bubble-Rise Velocity Of Gas Kicks," *J. Pet. Technol.*, vol. 27, no. 05, pp. 571–584, May 1975, doi:

10.2118/4647-PA.

[14]   R. Rommetveit *et al.*, "Ultra-Deepwater Hydraulics and Well Control Tests with Extensive Instrumentation: Field Tests and Data Analysis," *SPE Drill. Complet.*, vol. 20, no. 04, pp. 251–257, Dec. 2005, doi: 10.2118/84316-PA.

[15]   H. V. Nickens, "A Dynamic Computer Model of a Kicking Well," *SPE Drill. Eng.*, vol. 2, no. 02, pp. 159–173, Jun. 1987, doi: 10.2118/14183-PA.

[16]   A. R. Hasan, C. S. Kabir, and M. Sayarpour, "A Basic Approach to Wellbore Two-Phase Flow Modeling," in *SPE Annual Technical Conference and Exhibition*, Anaheim, California, USA., 2007, doi: 10.2118/109868-MS.

[17]   J. Bysveen, B. Fossli, P. C. Stenshorne, G. Skärgård, and L. Hollman, "Planning of an MPD and Controlled Mud Cap Drilling CMCD Operation in the Barents Sea Using the CML Technology," in *IADC/SPE Managed Pressure Drilling & Underbalanced Operations Conference & Exhibition*, Rio de Janeiro, Brazil, 2017, doi: 10.2118/185286-MS.

[18]   O. Kaldirim and J. J. Schubert, "Experimental setup at Texas A&M Dual Gradient Drilling Lab aims to study riser gas migration in controlled mud level drilling system," *Drilling Contractor*, Oct. 03, 2017. https://www.drillingcontractor.org/experimental-setup-at-texas-am-dual-gradient-drilling-lab-aims-to-study-riser-gas-migration-in-controlled-mud-level-drilling-system-41811. (Accessed Mar. 28th, 2020).

[19]   W. L. Lloyd, M. D. Andrea, and J. R. Kozicz, "New Considerations for Handling Gas in a Deepwater Riser," in *IADC/SPE Drilling Conference*, New Orleans, Louisiana, USA, 2000, doi: 10.2118/59183-MS.

[20]   P. R. Erb, T.-C. Ma, and M. P. Stockinger, "Riser Collapse A Unique Problem in Deep-Water Drilling," in *IADC/SPE Drilling Conference*, New Orleans, Louisiana, USA, 1983, doi: 10.2118/11394-MS.

[21]   H. Shi *et al.*, "Drift-Flux Modeling of Two-Phase Flow in Wellbores," *SPE J.*, vol. 10, no. 01, pp. 24–33, Mar. 2005, doi: 10.2118/84228-PA.

[22]   E. Al-Safran, C. Kora, and C. Sarica, "Prediction of Liquid Volume Fraction in Slugs in Two-Phase Horizontal Pipe Flow With High Viscosity Liquid," presented at the 16th International Conference on Multiphase Production Technology, Jun. 2013, Accessed: Feb. 26, 2020. [Online]. Available: https://www.onepetro.org/conference-paper/BHR-2013-H4.

[23]   D. H. Beggs and J. P. Brill, "A Study of Two-Phase Flow in Inclined Pipes," *J. Pet. Technol.*, vol. 25, no. 05, pp. 607–617, May 1973, doi: 10.2118/4007-PA.

[24]   N. Zuber and J. A. Findlay, "Average Volumetric Concentration in Two-Phase Flow Systems," *J. Heat Transf.*, vol. 87, no. 4, pp. 453–468, Nov. 1965, doi: 10.1115/1.3689137.

[25]   J. Choi, E. Pereyra, C. Sarica, C. Park, and J. Kang, "An Efficient Drift-Flux Closure Relationship to Estimate Liquid Holdups of Gas-Liquid Two-Phase Flow in Pipes," *Energies*, vol. 5, no. 12, pp. 5294–5306, Dec. 2012, doi: 10.3390/en5125294.

[26]   H.-Q. Zhang, Q. Wang, C. Sarica, and J. P. Brill, "Unified Model for Gas-Liquid Pipe Flow via Slug Dynamics—Part 1: Model Development," *J. Energy Resour. Technol.*, vol. 125, no. 4, pp. 266–273, Dec. 2003, doi: 10.1115/1.1615246.

[27]   S. Wang, H.-Q. Zhang, C. Sarica, and E. Pereyra, "A Mechanistic Slug-Liquid-Holdup Model for Different Oil Viscosities and Pipe-Inclination Angles," *SPE Prod. Oper.*, vol. 29, no. 04, pp. 329–336, Nov. 2014, doi: 10.2118/171563-PA.

[28]   N. Petalas and K. Aziz, "A Mechanistic Model For Multiphase Flow In Pipes," in *Annual Technical Meeting*, Calgary, Alberta, Canada, 1998, doi: 10.2118/98-39.

[29]   K. K. Fjelde, R. Rommetveit, A. Merlo, and A. C. V. M. Lage, "Improvements in Dynamic Modeling of Underbalanced Drilling," in *IADC/SPE Underbalanced Technology Conference and Exhibition*, Houston, Texas, USA, 2003, doi: 10.2118/81636-MS.

[30]   Z. Liu, R. Liao, W. Luo, Y. Su, and J. X. F. Ribeiro, "A New Model for Predicting Slug Flow Liquid Holdup in Vertical Pipes with Different Viscosities," *Arab. J. Sci. Eng.*, Feb. 2020, doi: 10.1007/s13369-019-04308-5.

[31]   Y. Taitel, D. Bornea, and A. E. Dukler, "Modelling flow pattern transitions for steady upward gas-liquid flow in vertical tubes," *AIChE J.*, vol. 26, no. 3, pp. 345–354, May 1980, doi: 10.1002/aic.690260304.

[32]   C. E. Lacy, "Applicability of Slug Flow Models to Heavy Oils," in *SPE Heavy Oil Conference Canada*, Calgary, Alberta, Canada, 2012, doi: 10.2118/147114-MS.

[33]   A. C. V. M. Lage and R. W. Time, "An Experimental and Theoretical Investigation of Upward Two-Phase Flow in Annuli," in *SPE Asia Pacific Oil and Gas Conference and Exhibition*, Brisbane, Australia, 2000, doi: 10.2118/64525-MS.

[34]   L. E. Gomez, O. Shoham, Z. Schmidt, R. N. Chokshi, and T. Northug, "Unified Mechanistic Model for Steady-State Two-Phase Flow: Horizontal to Vertical Upward Flow," *SPE J.*, vol. 5, no. 03, pp. 339–350, Sep. 2000, doi: 10.2118/65705-PA.

[35]   R. N. Chokshi, Z. Schmidt, and D. R. Doty, "Experimental Study and the Development of a Mechanistic Model for Two-Phase Flow Through Vertical Tubing," in *SPE Western Regional Meeting*, Anchorage, Alaska, USA, 1996, doi: 10.2118/35676-MS.

[36]   D. Barnea, "A unified model for predicting flow-pattern transitions for the whole range of pipe inclinations," *Int. J. Multiph. Flow*, vol. 13, no. 1, pp. 1–12, Jan. 1987, doi: 10.1016/0301-9322(87)90002-4.

[37]   Y. Taitel and A. E. Dukler, "A model for predicting flow regime transitions in horizontal and near horizontal gas-liquid flow," *AIChE J.*, vol. 22, no. 1, pp. 47–55, Jan. 1976, doi: 10.1002/aic.690220105.

[38]   J. J. Xiao, O. Shonham, and J. P. Brill, "A Comprehensive Mechanistic Model for Two-Phase Flow in Pipelines," in *SPE Annual Technical Conference and Exhibition*, New Orleans, Louisiana, USA, 1990, doi: 10.2118/20631-MS.

[39]   J. E. Julia and T. Hibiki, "Flow regime transition criteria for two-phase flow in a vertical annulus," *Int. J. Heat Fluid Flow*, vol. 32, no. 5, pp. 993–1004, Oct. 2011, doi: 10.1016/j.ijheatfluidflow.2011.06.001.

[40]   P. W. James, N. S. Wilkes, W. Conkie, and A. Burns, "Developments in the modelling of horizontal annular two-phase flow," *Int. J. Multiph. Flow*, vol. 13, no. 2, pp. 173–198, Mar. 1987, doi: 10.1016/0301-9322(87)90028-0.

[41]   N. Singhal, S. N. Shah, and S. Jain, "Friction Pressure Correlations for Newtonian and Non-Newtonian Fluids in Concentric Annuli," in *SPE Production Operations Symposium*, Oklahoma City, Oklahoma, USA, 2005, doi: 10.2118/94280-MS.

[42]   W. Kozicki, C. H. Chou, and C. Tiu, "Non-Newtonian flow in ducts of arbitrary cross-sectional shape," *Chem. Eng. Sci.*, vol. 21, no. 8, pp. 665–679, Aug. 1966, doi: 10.1016/0009-2509(66)80016-7.

[43]   T. D. Reed and A. A. Pilehvari, "A New Model for Laminar, Transitional, and Turbulent Flow of Drilling Muds," in *SPE Production Operations Symposium*, Oklahoma City, Oklahoma, USA, 1993, doi: 10.2118/25456-MS.

[44]   D. W. Dodge and A. B. Metzner, "Turbulent flow of non-newtonian systems," *AIChE J.*, vol. 5, no. 2, pp. 189–204, Jun. 1959, doi: 10.1002/aic.690050214.

[45]   J. E. Udegbunam, K. K. Fjelde, S. Evje, and G. Nygaard, "On the Advection-Upstream-Splitting-Method Hybrid Scheme: A Simple Transient-Flow Model for Managed-Pressure-Drilling and Underbalanced-Drilling Applications," *SPE Drill. Complet.*, vol. 30, no. 02, pp. 098–109, Jun. 2015, doi: 10.2118/168960-PA.

[46]   Y. Wang, H. Fu, L. Yang, S. Wang, H. Liang, and K. Ling, "STUDY THE BOUNDARY OF TWO-PHASE FLOW REGIME FROM BUBBLE TO SLUG FLOW," in *Proceeding of 4th Thermal and Fluids Engineering Conference*, Las Vegas, NV, USA, 2019, pp. 965–980, doi: 10.1615/TFEC2019.fmi.027622.

[47]   M. S. Capovilla, R. P. Coutinho, P. C. de Sousa, and P. J. Waltrich, "Experimental investigation of upward vertical two-phase high-velocity flows in large-diameter pipes," *Exp. Therm. Fluid Sci.*, vol. 102, pp. 493–505, Apr. 2019, doi:

10.1016/j.expthermflusci.2018.12.024.

[48] E. F. Caetano, "Upward Two-Phase Flow Through an Annulus," Ph.D. dissertation, University of Tulsa, Oklahoma, USA, 1985.

[49] T. Z. Harmathy, "Velocity of large drops and bubbles in media of infinite or restricted extent," *AIChE J.*, vol. 6, no. 2, pp. 281–288, Jun. 1960, doi: 10.1002/aic.690060222.

[50] V. C. Kelessidis and A. E. Dukler, "Modeling flow pattern transitions for upward gas-liquid flow in vertical concentric and eccentric annuli," *Int. J. Multiph. Flow*, vol. 15, no. 2, pp. 173–191, Apr. 1989, doi: 10.1016/0301-9322(89)90069-4.

[51] A. B. Johnson and D. B. White, "Gas-Rise Velocities During Kicks," *SPE Drill. Eng.*, vol. 6, no. 04, pp. 257–263, Dec. 1991, doi: 10.2118/20431-PA.

[52] S. Evje and K. K. Fjelde, "Hybrid Flux-Splitting Schemes for a Two-Phase Flow Model," *J. Comput. Phys.*, vol. 175, no. 2, pp. 674–701, Jan. 2002, doi: 10.1006/jcph.2001.6962.

[53] S. Benzoni-Gavage, "Analyse Numerique des Modèles Hydrodynamiques d'Ecoulements Diphasique Instationnaires dans les Réseaux de Production Pétrolière," These, ENS, Lyon, France, 1991.

Appendices

Appendix A

The mathematical model and code used in this thesis was provided by the faculty supervisor. It is based on previous work in [7] and [8]. In [7], a gas slip model based on constant slip parameters was used. In [8], the gas slip model was extended to cover different flow regimes and suspension effects. The focus of the latter paper was unloading of riser scenarios. In this work, the focus was on pressure build up in a closed well when having a migrating kick. The same density models were used. This acknowledgement also applies to Appendix B and D.

The MATLAB code used in case 1 (the old model) is provided below. It is essentially the same model as used in [7]. The red text color indicates new element(s) implemented during the work of this thesis.

```
% Transient two-phase code based on AUSMV scheme: Gas and Water
% The code assumes uniform geometry

% time - Seconds

% p - pressure at new time level (Pa)
% dl - density of liquid at new time level (kg/m3)
% dg - density of gas at new time level (kg/m3)
% eg - phase volume fraction of liquid at new time level (0-1)
% ev - phase volume fraction og gas at new time level (0-1)
% vg - phase velocity of gas at new time level (m/s)
% vl - phase velocity of liquid at new time level (m/s)
% qv - conservative variables at new time level  ( 3 in each cell)
% temp - temperature in well (K)

% po - pressure at old time level (Pa)
% dlo - density of liquid at old time level (kg/m3)
% dgo - density of gas at new old level (kg/m3)
% ego - phase volume fraction of liquid at old time level (0-1)
% evo - phase volume fraction og gas at old time level (0-1)
% vgo - phase velocity of gas at old time level (m/s)
% vlo - phase velocity of liquid at old time level (m/s)
% qvo - conservative variables at old  time level  ( 3 in each cell)
% temp - temperature in well (K)

clear;
t = cputime
tic,

% Geometry data/ Must be specified
welldepth = 4000;
nobox = 25; % Number of boxes in the well; 25, 50, or 100 boxes

% Note that one can use more refined grid, 50, 100 boxes.
% When doing this, remember to reduce time step to keep the CFL number
```

108

```matlab
% fixed below 0.25.. dt < cfl x dx/ speed of sound in water. If boxes are
% doubled, then half the time step.

nofluxes = nobox+1;  % Number of cell boundaries
dx = welldepth/nobox; % Boxlength
%dt = 0.005;

% Welldepth. Cell 1 start at bottom
x(1)= -1.0*welldepth+0.5*dx;
for i=1:nobox-1
 x(i+1)=x(i)+ dx;
end

% VERY IMPORTANT: BELOW THE TIMESTEP IS SET. MAKE SURE THAT THE
% CFL CONDIDTION IS FULFILLED. IF NUMBER OF BOXES IS CHANGED. DX WILL
% CHANGE AND DT HAS TO BE ADJUSTED TO KEEP THE CFL NUMBER FIXED.

dt= 0.02;  % Timestep (seconds); 0.02, 0.01, 0.005 for 25, 50, and 100
boxes respectively to keep CFL fixed at 0.1875
dtdx = dt/dx;
time = 0.0; % initial time.
endtime = 12000; % Time for ending simulation  (seconds)
nosteps = endtime/dt;   %Number of total timesteps. Used in for loop.
timebetweensavingtimedata = 5;  % How often in s we save data vs time for
plotting.
nostepsbeforesavingtimedata = timebetweensavingtimedata/dt;

% Slip parameters used in the gas slip relation. vg =Kvmix+S
k = 1.2;
s = 0.55;

% Boundary condition at outlet
pbondout=100000; % Pascal  (1 bar)

% Initial temperature distribution. (Kelvin)
% Note that this is only used if we use density models that depend on
% temperature

tempbot = 110+273;
temptop = 50+273;
tempgrad= (tempbot-temptop)/welldepth;
tempo(1)=tempbot-dx/2*tempgrad;
for i = 1:nobox-2
  tempo(i+1)=tempo(i)-dx*tempgrad;
end
tempo(nobox)=tempo(nobox-1)-dx*tempgrad;

temp = tempo;

% Different fluid density parameters
% Note how we switch between different models later.
% These parameters are used when finding the
% primitive variables pressure, densities in an analytical manner.
% Changing parameters here, you must also change parameters inside the
% density routines roliq and rogas.
% Simple Water density model & Ideal Gas. See worknote Extension of AUSMV
% scheme.

rho0=1000;  % Water density at STC (Standard Condition) kg/m3
```

```matlab
Bheta=2.2*10^9; % Parameter that depend on the compressibility of water
Alpha=0.000207; % Parameter related to thermal expansion/compression
R = 286.9; % Ideal gas parameter
P0=100000; % Pressure at STC (Pa)
T0=15+273.15; % Temperature at STC (K)


% Very simple models (PET510 compendium)


al = 1500; % Speed of sound in water.
rt= 100000; % Ideal gas parameter in model rhog = p/rt  (rt = ag^2)
rho0=1000; % Water density at STC (Standard Condition) kg/m3
P0=100000; % Pressure at STC (Pa)
T0=15+273.15; % Temperature at STC (K)



% Viscosities (Pa*s)/Used in the frictional pressure loss model (dpfric).
viscl = 0.001; % Liquid phase
viscg = 0.0000182; % Gas phase

% Gravity constant

  g = 9.81; % Gravitational constant m/s2

% Well opening. opening = 1, fully open well, opening = 0 (<0.01), the well
% is fully closed. This variable will control what boundary conditions that
% will apply at the outlet (both physical and numerical): We must change
% this further below in the code if we want to change status on this.

  wellopening = 1.0;  % This variable determines if
%the well is closed or not, wellopening = 1.0 -> open. welllopening = 0
%-> Well is closed. This variable affects the boundary treatment.

  bullheading = 0.0; % This variable can be set to 1.0 if we want to
simulate
% a bullheading operation. But the normal is to set this to zero.



% Specify if the primitive variables shall be found either by
% a numerical or analytical approach. If analytical = 1, analytical
% solution is used. If analytical = 0. The numerical approach is used.
% using the itsolver subroutine where the bisection numerical method
% is used. We use analytical.

  analytical = 1;



% Initialization of rest of geometry.
% Here we specify the outer and inner diameter and the flow area
% We assume 12.25 x 5 inch annulus. But this can be modified.

    for i = 1:nobox

      do(i)=0.331;
      di(i) = 0.127;

      area(i) = 3.14/4*(do(i)*do(i)- di(i)*di(i));

    end
```

```matlab
% Initialization of slope limiters. These are used for
% reducing numerical diffusion and will be calculated for each timestep.
% They make the numerical scheme second order.
  for i = 1:nobox
    sl1(i)=0;
    sl2(i)=0;
    sl3(i)=0;
    sl4(i)=0;
    sl5(i)=0;
    sl6(i)=0;
  end


% Now comes the intialization of the physical variables in the well.
% First primitive variables, then the conservative ones.

% Below we intialize pressure and fluid densities. We start from top of
% the well and calculated downwards. The calculation is done twice with
% updated values to get better approximation. Only hydrostatic
% considerations since we start with a static well.

for i = 1:nobox
  eg(i)=0.0;  % Gas volume fraction
  ev(i)=1-eg(i); % Liquid volume fraction
end

p(nobox)= pbondout+0.5*9.81*dx*...
    (ev(nobox)*rholiq(P0,T0)+eg(nobox)*rogas(P0,T0));   % Pressure (Pa)
dl(nobox)=rholiq(p(nobox),tempo(nobox));  % Liquid density kg/m3
dg(nobox)=rogas(p(nobox),tempo(nobox));    % Gas density kg/m3

for i=nobox-1:-1:1
p(i)=p(i+1)+dx*9.81*(ev(i+1)*dl(i+1)+eg(i+1)*dg(i+1));
dl(i)=rholiq(p(i),tempo(i));
dg(i)=rogas(p(i),tempo(i));
end

 for i=nobox-1:-1:1
  rhoavg1= (ev(i+1)*dl(i+1)+eg(i+1)*dg(i+1));
  rhoavg2= (ev(i)*dl(i)+eg(i)*dg(i));
  p(i)=p(i+1)+dx*9.81*(rhoavg1+rhoavg2)*0.5;
  dl(i)=rholiq(p(i),tempo(i));
  dg(i)=rogas(p(i),tempo(i));

 end

% Intitialize phase velocities, volume fractions, conservative variables
% and friction and hydrostatic gradients.
% The basic assumption is static fluid, one phase liquid.

for i = 1:nobox
  vl(i)=0; % Liquid velocity new time level.
  vg(i)=0; % Gas velocity at new time level
  eg(i)=0.0;  % Gas volume fraction
  ev(i)=1-eg(i); % Liquid volume fraction
  qv(i,1)=dl(i)*ev(i)*area(i);  % Conservative variable for liquid mass
(kg/m)
  qv(i,2)=dg(i)*eg(i)*area(i);  % Conservative variable for gas mass (kg/m)
```

```matlab
  qv(i,3)=(dl(i)*ev(i)*vl(i)+dg(i)*eg(i)*vg(i))*area(i); % Conservative
variable for mixture moementum
  fricgrad(i)=0;    % Pa/m
  hydgrad(i)=g*(dl(i)*ev(i)+eg(i)*dg(i));  % Pa/m
end

% Section where we also initialize values at old time level

for i=1:nobox
  dlo(i)=dl(i);
  dgo(i)=dg(i);
  po(i)=p(i);
  ego(i)=eg(i);
  evo(i)=ev(i);
  vlo(i)=vl(i);
  vgo(i)=vg(i);
  qvo(i,1)=qv(i,1);
  qvo(i,2)=qv(i,2);
  qvo(i,3)=qv(i,3);
end

% Intialize fluxes between the cells/boxes

for i = 1:nofluxes
  for j =1:3
   flc(i,j)=0.0; % Flux of liquid over box boundary
   fgc(i,j)=0.0; % Flux of gas over box boundary
   fp(i,j)= 0.0; % Pressure flux over box boundary
  end
end

%  Main program. Here we will progress in time. First som intializations
% and definitions to take out results. The for loop below runs until the
% simulation is finished.

countsteps = 0;
counter=0;
printcounter = 1;
pin(printcounter) = (p(1)+dx*0.5*hydgrad(1))/100000; % Pressure in bar at
bottom for time storage
pout(printcounter)= pbondout/100000; % Pressure at outlet of uppermost cell
pnobox(printcounter)= p(nobox)/100000; % Pressure in middle of uppermost
cell
liquidmassrateout(printcounter) = 0;  % liquid mass rate at outlet kg/s
gasmassrateout(printcounter)=0;    % gass mass rate at outlet kg/s
timeplot(printcounter)=time;  % Array for time and plotting of variables vs
time
pitvolume=0;
pitrate =0;
pitgain(printcounter)=0;

kickvolume=0;
bullvolume=0;

% The temperature is not updated but kept fixed according to the
% initialization.

% Now comes the for loop that runs forward in time. This is repeated for
% every timestep.
```

```matlab
for i = 1:nosteps
    countsteps=countsteps+1;
    counter=counter+1;
    time = time+dt;   % Step one timestep and update time.

% Then a section where specify the boundary conditions.
% Here we specify the inlet rates of the different phases at the
% bottom of the pipe in kg/s. We interpolate to make things smooth.
% It is also possible to change the outlet boundary status of the well
% here. First we specify rates at the bottom and the pressure at the outlet
% in case we have an open well. This is a place where we can change the
% code to control simulations. If the well shall be close, wellopening must
% be set to 0. It is also possible to reverse the flow (bullheading).

% In the example below, we take a gas kick and then circulate this
% out of the well without closing the well. (how you not should perform
% well control)

% Note there are two variables wellopening and bullheading that can be
% changed in the control structure below to close the well or start
% reversing the flow i.e. pumping downwards.

% Note that if we will change to bullheading throughout the control
stucture,
% the variable inletligmassrate
% has to be defined as negative since pumping downwards at outlet will be
% in negative direction (postive direction of flow has been chosen to be
% upwards)

% NB, NOTE THAT THIS IS ONE OF THE MAIN PLACES WHERE YOU HAVE TO ADJUST THE
% CODE TO CONTROL THE SIMULATION SCENARIO.

XX = 16; % Gasrate in kg/s; 16, 31, or 46 to introduce 4 m3, 8 m3, or 16 m3
gas kick to the system respectively
%XX=0; % Static

YY= 40; % Liquidrate in kg/s
YY=0; % Static

if (time < 10)

    inletligmassrate=0.0;
    inletgasmassrate=0.0;

elseif ((time>=10) & (time < 20))
    inletligmassrate = YY*(time-10)/10;   % Interpolate the rate from 0 to
value wanted.
    inletgasmassrate = XX*(time-10)/10;

elseif ((time >=20) && (time<200))
    inletligmassrate = YY;
    inletgasmassrate = XX;
elseif ((time >=200) & (time<210))
%   inletligmassrate = YY-YY*(time-200)/10;
    inletligmassrate = YY-YY*(time-200)/10;
    inletgasmassrate = XX-XX*(time-200)/10;
elseif (time > 210)
    inletligmassrate=0;
```

```matlab
    inletgasmassrate=0;
    wellopening = 0;
end


% The commented code below are from some previous runs. It shows. e.g. how
% we can close the well.
%elseif((time>=500)&(time<510))
%    inletligmassrate = YY-YY*(time-500)/10;
%    inletgasmassrate = XX-XX*(time-500)/10;
% elseif(time>=510)
%    inletligmassrate=0;
%    inletgasmassrate=0;
%    wellopening=0.0;
% end


%XX = 4;
% XX (kg/s) is a variable for introducing a kick in the well.
%YY = 15; % Liquid flowrate (kg/s) (1 kg/s = 1 l/s approx)
% if (time < 10)
%
%    inletligmassrate=0.0;
%    inletgasmassrate=0.0;
%
% elseif ((time>=10) & (time < 20))
%    inletligmassrate = 0*(time-10)/10;
%    inletgasmassrate = XX*(time-10)/10;
%
% elseif ((time >=20) & (time<110))
%    inletligmassrate = 0;
%    inletgasmassrate = XX;
%
% elseif ((time>=110)& (time<120))
%    inletligmassrate = 0;
%    inletgasmassrate = XX-XX*(time-110)/10;
% elseif ((time>=120&time<130))
%    inletligmassrate =0;
%    inletgasmassrate =0;
% elseif ((time>=130)&(time<300))
%    inletligmassrate =0;
%    inletgasmassrate =0;
% elseif ((time>=300)&(time<310))
%    inletligmassrate= YY*(time-300)/10;
%    inletgasmassrate =0;
% elseif((time>=310))
%    inletligmassrate= YY;
%    inletgasmassrate =0;
% end


kickvolume = kickvolume+inletgasmassrate/dgo(1)*dt;   % Here we find the
kickvolume

% initially induced in the well.


% Here we specify the physical outlet pressure. Here we have given the
pressure as
% constant. It would be possible to adjust it during openwell conditions
% either by giving the wanted pressure directly (in the command lines
% above) or by finding it indirectly through a chokemodel where the
chokeopening
```

```matlab
% would have had to be  an input parameter. The chokeopening variable would equally had
% to be adjusted inside the controle structure given above.

 pressureoutlet = pbondout;

% Based on these given physical boundary values combined with use
% of extrapolations techniques
% for the remaining unknowns at the boundaries, we will define the mass and
% momentum fluxes at the boundaries (inlet and outlet of pipe).

% inlet/bottom fluxes first.
    if (bullheading<=0)
 % Here we pump from bottom
     flc(1,1)= inletligmassrate/area(1);
     flc(1,2)= 0.0;
     flc(1,3)= flc(1,1)*vlo(1);

     fgc(1,1)= 0.0;
     fgc(1,2)= inletgasmassrate/area(1);
     fgc(1,3)= fgc(1,2)*vgo(1);

     fp(1,1)= 0.0;
     fp(1,2)= 0.0;

% Old way of treating the boundary
%      fp(1,3)= po(1)+0.5*(po(1)-po(2)); %Interpolation used to find the
% pressure at the inlet/bottom of the well.

% New way of treating the boundary
     fp(1,3)= po(1)...
            +0.5*dx*(dlo(1)*evo(1)+dgo(1)*ego(1))*g...
            +0.5*dx*fricgrad(1);

   else
     % Here we pump from the top. All masses are assumed to flow out of the
     % well into the formation. We use first order extrapolation.
     flc(1,1)=dlo(1)*evo(1)*vlo(1);
     flc(1,2)=0.0;
     flc(1,3)=flc(1,1)*vlo(1);

     fgc(1,1)=0.0;
     fgc(1,2)=dgo(1)*ego(1)*vgo(1);
     fgc(1,3)=fgc(1,2)*vgo(1);

     fp(1,1)=0.0;
     fp(1,2)=0.0;
     fp(1,3)=20000000;   (Pa) % This was a fixed pressure set at bottom when bullheading
   end

% Outlet fluxes (open & closed conditions)

    if (wellopening>0.01)

% Here open end condtions are given. We distinguish between bullheading
% & normal circulation.
```

```matlab
        if (bullheading<=0)  % Here we dont bullhead, i.e we circulate from
bottom

            % Here the is normal ciruclation and open well)
            flc(nofluxes,1)= dlo(nobox)*evo(nobox)*vlo(nobox);
            flc(nofluxes,2)= 0.0;
            flc(nofluxes,3)= flc(nofluxes,1)*vlo(nobox);

            fgc(nofluxes,1)= 0.0;
            fgc(nofluxes,2)= dgo(nobox)*ego(nobox)*vgo(nobox);
%            fgc(nofluxes,2)=0; Activate if gas is sucked in!?
            fgc(nofluxes,3)= fgc(nofluxes,2)*vgo(nobox);

            fp(nofluxes,1)= 0.0;
            fp(nofluxes,2)= 0.0;
            fp(nofluxes,3)= pressureoutlet;
        else
            % Here we are bullheading.
            flc(nofluxes,1)= inletligmassrate/area(nobox);
            flc(nofluxes,2)= 0.0;
            flc(nofluxes,3)= flc(nofluxes,1)*vlo(nobox);

            fgc(nofluxes,1)=0.0;
            fgc(nofluxes,2)=0.0;
            fgc(nofluxes,3)=0.0;

            fp(nofluxes,1)=0.0;
            fp(nofluxes,2)=0.0;
            fp(nofluxes,3)= po(nobox)...
            -0.5*dx*(dlo(nobox)*evo(nobox)+dgo(nobox)*ego(nobox))*g...
            +0.5*dx*fricgrad(nobox); %check sign here on friction
            % Physcially, the friction should be added when going from
            % mid point in upper cell to outlet. But if fricgrad(nobox) is
            % negative there should be a minus in front of the term to have
            % + in the end.
        end
    else

% Here closed end conditions are given

        flc(nofluxes,1)= 0.0;
        flc(nofluxes,2)= 0.0;
        flc(nofluxes,3)= 0.0;

        fgc(nofluxes,1)= 0.0;
        fgc(nofluxes,2)= 0.0;
        fgc(nofluxes,3)= 0.0;

        fp(nofluxes,1)=0.0;
        fp(nofluxes,2)=0.0;

%       Old way of treating the boundary
%        fp(nofluxes,3)= po(nobox)-0.5*(po(nobox-1)-po(nobox));

%       New way of treating the boundary
        fp(nofluxes,3)= po(nobox)...
        -0.5*dx*(dlo(nobox)*evo(nobox)+dgo(nobox)*ego(nobox))*g;
%         -0.5*dx*fricgrad(nobox); % Neglect friction since well is closed.
        end
```

```
% Implementation of slopelimiters. They are applied on the physical
 % variables like phase densities, phase velocities and pressure.

% It was found that if the slopelimiters were set to zero in
% the boundary cells, the pressure in these became wrong. E.g. the upper
% cell get an interior pressure that is higher than it should be e.g. when
% being static (hydrostatic pressure was too high). The problem was reduced
% by copying the slopelimiters from the interior cells. However, both
% approaches seems to give the same BHP pressure vs time but the latter
% approach give a more correct pressure vs depth profile. It is also better
% to use when simulating pressure build up where the upper cell pressure
% must be monitored. It should be checked more in detail before concluding.
% BUT; there has been mass conservation problems with the scheme for the
% case where the slopelimiters were copied (see master thesis of Keino)
% A possible fix has been included below where the slopelimiter related to
% the gas volume fraction is set to zero in the first cell.

    for i=2:nobox-1
     sl1(i)=minmod(dlo(i-1),dlo(i),dlo(i+1),dx);
     sl2(i)=minmod(po(i-1),po(i),po(i+1),dx);
     sl3(i)=minmod(vlo(i-1),vlo(i),vlo(i+1),dx);
     sl4(i)=minmod(vgo(i-1),vgo(i),vgo(i+1),dx);
     sl5(i)=minmod(ego(i-1),ego(i),ego(i+1),dx);
     sl6(i)=minmod(dgo(i-1),dgo(i),dgo(i+1),dx);
    end

 % Slopelimiters in outlet boundary cell are set to zero!
%      sl1(nobox)=0;
%      sl2(nobox)=0;
%      sl3(nobox)=0;
%      sl4(nobox)=0;
%      sl5(nobox)=0;
%      sl6(nobox)=0;

 % Slopelimiters in outlet boundary cell are copied from neighbour cell!
     sl1(nobox)=sl1(nobox-1);
     sl2(nobox)=sl2(nobox-1);
     sl3(nobox)=sl3(nobox-1);
     sl4(nobox)=sl4(nobox-1);
     sl5(nobox)=sl5(nobox-1);
     sl6(nobox)=sl6(nobox-1);

% Slopelimiters in inlet boundary cell are set to zero!
%      sl1(1)=0;
%      sl2(1)=0;
%      sl3(1)=0;
%      sl4(1)=0;
%      sl5(1)=0;
%      sl6(1)=0;

% Slopelimiters in inlet boundary cell are copied from neighbour cell!
     sl1(1)=sl1(2);
     sl2(1)=sl2(2);
     sl3(1)=sl3(2);
     sl4(1)=sl4(2);
     sl5(1)=sl5(2);
     sl6(1)=sl6(2);

% FIX FOR OMITTING THE GAS MASS CONSERVATION PROBLEM
```

```matlab
        sl5(1)=0;
        sl5(nobox)=0;


% Now we will find the fluxes between the different cells.
% NB - IMPORTANE -  Note that if we change the compressibilities/sound
velocities of
% the fluids involved, we may need to do changes inside the csound
function.
% But the effect of this is unclear.

        for j = 2:nofluxes-1

  %%%%%%%%%%%%%%%%%%%%%%%%%%%%%%%%%%%%%%%%%%%%%%
  %%%%%%%%%%%%%%%%%%%%%%%%%%%%%%%%%%%%%%%%%%%%%%
  % First order method is from here: If you want to test this, activate this
  % and comment the second order code below.
  %         cl = csound(ego(j-1),po(j-1),dlo(j-1),k);
  %         cr = csound(ego(j),po(j),dlo(j),k);
  %         c = max(cl,cr);
  %         pll = psip(vlo(j-1),c,evo(j));
  %         plr = psim(vlo(j),c,evo(j-1));
  %         pgl = psip(vgo(j-1),c,ego(j));
  %         pgr = psim(vgo(j),c,ego(j-1));
  %         vmixr = vlo(j)*evo(j)+vgo(j)*ego(j);
  %         vmixl = vlo(j-1)*evo(j-1)+vgo(j-1)*ego(j-1);
  %
  %         pl = pp(vmixl,c);
  %         pr = pm(vmixr,c);
  %         mll= evo(j-1)*dlo(j-1);
  %         mlr= evo(j)*dlo(j);
  %         mgl= ego(j-1)*dgo(j-1);
  %         mgr= ego(j)*dgo(j);
  %
  %         flc(j,1)= mll*pll+mlr*plr;
  %         flc(j,2)= 0.0;
  %         flc(j,3)= mll*pll*vlo(j-1)+mlr*plr*vlo(j);
  %
  %         fgc(j,1)=0.0;
  %         fgc(j,2)= mgl*pgl+mgr*pgr;
  %         fgc(j,3)= mgl*pgl*vgo(j-1)+mgr*pgr*vgo(j);
  %
  %         fp(j,1)= 0.0;
  %         fp(j,2)= 0.0;
  %         fp(j,3)= pl*po(j-1)+pr*po(j);

  %  First order methods ends here
  %%%%%%%%%%%%%%%%%%%%%%%%%%%%%%%%%%%%%%%%%%%%%%%%%%%%%
  %%%%%%%%%%%%%%%%%%%%%%%%%%%%%%%%%%%%%%%%%%%%%%%%%%%%%


%%%%%%%%%%%%%%%%%%%%%%%%%%%%%%%%%%%%%%%%%%%%%%%%%%%%%%%%%%%
%%%%%%%%%%%%%%%%%%%%%%%%%%%%%%%%%%%%%%%%%%%%%%%%%%%%%%%%%%%
% Second order method starts here:
% Here slopelimiter is used on all variables except phase velocoties

        psll = po(j-1)+dx/2*sl2(j-1);
        pslr = po(j)-dx/2*sl2(j);
        dsll = dlo(j-1)+dx/2*sl1(j-1);
        dslr = dlo(j)-dx/2*sl1(j);
        dgll = dgo(j-1)+dx/2*sl6(j-1);
```

118

```matlab
        dglr = dgo(j)-dx/2*sl6(j);

        vlv = vlo(j-1)+dx/2*sl3(j-1);
        vlh = vlo(j)-dx/2*sl3(j);
        vgv = vgo(j-1)+dx/2*sl4(j-1);
        vgh = vgo(j)-dx/2*sl4(j);

        gvv = ego(j-1)+dx/2*sl5(j-1);
        gvh = ego(j)-dx/2*sl5(j);
        lvv = 1-gvv;
        lvh = 1-gvh;

        cl = csound(gvv,psll,dsll,k);
        cr = csound(gvh,pslr,dslr,k);
        c = max(cl,cr);

        pll = psip(vlo(j-1),c,lvh);
        plr = psim(vlo(j),c,lvv);
        pgl = psip(vgo(j-1),c,gvh);
        pgr = psim(vgo(j),c,gvv);
        vmixr = vlo(j)*lvh+vgo(j)*gvh;
        vmixl = vlo(j-1)*lvv+vgo(j-1)*gvv;

        pl = pp(vmixl,c);
        pr = pm(vmixr,c);

       mll= lvv*dsll;
       mlr= lvh*dslr;
       mgl= gvv*dgll;
       mgr= gvh*dglr;

       flc(j,1)= mll*pll+mlr*plr;
       flc(j,2)= 0.0;
       flc(j,3)= mll*pll*vlo(j-1)+mlr*plr*vlo(j);


       fgc(j,1)=0.0;
       fgc(j,2)= mgl*pgl+mgr*pgr;
       fgc(j,3)= mgl*pgl*vgo(j-1)+mgr*pgr*vgo(j);

       fp(j,1)= 0.0;
       fp(j,2)= 0.0;
       fp(j,3)= pl*psll+pr*pslr;

%%% Second order method ends here
%%%%%%%%%%%%%%%%%%%%%%%%%%%%%%%%%%%%%%%%%%%%%%%%%%%%%%%%%%%%%%%
%%%%%%%%%%%%%%%%%%%%%%%%%%%%%%%%%%%%%%%%%%%%%%%%%%%%%%%%%%%

% Here sloplimiters is used on all variables. This
% has not worked so well yet. Therefore it is commented away.

%        psll = po(j-1)+dx/2*sl2(j-1);
%        pslr = po(j)-dx/2*sl2(j);
%        dsll = dlo(j-1)+dx/2*sl1(j-1);
%        dslr = dlo(j)-dx/2*sl1(j);
%        dgll = dgo(j-1)+dx/2*sl6(j-1);
%        dglr = dgo(j)-dx/2*sl6(j);
%
%        vlv = vlo(j-1)+dx/2*sl3(j-1);
```

```matlab
%         vlh = vlo(j)-dx/2*sl3(j);
%         vgv = vgo(j-1)+dx/2*sl4(j-1);
%         vgh = vgo(j)-dx/2*sl4(j);
%
%         gvv = ego(j-1)+dx/2*sl5(j-1);
%         gvh = ego(j)-dx/2*sl5(j);
%         lvv = 1-gvv;
%         lvh = 1-gvh;
%
%         cl = csound(gvv,psll,dsll,k);
%         cr = csound(gvh,pslr,dslr,k);
%         c = max(cl,cr);
%
%         pll = psip(vlv,c,lvh);
%         plr = psim(vlh,c,lvv);
%         pgl = psip(vgv,c,gvh);
%         pgr = psim(vgh,c,gvv);
%         vmixr = vlh*lvh+vgh*gvh;
%         vmixl = vlv*lvv+vgv*gvv;
%
%         pl = pp(vmixl,c);
%         pr = pm(vmixr,c);
%         mll= lvv*dsll;
%         mlr= lvh*dslr;
%         mgl= gvv*dgll;
%         mgr= gvh*dglr;
%
%         flc(j,1)= mll*pll+mlr*plr;
%         flc(j,2)= 0.0;
%         flc(j,3)= mll*pll*vlv+mlr*plr*vlh;
%
%
%         fgc(j,1)=0.0;
%         fgc(j,2)= mgl*pgl+mgr*pgr;
%         fgc(j,3)= mgl*pgl*vgv+mgr*pgr*vgh;
%
%         fp(j,1)= 0.0;
%         fp(j,2)= 0.0;
%         fp(j,3)= pl*psll+pr*pslr;

    end

% Fluxes have now been calculated. We will now update the conservative
% variables in each of the numerical cells.

% The source terms can be calculated by using a
% for loop.
% Note that the model is sensitive to how we treat the model
% for low Reynolds numbers (possible discontinuity in the model)
    for j=1:nobox
        fricgrad(j)=dpfric(vlo(j),vgo(j),evo(j),ego(j),dlo(j),dgo(j), ...
          po(j),do(j),di(j),viscl,viscg); % Pa/m
        hydgrad(j)=g*(dlo(j)*evo(j)+dgo(j)*ego(j)); % Pa/m
     end

    sumfric = 0;
    sumhyd= 0;

    for j=1:nobox
```

```matlab
    % Here we solve the three conservation laws for each cell and update
    % the conservative variables qv

     ar = area(j);

     % Liquid mass conservation
     qv(j,1)=qvo(j,1)-dtdx*((ar*flc(j+1,1)-ar*flc(j,1))...
                           +(ar*fgc(j+1,1)-ar*fgc(j,1))...
                           +(ar*fp(j+1,1)-ar*fp(j,1)));

     % Gas mass conservation:

     qv(j,2)=qvo(j,2)-dtdx*((ar*flc(j+1,2)-ar*flc(j,2))...
                           +(ar*fgc(j+1,2)-ar*fgc(j,2))...
                           +(ar*fp(j+1,2)-ar*fp(j,2)));
     % Mixture momentum conservation:

     qv(j,3)=qvo(j,3)-dtdx*((ar*flc(j+1,3)-ar*flc(j,3))...
                           +(ar*fgc(j+1,3)-ar*fgc(j,3))...
                           +(ar*fp(j+1,3)-ar*fp(j,3)))...
                 -dt*ar*(fricgrad(j)+hydgrad(j));

%  Add up the hydrostatic pressure  and friction  in the whole well.
     sumfric=sumfric+fricgrad(j)*dx;
     sumhyd=sumhyd+hydgrad(j)*dx;

     end

% Section where we find the physical variables (pressures, densities etc)
% from the conservative variables. Some trickes to ensure stability. These
% are induced to avoid negative masses.

     gasmass=0;
     liqmass=0;

     for j=1:nobox

% Remove the area from the conservative variables to find the
% the primitive variables from the conservative ones.

     qv(j,1)= qv(j,1)/area(j);
     qv(j,2)= qv(j,2)/area(j);

     if (qv(j,1)<0.00000001)  % Trick to avoid negative masses.
       qv(j,1)=0.00000001;
     end

     if (qv(j,2)< 0.00000001)  % Trick to avoid negative masses.
       qv(j,2)=0.00000001;
     end

 % Here we summarize the mass of gas and liquid in the well respectively.
 % These variables are important to show that the scheme is conserving
 % mass. (if e.g. gas leaks in our out of the well unintentionally in the
simulation
 % without being specified in the code,something fundamental is wrong.

     gasmass = gasmass+qv(j,2)*area(j)*dx;
```

```matlab
        liqmass = liqmass+qv(j,1)*area(j)*dx;

% Below, we find the primitive variables pressure and densities based on
% the conservative variables q1,q2. One can choose between getting them by
% analytical or numerical solution approach specified in the beginning of
% the program. Ps. For more advanced density models, this must be changed.

        if (analytical == 1)
%          % Analytical solution:

% here the simple density models used in PET 510 Wellflow modelling
% compendium is used.

            t1=rho0-P0/al^2;

%  Coefficients:
            a = 1/(al*al);
            b = t1-qv(j,1)-rt*qv(j,2)/(al*al);
            c = -1.0*t1*rt*qv(j,2);
%

%          Note here we use the very simple models from the PET510 course
            p(j)=(-b+sqrt(b*b-4*a*c))/(2*a);   % Pressure
            dl(j)=rholiq(p(j),temp(j)); % Density of liquid
            dg(j)=rogas(p(j),temp(j)); % Density of gas

%      The code below can be activated if we want to switch to the other set
%      of density models. Also then remember to do the changes inside
%      functions rogas og rholiq if we change density models.

%            x1=rho0-P0*rho0/Bheta-rho0*Alpha*(temp(j)-T0);
%            x2=rho0/Bheta;
%            x3=-qv(j,2)*R*temp(j);

%            a = x2;
%            b = x1+x2*x3-qv(j,1);
%            c = x1*x3;

%            p(j)=(-b+sqrt(b*b-4*a*c))/(2*a);   % Pressure
%            dl(j)=rholiq(p(j),temp(j));
%            dg(j)=rogas(p(j),temp(j));
        else

        %Numerical Solution: This might be used if we use more complex
        %density models. Has not been used for years.

         [p(j),error]=itsolver(po(j),qv(j,1),qv(j,2)); % Pressure
         dl(j)=rholiq(p(j),temp(j)); % Density of liquid
         dg(j)=rogas(p(j)); % Density of gas

        % Incase a numerical solution is not found, the program will write
out "error":
         if error > 0
            error
         end
        end

%   Find phase volume fractions
        eg(j)= qv(j,2)/dg(j);
```

```
      ev(j)=1-eg(j);

 %    Reset average conservative varibles in cells with area included in
the variables.

      qv(j,1)=qv(j,1)*area(j);
      qv(j,2)=qv(j,2)*area(j);

      end  % end of loop

 %    Below we find the phase velocities by combining the
 %    conservative variable defined by the mixture momentum equation
 %    with the gas slip relation.
 %    At the same time we try to summarize the gas volume in the well. This
 %    also measure the size of the kick.

   gasvol=0;

   for j=1:nobox

   % The  interpolations introduced below are included
   % to omit a singularity in the slip relation when the gas volume
   % fraction becomes equal to 1/K. In additon, S is interpolated to
   % zero when approaching one phase gas flow. In the transition to
   % one phase gas flow, we have no slip condtions (K=1, S=0)
   % We will let the k0,s0,k1,s1 be arrays to make it easier to incorporate
   % different flow regimes later.  In that case, the slip parameters will
   % vary from cell to cell and we must have slip parameter values for each
   % cell.

      ktemp=k;
      stemp=s;

      k0(j) = ktemp;
      s0(j) = stemp;

    % Interpolation to handle that (1-Kxgasvolumefraction) does not become
zero
      if ((eg(j)>=0.7) & (eg(j)<=0.8))
        xint = (eg(j)-0.7)/0.1;
        k0(j) =1.0*xint+k*(1-xint);
      elseif(eg(j)>0.8)
        k0(j)=1.0;
      end

    % Interpolate S to zero in transition to pure gas phase
       if ((eg(j)>=0.9) & (eg(j)<=1.0))
         xint = (eg(j)-0.9)/0.1;
         s0(j) = 0.0*xint+s*(1-xint);
       end

  % Note that the interpolations above and below can be changed
  % if numerical stability problems
  % are encountered.

  %
      if (eg(j)>=0.999999)
       % Pure gas
        k1(j) = 1.0;
```

123

```matlab
            s1(j) = 0.0;
          else
            %Two phase flow
            k1(j) = (1-k0(j)*eg(j))/(1-eg(j));
            s1(j) = -1.0*s0(j)*eg(j)/(1-eg(j));
          end

          help1 = dl(j)*ev(j)*k1+dg(j)*eg(j)*k0;
          help2 = dl(j)*ev(j)*s1+dg(j)*eg(j)*s0;



          vmixhelpl = (qv(j,3)/area(j)-help2)/help1;
          vg(j)=k0(j)*vmixhelpl+s0(j);
          vl(j)=k1(j)*vmixhelpl+s1(j);

          % Variable for summarizing the gas volume content in the well.
          gasvol=gasvol+eg(j)*area(j)*dx;


    end

% Old values are now set equal to new values in order to prepare
% computation of next time level.


    po=p;
    dlo=dl;
    dgo=dg;
    vlo=vl;
    vgo=vg;
    ego=eg;
    evo=ev;
    qvo=qv;

% Section where we save some timedependent variables in arrays.
% e.g. the bottom hole pressure. They will be saved for certain
% timeintervalls defined in the start of the program in order to ensure
% that the arrays do not get to long!

  if (counter>=nostepsbeforesavingtimedata)
    printcounter=printcounter+1;
    time   % Write time to screen.

    % Outlet massrates (kg/s) vs time

liquidmassrateout(printcounter)=dl(nobox)*ev(nobox)*vl(nobox)*area(nobox);
    gasmassrateout(printcounter)=dg(nobox)*eg(nobox)*vg(nobox)*area(nobox);

    % Outlet flowrates (lpm) vs time
    liquidflowrateout(printcounter)=liquidmassrateout(printcounter)/...
        rholiq(P0,T0)*1000*60;
    gasflowrateout(printcounter)=gasmassrateout(printcounter)/...
        rogas(P0,T0)*1000*60;

    % Hydrostatic and friction pressure (bar) in well vs time
    hyd(printcounter)=sumhyd/100000;
    fric(printcounter)=sumfric/100000;
```

```matlab
    % Volume of gas in well vs time (m3). Also used for indicating kick
    % size in well.

    volgas(printcounter)=gasvol;

    % Total phase masses (kg) in the well vs time
    % Used for checking mass conservation.

     massgas(printcounter)=gasmass;
     massliq(printcounter)=liqmass;

    % pout calculates the pressure at the outletboundary. I.e. upper edge
    % of uppermost cell. Corresponds where the well ends at surface. The
    % reason we do this is the fact than in AUSMV is all variables defined
    % in the mid point of the numerical cells.
    pout(printcounter)=(p(nobox)-0.5*dx*...
    (dlo(nobox)*evo(nobox)+dgo(nobox)*ego(nobox))*g-
dx*0.5*fricgrad(nobox))/100000;

    % pin (bar) defines the  pressure at the inlet boundary, I.e lower edge
    % of the lowermost cell. Corresponds to TD of well.
    pin(printcounter)=
(p(1)+0.5*dx*(dlo(1)*evo(1)+dgo(1)*ego(1))*g+0.5*dx*fricgrad(1))/100000;

    % Pressure in the middle of top box (bar).
    pnobox(printcounter)=p(nobox)/100000;  %

    % Time variable
    timeplot(printcounter)=time;

    counter = 0;

  end
end

% end of stepping forward in time.

% Printing of resultssection

countsteps % Marks number of simulation steps.

% Plot commands for variables vs time. The commands can also
% be copied to command screen where program is run for plotting other
% variables.

toc,
e = cputime-t

% Plot bottom hole pressure
plot(timeplot,pin)

% Show cfl number used.
disp('cfl')
cfl = al*dt/dx

 plot(timeplot,pin)
%plot(timeplot,hyd)
%plot(timeplot,fric)
```

```
%plot(timeplot,liquidmassrateout)
%plot(timeplot,gasmassrateout)
%plot(timeplot,volgas)
%plot(timeplot,liquidflowrateout)
%plot(timeplot,gasflowrateout)
%plot(timeplot,massgas)
%plot(timeplot,massliq)
%plot(timeplot,pout)
%plot(timeplot,pnobox)

%Plot commands for variables vs depth/Only the last simulated
%values at endtime is visualised

%plot(vl,x);
%plot(vg,x);
%plot(eg,x);
%plot(p,x);
%plot(dl,x);
%plot(dg,x);
```

Appendix B

The MATLAB code used in case 2 through 7 (the new model) is provided below. It is based on the model used in [8], but extended further to account for well deviation and annular geometry corrections. The corrections have not been used for the simulations in this thesis and are therefore commented away, but they are kept for further studies. The red text color indicates new elements implemented during the work of this thesis.

```matlab
% Transient two-phase code based on AUSMV scheme: Gas and Water
% The code assumes uniform geometry

% time - seconds

% p - pressure at new time level (Pa)
% dl - density of liquid at new time level (kg/m3)
% dg - density of gas at new time level (kg/m3)
% eg - phase volume fraction of liquid at new time level (0-1)
% ev - phase volume fraction og gas at new time level (0-1)
% vg - phase velocity of gas at new time level (m/s)
% vl - phase velocity of liquid at new time level (m/s)
% qv - conservative variables at new time level  ( 3 in each cell)
% temp - temperature in well (K)

% po - pressure at old time level (Pa)
% dlo - density of liquid at old time level (kg/m3)
% dgo - density of gas at new old level (kg/m3)
% ego - phase volume fraction of liquid at old time level (0-1)
% evo - phase volume fraction og gas at old time level (0-1)
% vgo - phase velocity of gas at old time level (m/s)
% vlo - phase velocity of liquid at old time level (m/s)
% qvo - conservative variables at old  time level  ( 3 in each cell)
% temp - temperature in well (K)

clear;
t = cputime
tic,

% Geometry data/ Must be specified
welldepth = 4000;
nobox = 50; %Number of boxes in the well; 25, 50, or 100 boxes

% Note that one can use more refined grid, 50, 100 boxes.
% When doing this, remember to reduce time step to keep the CFL number
% fixed below 0.25.. dt < cfl x dx/ speed of sound in water. If boxes are
% doubled, then half the time step.

nofluxes = nobox+1;  % Number of cell boundaries
dx = welldepth/nobox; % Boxlength
%dt = 0.005;
% angle=0; % Well inclination
% dx=dx*cosd(angle); % New boxlength

% Welldepth. Cell 1 start at bottom
x(1)= -1.0*welldepth+0.5*dx;
for i=1:nobox-1
```

```
 x(i+1)=x(i)+ dx;
end


% VERY IMPORTANT: BELOW THE TIMESTEP IS SET. MAKE SURE THAT THE
% CFL CONDIDTION IS FULFILLED. IF NUMBER OF BOXES IS CHANGED. DX WILL
% CHANGE AND DT HAS TO BE ADJUSTED TO KEEP THE CFL NUMBER FIXED.

dt= 0.01;  % Timestep (seconds); 0.02, 0.01, 0.005 for 25, 50, and 100
boxes respectively to keep CFL fixed at 0.1875
dtdx = dt/dx;
time = 0.0; % Initial time.
endtime = 20000; % Time for ending simulation  (seconds)
nosteps = endtime/dt;  % Number of total timesteps. Used in for loop.
timebetweensavingtimedata = 5;  % How often in s we save data vs time for
plotting.
nostepsbeforesavingtimedata = timebetweensavingtimedata/dt;


% Slip parameters used in the gas slip relation. vg =Kvmix+S
k = 1.2;
s = 0.55;


% Boundary condition at outlet
pbondout=100000; % Pascal  (1 bar)

% Initial temperature distribution. (Kelvin)
% Note that this is only used if we use density models that depend on
% temperature

tempbot = 110+273;
temptop = 50+273;
tempgrad= (tempbot-temptop)/welldepth;
tempo(1)=tempbot-dx/2*tempgrad;
for i = 1:nobox-2
  tempo(i+1)=tempo(i)-dx*tempgrad;
end
tempo(nobox)=tempo(nobox-1)-dx*tempgrad;


temp = tempo;

% Different fluid density parameters
% Note how we switch between different models later.
% These parameters are used when finding the
% primitive variables pressure, densities in an analytical manner.
% Changing parameters here, you must also change parameters inside the
% density routines roliq and rogas.
% Simple Water density model & Ideal Gas. See worknote Extension of AUSMV
% scheme.

rho0=1000;  % Water density at STC (Standard Condition) kg/m3
Bheta=2.2*10^9; % Parameter that depend on the compressibility of water
Alpha=0.000207; % Parameter related to thermal expansion/compression
R = 286.9; % Ideal gas parameter
P0=100000; % Pressure at STC (Pa)
T0=15+273.15; % Temperature at STC (K)


% Very simple models (PET510 compendium)

al = 1500; % Speed of sound in water.
rt= 100000; % Ideal gas parameter in model rhog = p/rt  (rt = ag^2)
```

```matlab
rho0=1000; % Water density at STC (Standard Condition) kg/m3
P0=100000; % Pressure at STC (Pa)
T0=15+273.15; % Temperature at STC (K)

% Viscosities (Pa*s)/Used in the frictional pressure loss model (dpfric).
viscl = 0.001; % Liquid phase
viscg = 0.0000182; % Gas phase
sigma=0.0772; % Interfacial tension between phases in N/m

% Gravity constant

  g = 9.81; % Gravitational constant m/s2

% Well opening. opening = 1, fully open well, opening = 0 (<0.01), the well
% is fully closed. This variable will control what boundary conditions that
% will apply at the outlet (both physical and numerical): We must change
% this further below in the code if we want to change status on this.

  wellopening = 1.0;  % This variable determines if
%the well is closed or not, wellopening = 1.0 -> open. welllopening = 0
%-> Well is closed. This variable affects the boundary treatment.

  bullheading = 0.0; % This variable can be set to 1.0 if we want to
simulate
% a bullheading operation. But the normal is to set this to zero.

% Specify if the primitive variables shall be found either by
% a numerical or analytical approach. If analytical = 1, analytical
% solution is used. If analytical = 0. The numerical approach is used.
% using the itsolver subroutine where the bisection numerical method
% is used. We use analytical.

  analytical = 1;

% Initialization of rest of geometry.
% Here we specify the outer and inner diameter and the flow area
% We assume 12.25 x 5 inch annulus. But this can be modified.

   for i = 1:nobox

    do(i)=12.25*0.0254;
    di(i)=5*0.0254;

    area(i) = pi/4*(do(i)*do(i)- di(i)*di(i));

   end


% Initialization of slope limiters. These are used for
% reducing numerical diffusion and will be calculated for each timestep.
% They make the numerical scheme second order.
   for i = 1:nobox
     sl1(i)=0;
     sl2(i)=0;
     sl3(i)=0;
     sl4(i)=0;
     sl5(i)=0;
     sl6(i)=0;
```

```matlab
    end

% Now comes the intialization of the physical variables in the well.
% First primitive variables, then the conservative ones.

% Below we intialize pressure and fluid densities. We start from top of
% the well and calculated downwards. The calculation is done twice with
% updated values to get better approximation. Only hydrostatic
% considerations since we start with a static well.

for i = 1:nobox
  eg(i)=0.0;  % Gas volume fraction
  ev(i)=1-eg(i); % Liquid volume fraction
end

p(nobox)= pbondout+0.5*9.81*dx*...
    (ev(nobox)*rholiq(P0,T0)+eg(nobox)*rogas(P0,T0));   % Pressure (Pa)
dl(nobox)=rholiq(p(nobox),tempo(nobox));  % Liquid density kg/m3
dg(nobox)=rogas(p(nobox),tempo(nobox));    % Gas density kg/m3

for i=nobox-1:-1:1
p(i)=p(i+1)+dx*9.81*(ev(i+1)*dl(i+1)+eg(i+1)*dg(i+1));
dl(i)=rholiq(p(i),tempo(i));
dg(i)=rogas(p(i),tempo(i));
end

 for i=nobox-1:-1:1
  rhoavg1= (ev(i+1)*dl(i+1)+eg(i+1)*dg(i+1));
  rhoavg2= (ev(i)*dl(i)+eg(i)*dg(i));
  p(i)=p(i+1)+dx*9.81*(rhoavg1+rhoavg2)*0.5;
  dl(i)=rholiq(p(i),tempo(i));
  dg(i)=rogas(p(i),tempo(i));

 end

% Intitialize phase velocities, volume fractions, conservative variables
% and friction and hydrostatic gradients.
% The basic assumption is static fluid, one phase liquid.

for i = 1:nobox
  vl(i)=0; % Liquid velocity new time level.
  vg(i)=0; % Gas velocity at new time level
  eg(i)=0.0;  % Gas volume fraction
  ev(i)=1-eg(i); % Liquid volume fraction
  qv(i,1)=dl(i)*ev(i)*area(i);  % Conservative variable for liquid mass
(kg/m)
  qv(i,2)=dg(i)*eg(i)*area(i);  % Conservative variable for gas mass (kg/m)
  qv(i,3)=(dl(i)*ev(i)*vl(i)+dg(i)*eg(i)*vg(i))*area(i); % Conservative
variable for mixture moementum
  fricgrad(i)=0;   % Pa/m
  hydgrad(i)=g*(dl(i)*ev(i)+eg(i)*dg(i));  % Pa/m
end

% Section where we also initialize values at old time level

for i=1:nobox
  dlo(i)=dl(i);
  dgo(i)=dg(i);
  po(i)=p(i);
```

```
      ego(i)=eg(i);
      evo(i)=ev(i);
      vlo(i)=vl(i);
      vgo(i)=vg(i);
      qvo(i,1)=qv(i,1);
      qvo(i,2)=qv(i,2);
      qvo(i,3)=qv(i,3);
end


% Intialize fluxes between the cells/boxes

for i = 1:nofluxes
  for j =1:3
    flc(i,j)=0.0; % Flux of liquid over box boundary
    fgc(i,j)=0.0; % Flux of gas over box boundary
    fp(i,j)= 0.0; % Pressure flux over box boundary
  end
end


%  Main program. Here we will progress in time. First some intializations
% and definitions to take out results. The for loop below runs until the
% simulation is finished.

countsteps = 0;
counter=0;
printcounter = 1;
pin(printcounter) = (p(1)+dx*0.5*hydgrad(1))/100000; % Pressure in bar at
bottom for time storage
pout(printcounter)= pbondout/100000; % Pressure at outlet of uppermost cell
pnobox(printcounter)= p(nobox)/100000; % Pressure in middle of uppermost
cell
liquidmassrateout(printcounter) = 0;  % liquid mass rate at outlet kg/s
gasmassrateout(printcounter)=0;    % gass mass rate at outlet kg/s
timeplot(printcounter)=time;  % Array for time and plotting of variables vs
time
pitvolume=0;
pitrate =0;
pitgain(printcounter)=0;

kickvolume=0;
bullvolume=0;

% The temperature is not updated but kept fixed according to the
% initialization.

% Now comes the for loop that runs forward in time. This is repeated for
% every timestep.

for i = 1:nosteps
   countsteps=countsteps+1;
   counter=counter+1;
   time = time+dt;  % Step one timestep and update time.

% Then a section where specify the boundary conditions.
% Here we specify the inlet rates of the different phases at the
% bottom of the pipe in kg/s. We interpolate to make things smooth.
% It is also possible to change the outlet boundary status of the well
% here. First we specify rates at the bottom and the pressure at the outlet
% in case we have an open well. This is a place where we can change the
% code to control simulations. If the well shall be close, wellopening must
```

131

```matlab
% be set to 0. It is also possible to reverse the flow (bullheading).

% In the example below, we take a gas kick and then circulate this
% out of the well without closing the well. (how you not should perform
% well control)

% Note there are two variables wellopening and bullheading that can be
% changed in the control structure below to close the well or start
% reversing the flow i.e. pumping downwards.

% Note that if we will change to bullheading throughout the control
stucture,
% the variable inletligmassrate
% has to be defined as negative since pumping downwards at outlet will be
% in negative direction (postive direction of flow has been chosen to be
% upwards)

% NB, NOTE THAT THIS IS ONE OF THE MAIN PLACES WHERE YOU HAVE TO ADJUST THE
% CODE TO CONTROL THE SIMULATION SCENARIO.

XX = 16; % Gasrate in kg/s; 16, 31, or 46 to introduce 4 m3, 8 m3, or 16 m3
gas kick to the system respectively
%XX=0; % Static

YY= 40; % Liquidrate in kg/s
YY=0; % Static

if (time < 10)

  inletligmassrate=0.0;
  inletgasmassrate=0.0;

elseif ((time>=10) & (time < 20))
  inletligmassrate = YY*(time-10)/10;  % Interpolate the rate from 0 to
value wanted.
  inletgasmassrate = XX*(time-10)/10;

elseif ((time >=20) && (time<110))
  inletligmassrate = YY;
  inletgasmassrate = XX;
elseif ((time >=110) & (time<120))
  inletligmassrate = YY-YY*(time-110)/10;
  inletgasmassrate = XX-XX*(time-110)/10;
elseif (time>=120)
  inletligmassrate=0;
  inletgasmassrate=0;
  wellopening = 0;
end

% The commented code below are from some previous runs. It shows. e.g. how
% we can close the well.
% elseif((time>=500)&(time<510))
%   inletligmassrate = YY-YY*(time-500)/10;
%   inletgasmassrate = XX-XX*(time-500)/10;
% elseif(time>=510)
%   inletligmassrate=0;
%   inletgasmassrate=0;
%   wellopening=0.0;
% end
```

```
%

%XX = 4;
% XX (kg/s) is a variable for introducing a kick in the well.
%YY = 15; % Liquid flowrate (kg/s) (1 kg/s = 1 l/s approx)
% if (time < 10)
%
%    inletligmassrate=0.0;
%    inletgasmassrate=0.0;
%
% elseif ((time>=10) & (time < 20))
%    inletligmassrate = 0*(time-10)/10;
%    inletgasmassrate = XX*(time-10)/10;
%
% elseif ((time >=20) & (time<110))
%    inletligmassrate = 0;
%    inletgasmassrate = XX;
%
% elseif ((time>=110)& (time<120))
%    inletligmassrate = 0;
%    inletgasmassrate = XX-XX*(time-110)/10;
% elseif ((time>=120&time<130))
%    inletligmassrate =0;
%    inletgasmassrate =0;
% elseif ((time>=130)&(time<300))
%    inletligmassrate =0;
%    inletgasmassrate =0;
% elseif ((time>=300)&(time<310))
%    inletligmassrate= YY*(time-300)/10;
%    inletgasmassrate =0;
% elseif((time>=310))
%    inletligmassrate= YY;
%    inletgasmassrate =0;
% end

kickvolume = kickvolume+inletgasmassrate/dgo(1)*dt;  % Here we find the
kickvolume

% initially induced in the well.

% Here we specify the physical outlet pressure. Here we have given the
pressure as
% constant. It would be possible to adjust it during openwell conditions
% either by giving the wanted pressure directly (in the command lines
% above) or by finding it indirectly through a chokemodel where the
chokeopening
% would have had to be  an input parameter. The chokeopening variable would
equally had
% to be adjusted inside the controle structure given above.

 pressureoutlet = pbondout;

% Based on these given physical boundary values combined with use
% of extrapolations techniques
% for the remaining unknowns at the boundaries, we will define the mass and
% momentum fluxes at the boundaries (inlet and outlet of pipe).

% inlet/bottom fluxes first.
    if (bullheading<=0)
 % Here we pump from bottom
```

```matlab
        flc(1,1)= inletligmassrate/area(1);
        flc(1,2)= 0.0;
        flc(1,3)= flc(1,1)*vlo(1);

        fgc(1,1)= 0.0;
        fgc(1,2)= inletgasmassrate/area(1);
        fgc(1,3)= fgc(1,2)*vgo(1);

        fp(1,1)= 0.0;
        fp(1,2)= 0.0;

% Old way of treating the boundary
%     fp(1,3)= po(1)+0.5*(po(1)-po(2)); %Interpolation used to find the
% pressure at the inlet/bottom of the well.

% New way of treating the boundary
        fp(1,3)= po(1)...
            +0.5*dx*(dlo(1)*evo(1)+dgo(1)*ego(1))*g...
            +0.5*dx*fricgrad(1);

    else
      % Here we pump from the top. All masses are assumed to flow out of the
      % well into the formation. We use first order extrapolation.
      flc(1,1)=dlo(1)*evo(1)*vlo(1);
      flc(1,2)=0.0;
      flc(1,3)=flc(1,1)*vlo(1);

      fgc(1,1)=0.0;
      fgc(1,2)=dgo(1)*ego(1)*vgo(1);
      fgc(1,3)=fgc(1,2)*vgo(1);

      fp(1,1)=0.0;
      fp(1,2)=0.0;
      fp(1,3)=20000000;
%       (Pa) This was a fixed pressure set at bottom when bullheading
    end

% Outlet fluxes (open & closed conditions)

    if (wellopening>0.01)

% Here open end condtions are given. We distinguish between bullheading
% & normal circulation.

        if (bullheading<=0)  % Here we dont bullhead, i.e we circulate from
bottom

           % Here the is normal ciruclation and open well)
             flc(nofluxes,1)= dlo(nobox)*evo(nobox)*vlo(nobox);
             flc(nofluxes,2)= 0.0;
             flc(nofluxes,3)= flc(nofluxes,1)*vlo(nobox);

             fgc(nofluxes,1)= 0.0;
             fgc(nofluxes,2)= dgo(nobox)*ego(nobox)*vgo(nobox);
%             fgc(nofluxes,2)=0; Activate if gas is sucked in!?
             fgc(nofluxes,3)= fgc(nofluxes,2)*vgo(nobox);

             fp(nofluxes,1)= 0.0;
             fp(nofluxes,2)= 0.0;
```

134

```matlab
                fp(nofluxes,3)= pressureoutlet;
        else
            % Here we are bullheading.
            flc(nofluxes,1)= inletligmassrate/area(nobox);
            flc(nofluxes,2)= 0.0;
            flc(nofluxes,3)= flc(nofluxes,1)*vlo(nobox);

            fgc(nofluxes,1)=0.0;
            fgc(nofluxes,2)=0.0;
            fgc(nofluxes,3)=0.0;

            fp(nofluxes,1)=0.0;
            fp(nofluxes,2)=0.0;
            fp(nofluxes,3)= po(nobox)...
            -0.5*dx*(dlo(nobox)*evo(nobox)+dgo(nobox)*ego(nobox))*g...
            +0.5*dx*fricgrad(nobox); %check sign here on friction
            % Physcially, the friction should be added when going from
            % mid point in upper cell to outlet. But if fricgrad(nobox) is
            % negative there should be a minus in front of the term to have
            % + in the end.
        end
    else

% Here closed end conditions are given

            flc(nofluxes,1)= 0.0;
            flc(nofluxes,2)= 0.0;
            flc(nofluxes,3)= 0.0;

            fgc(nofluxes,1)= 0.0;
            fgc(nofluxes,2)= 0.0;
            fgc(nofluxes,3)= 0.0;

            fp(nofluxes,1)=0.0;
            fp(nofluxes,2)=0.0;

    %     Old way of treating the boundary
    %      fp(nofluxes,3)= po(nobox)-0.5*(po(nobox-1)-po(nobox));

    %     New way of treating the boundary
            fp(nofluxes,3)= po(nobox)...
            -0.5*dx*(dlo(nobox)*evo(nobox)+dgo(nobox)*ego(nobox))*g;
    %      -0.5*dx*fricgrad(nobox); % Neglect friction since well is closed.
        end

% Implementation of slopelimiters. They are applied on the physical
 % variables like phase densities, phase velocities and pressure.

% It was found that if the slopelimiters were set to zero in
% the boundary cells, the pressure in these became wrong. E.g. the upper
% cell get an interior pressure that is higher than it should be e.g. when
% being static (hydrostatic pressure was too high). The problem was reduced
% by copying the slopelimiters from the interior cells. However, both
% approaches seems to give the same BHP pressure vs time but the latter
% approach give a more correct pressure vs depth profile. It is also better
% to use when simulating pressure build up where the upper cell pressure
% must be monitored. It should be checked more in detail before concluding.
% BUT; there has been mass conservation problems with the scheme for the
% case where the slopelimiters were copied (see master thesis of Keino)
```

```matlab
% A possible fix has been included below where the slopelimiter related to
% the gas volume fraction is set to zero in the first cell.

    for i=2:nobox-1
     sl1(i)=minmod(dlo(i-1),dlo(i),dlo(i+1),dx);
     sl2(i)=minmod(po(i-1),po(i),po(i+1),dx);
     sl3(i)=minmod(vlo(i-1),vlo(i),vlo(i+1),dx);
     sl4(i)=minmod(vgo(i-1),vgo(i),vgo(i+1),dx);
     sl5(i)=minmod(ego(i-1),ego(i),ego(i+1),dx);
     sl6(i)=minmod(dgo(i-1),dgo(i),dgo(i+1),dx);
    end

 % Slopelimiters in outlet boundary cell are set to zero!
%      sl1(nobox)=0;
%      sl2(nobox)=0;
%      sl3(nobox)=0;
%      sl4(nobox)=0;
%      sl5(nobox)=0;
%      sl6(nobox)=0;

 % Slopelimiters in outlet boundary cell are copied from neighbour cell!
    sl1(nobox)=sl1(nobox-1);
    sl2(nobox)=sl2(nobox-1);
    sl3(nobox)=sl3(nobox-1);
    sl4(nobox)=sl4(nobox-1);
    sl5(nobox)=sl5(nobox-1);
    sl6(nobox)=sl6(nobox-1);

% Slopelimiters in inlet boundary cell are set to zero!
%      sl1(1)=0;
%      sl2(1)=0;
%      sl3(1)=0;
%      sl4(1)=0;
%      sl5(1)=0;
%      sl6(1)=0;

% Slopelimiters in inlet boundary cell are copied from neighbour cell!
    sl1(1)=sl1(2);
    sl2(1)=sl2(2);
    sl3(1)=sl3(2);
    sl4(1)=sl4(2);
    sl5(1)=sl5(2);
    sl6(1)=sl6(2);

% FIX FOR OMITTING THE MASS CONSERVATION PROBLEMS
    sl5(1)=0;
    sl5(nobox)=0;

% Now we will find the fluxes between the different cells.
% NB - IMPORTANT -  Note that if we change the compressibilities/sound
velocities of
% the fluids involved, we may need to do changes inside the csound
function.
% But the effect of this is unclear.

    for j = 2:nofluxes-1

 %%%%%%%%%%%%%%%%%%%%%%%%%%%%%%%%%%%%%%%%%%%%%%%%
 %%%%%%%%%%%%%%%%%%%%%%%%%%%%%%%%%%%%%%%%%%%%%%%%
% First order method is from here: If you want to test this, activate this
```

```
%  and comment the second order code below.
%         cl = csound(ego(j-1),po(j-1),dlo(j-1),k);
%         cr = csound(ego(j),po(j),dlo(j),k);
%         c = max(cl,cr);
%         pll = psip(vlo(j-1),c,evo(j));
%         plr = psim(vlo(j),c,evo(j-1));
%         pgl = psip(vgo(j-1),c,ego(j));
%         pgr = psim(vgo(j),c,ego(j-1));
%         vmixr = vlo(j)*evo(j)+vgo(j)*ego(j);
%         vmixl = vlo(j-1)*evo(j-1)+vgo(j-1)*ego(j-1);
%
%         pl = pp(vmixl,c);
%         pr = pm(vmixr,c);
%         mll= evo(j-1)*dlo(j-1);
%         mlr= evo(j)*dlo(j);
%         mgl= ego(j-1)*dgo(j-1);
%         mgr= ego(j)*dgo(j);
%
%         flc(j,1)= mll*pll+mlr*plr;
%         flc(j,2)= 0.0;
%         flc(j,3)= mll*pll*vlo(j-1)+mlr*plr*vlo(j);
%
%         fgc(j,1)=0.0;
%         fgc(j,2)= mgl*pgl+mgr*pgr;
%         fgc(j,3)= mgl*pgl*vgo(j-1)+mgr*pgr*vgo(j);
%
%         fp(j,1)= 0.0;
%         fp(j,2)= 0.0;
%         fp(j,3)= pl*po(j-1)+pr*po(j);


 %  First order methods ends here
 %%%%%%%%%%%%%%%%%%%%%%%%%%%%%%%%%%%%%%%%%%%%%%%%%%%%%%
 %%%%%%%%%%%%%%%%%%%%%%%%%%%%%%%%%%%%%%%%%%%%%%%%%%%%%%


%%%%%%%%%%%%%%%%%%%%%%%%%%%%%%%%%%%%%%%%%%%%%%%%%%%%%%%%%%%
%%%%%%%%%%%%%%%%%%%%%%%%%%%%%%%%%%%%%%%%%%%%%%%%%%%%%%%%%%%
% Second order method starts here:
% Here slopelimiter is used on all variables except phase velocoties

        psll = po(j-1)+dx/2*sl2(j-1);
        pslr = po(j)-dx/2*sl2(j);
        dsll = dlo(j-1)+dx/2*sl1(j-1);
        dslr = dlo(j)-dx/2*sl1(j);
        dgll = dgo(j-1)+dx/2*sl6(j-1);
        dglr = dgo(j)-dx/2*sl6(j);

        vlv = vlo(j-1)+dx/2*sl3(j-1);
        vlh = vlo(j)-dx/2*sl3(j);
        vgv = vgo(j-1)+dx/2*sl4(j-1);
        vgh = vgo(j)-dx/2*sl4(j);

        gvv = ego(j-1)+dx/2*sl5(j-1);
        gvh = ego(j)-dx/2*sl5(j);
        lvv = 1-gvv;
        lvh = 1-gvh;

        cl = csound(gvv,psll,dsll,k);
        cr = csound(gvh,pslr,dslr,k);
        c = max(cl,cr);
```

```
        pll = psip(vlo(j-1),c,lvh);
        plr = psim(vlo(j),c,lvv);
        pgl = psip(vgo(j-1),c,gvh);
        pgr = psim(vgo(j),c,gvv);
        vmixr = vlo(j)*lvh+vgo(j)*gvh;
        vmixl = vlo(j-1)*lvv+vgo(j-1)*gvv;


        pl = pp(vmixl,c);
        pr = pm(vmixr,c);

     mll= lvv*dsll;
     mlr= lvh*dslr;
     mgl= gvv*dgll;
     mgr= gvh*dglr;

     flc(j,1)= mll*pll+mlr*plr;
     flc(j,2)= 0.0;
     flc(j,3)= mll*pll*vlo(j-1)+mlr*plr*vlo(j);

     fgc(j,1)=0.0;
     fgc(j,2)= mgl*pgl+mgr*pgr;
     fgc(j,3)= mgl*pgl*vgo(j-1)+mgr*pgr*vgo(j);

     fp(j,1)= 0.0;
     fp(j,2)= 0.0;
     fp(j,3)= pl*psll+pr*pslr;
%%% Second order method ends here
%%%%%%%%%%%%%%%%%%%%%%%%%%%%%%%%%%%%%%%%%%%%%%%%%%%%%%%%%%%%%%%
%%%%%%%%%%%%%%%%%%%%%%%%%%%%%%%%%%%%%%%%%%%%%%%%%%%%%%%%%%%%%%%


% Here slopelimiters is used on all variables. This
% has not worked so well yet. Therefore it is commented away.

%        psll = po(j-1)+dx/2*sl2(j-1);
%        pslr = po(j)-dx/2*sl2(j);
%        dsll = dlo(j-1)+dx/2*sl1(j-1);
%        dslr = dlo(j)-dx/2*sl1(j);
%        dgll = dgo(j-1)+dx/2*sl6(j-1);
%        dglr = dgo(j)-dx/2*sl6(j);
%
%        vlv = vlo(j-1)+dx/2*sl3(j-1);
%        vlh = vlo(j)-dx/2*sl3(j);
%        vgv = vgo(j-1)+dx/2*sl4(j-1);
%        vgh = vgo(j)-dx/2*sl4(j);
%
%        gvv = ego(j-1)+dx/2*sl5(j-1);
%        gvh = ego(j)-dx/2*sl5(j);
%        lvv = 1-gvv;
%        lvh = 1-gvh;
%
%        cl = csound(gvv,psll,dsll,k);
%        cr = csound(gvh,pslr,dslr,k);
%        c = max(cl,cr);
%
%        pll = psip(vlv,c,lvh);
%        plr = psim(vlh,c,lvv);
%        pgl = psip(vgv,c,gvh);
%        pgr = psim(vgh,c,gvv);
%        vmixr = vlh*lvh+vgh*gvh;
%        vmixl = vlv*lvv+vgv*gvv;
```

```matlab
%
%          pl = pp(vmixl,c);
%          pr = pm(vmixr,c);
%          mll= lvv*dsll;
%          mlr= lvh*dslr;
%          mgl= gvv*dgll;
%          mgr= gvh*dglr;
%
%          flc(j,1)= mll*pll+mlr*plr;
%          flc(j,2)= 0.0;
%          flc(j,3)= mll*pll*vlv+mlr*plr*vlh;
%
%
%          fgc(j,1)=0.0;
%          fgc(j,2)= mgl*pgl+mgr*pgr;
%          fgc(j,3)= mgl*pgl*vgv+mgr*pgr*vgh;
%
%          fp(j,1)= 0.0;
%          fp(j,2)= 0.0;
%          fp(j,3)= pl*psll+pr*pslr;

      end

% Fluxes have now been calculated. We will now update the conservative
% variables in each of the numerical cells.

% The source terms can be calculated by using a
% for loop.
% Note that the model is sensitive to how we treat the model
% for low Reynolds numbers (possible discontinuity in the model)
      for j=1:nobox
        fricgrad(j)=dpfric(vlo(j),vgo(j),evo(j),ego(j),dlo(j),dgo(j), ...
          po(j),do(j),di(j),viscl,viscg); % Pa/m
        hydgrad(j)=g*(dlo(j)*evo(j)+dgo(j)*ego(j)); % Pa/m
      end

     sumfric = 0;
     sumhyd= 0;

     for j=1:nobox

   % Here we solve the three conservation laws for each cell and update
   % the conservative variables qv

     ar = area(j);

    % Liquid mass conservation
    qv(j,1)=qvo(j,1)-dtdx*((ar*flc(j+1,1)-ar*flc(j,1))...
                         +(ar*fgc(j+1,1)-ar*fgc(j,1))...
                         +(ar*fp(j+1,1)-ar*fp(j,1)));

    % Gas mass conservation:

    qv(j,2)=qvo(j,2)-dtdx*((ar*flc(j+1,2)-ar*flc(j,2))...
                         +(ar*fgc(j+1,2)-ar*fgc(j,2))...
                         +(ar*fp(j+1,2)-ar*fp(j,2)));
    % Mixture momentum conservation:

    qv(j,3)=qvo(j,3)-dtdx*((ar*flc(j+1,3)-ar*flc(j,3))...
```

```
                              +(ar*fgc(j+1,3)-ar*fgc(j,3))...
                              +(ar*fp(j+1,3)-ar*fp(j,3)))...
                    -dt*ar*(fricgrad(j)+hydgrad(j));

%  Add up the hydrostatic pressure  and friction  in the whole well.
      sumfric=sumfric+fricgrad(j)*dx;
      sumhyd=sumhyd+hydgrad(j)*dx;


      end

% Section where we find the physical variables (pressures, densities etc)
% from the conservative variables. Some trickes to ensure stability. These
% are induced to avoid negative masses.

      gasmass=0;
      liqmass=0;

      for j=1:nobox

% Remove the area from the conservative variables to find the
% the primitive variables from the conservative ones.

      qv(j,1)= qv(j,1)/area(j);
      qv(j,2)= qv(j,2)/area(j);

      if (qv(j,1)<0.00000001)  % Trick to avoid negative masses.
        qv(j,1)=0.00000001;
      end

      if (qv(j,2)< 0.00000001)  % Trick to avoid negative masses.
        qv(j,2)=0.00000001;
      end

 % Here we summarize the mass of gas and liquid in the well respectively.
 % These variables are important to show that the scheme is conserving
 % mass. (if e.g. gas leaks in our out of the well unintentionally in the
simulation
 % without being specified in the code,something fundamental is wrong.

      gasmass = gasmass+qv(j,2)*area(j)*dx;
      liqmass = liqmass+qv(j,1)*area(j)*dx;

% Below, we find the primitive variables pressure and densities based on
% the conservative variables q1,q2. One can choose between getting them by
% analytical or numerical solution approach specified in the beginning of
% the program. Ps. For more advanced density models, this must be changed.


      if (analytical == 1)
%         % Analytical solution:

% here the simple density models used in PET 510 Wellflow modelling
% compendium is used.

      t1=rho0-P0/al^2;

%  Coefficients:
      a = 1/(al*al);
```

140

```matlab
        b = t1-qv(j,1)-rt*qv(j,2)/(al*al);
        c = -1.0*t1*rt*qv(j,2);

%        Note here we use the very simple models from the PET510 course
        p(j)=(-b+sqrt(b*b-4*a*c))/(2*a);   % Pressure
        dl(j)=rholiq(p(j),temp(j)); % Density of liquid
        dg(j)=rogas(p(j),temp(j)); % Density of gas

%     The code below can be activated if we want to switch to the other set
%     of density models. Also then remember to do the changes inside
%     functions rogas og rholiq if we change density models.

%          x1=rho0-P0*rho0/Bheta-rho0*Alpha*(temp(j)-T0);
%          x2=rho0/Bheta;
%          x3=-qv(j,2)*R*temp(j);

%          a = x2;
%          b = x1+x2*x3-qv(j,1);
%          c = x1*x3;

%          p(j)=(-b+sqrt(b*b-4*a*c))/(2*a);   % Pressure
%          dl(j)=rholiq(p(j),temp(j));
%          dg(j)=rogas(p(j),temp(j));
        else

        % Numerical Solution: This might be used if we use more complex
        %density models. Has not been used for years.

         [p(j),error]=itsolver(po(j),qv(j,1),qv(j,2)); % Pressure
         dl(j)=rholiq(p(j),temp(j)); % Density of liquid
         dg(j)=rogas(p(j)); % Density of gas

        % In case a numerical solution is not found, the program will write
out "error":
        if error > 0
           error
        end
        end

%   Find phase volume fractions
        eg(j)= qv(j,2)/dg(j);
        ev(j)=1-eg(j);

 %  Reset average conservative varibles in cells with area included in the
variables.

     qv(j,1)=qv(j,1)*area(j);
     qv(j,2)=qv(j,2)*area(j);

     end  % End of loop

 %    Below we find the phase velocities by combining the
 %    conservative variable defined by the mixture momentum equation
 %    with the gas slip relation.
 %    At the same time we try to summarize the gas volume in the well. This
 %    also measure the size of the kick.

%%% BEFORE IMPLEMENTATION OF GAS SLIP VARIATIONS %%%
%
```

```
%       gasvol=0;
%
%     for j=1:nobox
%     % The  interpolations introduced below are included
%     % to omit a singularity in the slip relation when the gas volume
%     % fraction becomes equal to 1/K. In additon, S is interpolated to
%     % zero when approaching one phase gas flow. In the transition to
%     % one phase gas flow, we have no slip condtions (K=1, S=0)
%     % We will let the k0,s0,k1,s1 be arrays to make it easier to
incorporate
%     % different flow regimes later.  In that case, the slip parameters
will
%     % vary from cell to cell and we must have slip parameter values for
each
%     % cell.
%
%         ktemp=k;
%         stemp=s;
%
%         k0(j) = ktemp;
%         s0(j) = stemp;
%
%      % Interpolation to handle that (1-Kxgasvolumefraction) does not
become zero
%         if ((eg(j)>=0.7) & (eg(j)<=0.8))
%           xint = (eg(j)-0.7)/0.1;
%           k0(j) =1.0*xint+k*(1-xint);
%         elseif(eg(j)>0.8)
%           k0(j)=1.0;
%         end
%
%
%      % Interpolate S to zero in transition to pure gas phase
%         if ((eg(j)>=0.9) & (eg(j)<=1.0))
%           xint = (eg(j)-0.9)/0.1;
%           s0(j) = 0.0*xint+s*(1-xint);
%         end
%
%     % Note that the interpolations above and below can be changed
%     % if numerical stability problems
%     % are encountered.
%
%
%         if (eg(j)>=0.99999)
%          % Pure gas
%           k1(j) = 1.0;
%           s1(j) = 0.0;
%         else
%           %Two phase flow
%           k1(j) = (1-k0(j)*eg(j))/(1-eg(j));
%           s1(j) = -1.0*s0(j)*eg(j)/(1-eg(j));
%         end
%
%
%
%         help1 = dl(j)*ev(j)*k1(j)+dg(j)*eg(j)*k0(j);
%         help2 = dl(j)*ev(j)*s1(j)+dg(j)*eg(j)*s0(j);
%
%
%         vmixhelpl = (qv(j,3)/area(j)-help2)/help1;
%         vg(j)=k0(j)*vmixhelpl+s0(j);
```

```matlab
%         vl(j)=k1(j)*vmixhelpl+s1(j);
%
%
%
%
%
%
%         % Variable for summarizing the gas volume content in the well.
%         gasvol=gasvol+eg(j)*area(j)*dx;
%
%
%     end
%
%
% % Old values are now set equal to new values in order to prepare
% % computation of next time level.
%
%
%     po=p;
%     dlo=dl;
%     dgo=dg;
%     vlo=vl;
%     vgo=vg;
%     ego=eg;
%     evo=ev;
%     qvo=qv;
%
%
%
% % Section where we save some timedependent variables in arrays.
% % e.g. the bottom hole pressure. They will be saved for certain
% % timeintervalls defined in the start of the program in order to ensure
% % that the arrays do not get to long!
%
%   if (counter>=nostepsbeforesavingtimedata)
%     printcounter=printcounter+1;
%     time  % Write time to screen.
%
%     % Outlet massrates (kg/s) vs time
%
liquidmassrateout(printcounter)=dl(nobox)*ev(nobox)*vl(nobox)*area(nobox);
%
gasmassrateout(printcounter)=dg(nobox)*eg(nobox)*vg(nobox)*area(nobox);
%
%     % Outlet flowrates (lpm) vs time
%     liquidflowrateout(printcounter)=liquidmassrateout(printcounter)/...
%         rholiq(P0,T0)*1000*60;
%     gasflowrateout(printcounter)=gasmassrateout(printcounter)/...
%         rogas(P0,T0)*1000*60;
%
%     % Hydrostatic and friction pressure (bar) in well vs time
%     hyd(printcounter)=sumhyd/100000;
%     fric(printcounter)=sumfric/100000;
%
%     % Volume of gas in well vs time (m3). Also used for indicating kick
%     % size in well.
%
%     volgas(printcounter)=gasvol;
%
%     % Total phase masses (kg) in the well vs time
%     % Used for checking mass conservation.
%
%      massgas(printcounter)=gasmass;
```

143

```matlab
%       massliq(printcounter)=liqmass;
%
%
%       % pout calculates the pressure at the outletboundary. I.e. upper edge
%       % of uppermost cell. Corresponds where the well ends at surface. The
%       % reason we do this is the fact than in AUSMV is all variables
defined
%       % in the mid point of the numerical cells.
%       pout(printcounter)=(p(nobox)-0.5*dx*...
%       (dlo(nobox)*evo(nobox)+dgo(nobox)*ego(nobox))*g-
dx*0.5*fricgrad(nobox))/100000;
%
%
%       % pin (bar) defines the  pressure at the inlet boundary, I.e lower
edge
%       % of the lowermost cell. Corresponds to TD of well.
%       pin(printcounter)=
(p(1)+0.5*dx*(dlo(1)*evo(1)+dgo(1)*ego(1))*g+0.5*dx*fricgrad(1))/100000;
%
%       % Pressure in the middle of top box (bar).
%       pnobox(printcounter)=p(nobox)/100000;   %
%
%
%       % Time variable
%       timeplot(printcounter)=time;
%
%       counter = 0;
%
%
%    end
%    end
%
%
% % end of stepping forward in time.
%
%%% MODEL ENDS HERE %%%

%%% MODEL TO CONTROL FROM WHERE SUSPENSION GOES TO BUBBLE FLOW %%%

   gasvol=0;

      ksusp=1; %%% suspended k-value
      ssusp=0; %%% suspended s-value
      kbubble=1; %%% bubble k-value
      kslug=1.2; %%% slug k-value

minsusplim=0.00; % For all gas volume fractions below - fully suspended;
0.00, 0.01, 0.03, 0.05, 0.07 for 0%, 1%, 3%, 5%, 7% suspension respectively
maxsusplim=0.00; % Fully developed bubble flow;  0.00, 0.03, 0.05, 0.07,
0.09 for 0%, 1%, 3%, 5%, 7% suspension respectively (2% transition
interval)
                % 0.00, 0.05, 0.07 for 0%, 1%, 3% suspension respectively
(4% transition interval)

for j=1:nobox
    %   WELL DEVIATION AND ANNULAR GEOMETRY CORRECTIONS FOR SLUG FLOW
    %ftheta=cosd(angle)^0.5*(1+sind(angle)).^1.2; % Well-deviation factor
in terms of deviation angle from vertical (eq. A-10 in SPE-109868)
    %fa(j)=(1+(0.29*di(j))/do(j)); % Annulus factor in terms of the annulus
inside/outside diameter ratio (eq. A-11 in SPE-109868)
```

```matlab
    if (eg(j)<=minsusplim) % Case of suspension
        ktemp=ksusp;
        stemp=ssusp;
        flowregime(j)=1;
    elseif((eg(j)>minsusplim)&(eg(j)<maxsusplim)) % Transition from
suspension to bubble flow
        xinttemp=(eg(j)-minsusplim)/(maxsusplim-minsusplim);
        ktemp=xinttemp*kbubble+(1-xinttemp)*ksusp;
        sbubble=1.53*(g*(dlo(j)-dgo(j))*sigma/(dlo(j)^2))^0.25;
        stemp=xinttemp*sbubble+(1-xinttemp)*ssusp;
        flowregime(j)=2 ;
    elseif((eg(j)>=maxsusplim)&(eg(j)<0.20)) % Case of bubble flow for high
transition zone from bubble to slug flow (gas fractions at 20-25%)
%   elseif((eg(j)>=maxsusplim)&(eg(j)<0.10)) % For low transition zone from
bubble to slug flow (gas fractions at 10-15%)
        ktemp=kbubble;
        sbubble=1.53*(g*(dlo(j)-dgo(j))*sigma/(dlo(j)^2))^.25;
        stemp=sbubble;
        flowregime(j)=3;
    elseif((eg(j)>=0.20)&(eg(j)<0.25))% Transition from bubble to slug flow
for high transition zone from bubble to slug flow (gas fractions at 20-25%)
%   elseif((eg(j)>=0.10)&(eg(j)<0.15)) % For low transition zone from
bubble to slug flow (gas fractions at 10-15%)
        xinttemp=(eg(j)-0.20)/0.05;
%       xinttemp=(eg(j)-0.10)/0.05; % For low transition zone from bubble
to slug flow (gas fractions at 10-15%)
        ktemp=xinttemp*kslug+(1-xinttemp)*kbubble;
        sbubble=1.53*(g*(dlo(j)-dgo(j))*sigma/(dlo(j)^2))^0.25;
        sslug=(0.35*(g*do(j)*(dlo(j)-dgo(j))/dlo(j))^0.5);%*ftheta*fa(j);

        stemp=xinttemp*sslug+(1-xinttemp)*sbubble;
        flowregime(j)=4;
    else % Case of slug flow
        ktemp=kslug;
        sslug=(0.35*(g*do(j)*(dlo(j)-dgo(j))/dlo(j))^0.5);%*ftheta*fa(j);

        stemp=sslug;
        flowregime(j)=5;
    end

    k0(j)=ktemp;
    s0(j)=stemp;

%%% MODEL ENDS HERE %%%

%     k0(j)=1.20; % To keep fixed gas slip model, i.e. slug flow
%     s0(j)=0.55; % Commented away to test gas slip interpolation

    % Interpolation to handle that (1-Kxgasvolumefraction) does not become
    % zero

    if ((eg(j))>=0.7)&(eg(j)<=0.8) % K interpolated to 1.0 at [0.7,0.8]
%   if ((eg(j))>=0.6)&(eg(j)<=0.8) % K interpolated to 1.0 at [0.6,0.8]
        xint=(eg(j)-0.7)/0.1;
%       xint=(eg(j)-0.6)/0.2; % K interpolated to 1.0 at [0.6,0.8]
        k0(j)=1.0*xint+kslug*(1-xint);
    elseif(eg(j)>0.8)
        k0(j)=1.0;
    end
```

```matlab
    % Interpolate S to zero in transition to pure gas phase

    if (eg(j)>=0.9 &(eg(j)<=1.0)) % S interpolated to 0 at [0.9,1.0]
%   if (eg(j)>=0.6 &(eg(j)<=1.0)) % S interpolated to 0 at [0.6,1.0]
        xint=(eg(j)-0.9)/0.1;
%       xint=(eg(j)-0.6)/0.4; % S interpolated to 0 at [0.6,1.0]
        s0(j)=0.0*xint+sslug*(1-xint);
    end

    if (eg(j)>=0.99999)
        k1(j)=1.0;
        s1(j)=0.0;
    else % Two phase flow
        k1(j)=(1-k0(j)*eg(j))/(1-eg(j));
        s1(j)=-1.0*s0(j)*eg(j)/(1-eg(j));
    end

    help1=dl(j)*ev(j)*k1(j)+dg(j)*eg(j)*k0(j);
    help2=dl(j)*ev(j)*s1(j)+dg(j)*eg(j)*s0(j);

    vmixhelp1=(qv(j,3)/area(j)-help2)/help1;
    vg(j)=k0(j)*vmixhelp1+s0(j);
    vl(j)=k1(j)*vmixhelp1+s1(j);

    vgcosmetic(j)=vg(j);
    if eg(j)<0.01
        vgcosmetic(j)=0;
    end

    % Variable for summarizing the gas volume content in the well

    gasvol=gasvol+eg(j)*area(j)*dx;

end

% Old values are now set equal to new values in order to prepare
% computation of next time level.


po=p;
dlo=dl;
dgo=dg;
vlo=vl;
vgo=vg;
ego=eg;
evo=ev;
qvo=qv;

% Section where we save some timedependent variables in arrays.
% e.g. the bottom hole pressure. They will be saved for certain
% timeintervalls defined in the start of the program in order to ensure
% that the arrays do not get to long!

if (counter>=nostepsbeforesavingtimedata)
    printcounter=printcounter+1;
    time   % Write time to screen.
```

```matlab
    % Outlet massrates (kg/s) vs time

liquidmassrateout(printcounter)=dl(nobox)*ev(nobox)*vl(nobox)*area(nobox);
    gasmassrateout(printcounter)=dg(nobox)*eg(nobox)*vg(nobox)*area(nobox);

    % Outlet flowrates (lpm) vs time
    liquidflowrateout(printcounter)=liquidmassrateout(printcounter)/...
        rholiq(P0,T0)*1000*60;
    gasflowrateout(printcounter)=gasmassrateout(printcounter)/...
        rogas(P0,T0)*1000*60;

    % Hydrostatic and friction pressure (bar) in well vs time
    hyd(printcounter)=sumhyd/100000;
    fric(printcounter)=sumfric/100000;

    % Volume of gas in well vs time (m3). Also used for indicating kick
    % size in well.

    volgas(printcounter)=gasvol;

    % Total phase masses (kg) in the well vs time
    % Used for checking mass conservation.

     massgas(printcounter)=gasmass;
     massliq(printcounter)=liqmass;

    % pout calculates the pressure at the outletboundary. I.e. upper edge
    % of uppermost cell. Corresponds where the well ends at surface. The
    % reason we do this is the fact than in AUSMV is all variables defined
    % in the mid point of the numerical cells.
    pout(printcounter)=(p(nobox)-0.5*dx*...
    (dlo(nobox)*evo(nobox)+dgo(nobox)*ego(nobox))*g-
dx*0.5*fricgrad(nobox))/100000;

    % pin (bar) defines the  pressure at the inlet boundary, I.e lower edge
    % of the lowermost cell. Corresponds to TD of well.
    pin(printcounter)=
(p(1)+0.5*dx*(dlo(1)*evo(1)+dgo(1)*ego(1))*g+0.5*dx*fricgrad(1))/100000;

    % Pressure in the middle of top box (bar).
    pnobox(printcounter)=p(nobox)/100000;  %

     % Time variable
    timeplot(printcounter)=time;

    counter = 0;

  end
end


% Printing of results section

countsteps % Marks number of simulation steps.

% Plot commands for variables vs time. The commands can also
% be copied to command screen where program is run for plotting other
% variables.
```

```
toc,
e = cputime-t

% Plot bottom hole pressure
%plot(timeplot,pin)

% Show cfl number used.
disp('cfl')
cfl = al*dt/dx

%plot(timeplot,pin)
%plot(timeplot,hyd)
%plot(timeplot,fric)
%plot(timeplot,liquidmassrateout)
%plot(timeplot,gasmassrateout)
%plot(timeplot,volgas)
%plot(timeplot,liquidflowrateout)
%plot(timeplot,gasflowrateout)
%plot(timeplot,massgas)
%plot(timeplot,massliq)
%plot(timeplot,pout)
%plot(timeplot,pnobox)

% Plot commands for variables vs depth/Only the last simulated
%values at endtime is visualised

%plot(vl,x);
%plot(vg,x);
%plot(eg,x);
%plot(p,x);
%plot(dl,x);
%plot(dg,x);
```

Appendix C

Example of MATLAB code to display plots (Case 4 – Effect of Different Suspension Limits):

```
load 0percent_20000_4
pb1=pin;
ps1=pout;
tid1=timeplot;
x1=x;
ml1=massliq;
mg1=massgas;
vol1=volgas;


load 1percent_20000_4

pb2=pin;
ps2=pout;
tid2=timeplot;
x2=x;
ml2=massliq;
mg2=massgas;
vol2=volgas;


load 3percent_20000_4

pb3=pin;
ps3=pout;
tid3=timeplot;
x3=x;
ml3=massliq;
mg3=massgas;
vol3=volgas;


load 5percent_20000_4

pb4=pin;
ps4=pout;
tid4=timeplot;
x4=x;
ml4=massliq;
mg4=massgas;
vol4=volgas;


load 7percent_20000_4

pb5=pin;
ps5=pout;
tid5=timeplot;
x5=x;
ml5=massliq;
mg5=massgas;
vol5=volgas;


load 0percent_4000_4

vl1=vl;
vg1=vgcosmetic;
eg1=eg;
```

```matlab
x1=x;

load 1percent_4000_4

vl2=vl;
vg2=vg;
eg2=eg;
x2=x;

load 3percent_4000_4

vl3=vl;
vg3=vg;
eg3=eg;
x3=x;

load 5percent_4000_4

vl4=vl;
vg4=vg;
eg4=eg;
x4=x;

load 7percent_4000_4

vl5=vl;
vg5=vg;
eg5=eg;
x5=x;

%%% PLOT MASSLIQ, MASSGAS
% subplot(1,2,1)
%  plot(tid1,ml1,'black',tid2,ml2,'g',tid3,ml3,'b',tid4,ml4,'r',tid5,ml5,'-
-b','linewidth',1.5)
%  xlabel ('time (s)')
%  ylabel('total gas mass (kg)')
%  title('Liquid mass')
%  legend('0%','1%','3%','5%','7%','location','best')
%  grid on
% subplot(1,2,2)
%
plot(tid1,mg1,'black',tid2,mg2,'g',tid3,mg3,'b',tid4,mg4,'r',tid5,mg5,'--
b','linewidth',1.5)
%  xlabel('time (s)')
%  ylabel('total liquid mass (kg)')
%  title('Gas mass')
%  legend('0%','1%','3%','5%','7%','location','best')
%  grid on

%%% PLOT VOLGAS, BHP, WHP
%
plot(tid1,vol1,'black',tid2,vol2,'g',tid3,vol3,'b',tid4,vol4,'red',tid5,vol
5,'--b','linewidth',2)
%  xlabel ('time (s)')
%  ylabel('total gas volume (m3)')
%  title('Gas volume')
%  legend('0%','1%','3%','5%','7%','location','best')
%  grid on
```

```matlab
% subplot(1,2,1)
%
plot(tid1,pb1,'black',tid2,pb2,'g',tid3,pb3,'b',tid4,pb4,'red',tid5,pb5,'--
b','linewidth',2)
%  xlabel ('time (s)')
%  ylabel('BHP (bar)')
%  title('BHP')
%  legend('0%','1%','3%','5%','7%','location','best')
%  axis([0 20000 350 700])
%  grid on
% subplot(1,2,2)
%
plot(tid1,ps1,'black',tid2,ps2,'g',tid3,ps3,'b',tid4,ps4,'red',tid5,ps5,'--
b','linewidth',2)
%  xlabel ('time (s)')
%  ylabel('WHP (bar)')
%  title('WHP')
%  legend('0%','1%','3%','5%','7%','location','best')
%  axis([0 20000 0 300])
%  grid on

%%% PLOT EG, VL, VG
%  plot(eg1,x1,'black',eg2,x2,'g',eg3,x3,'b',eg4,x4,'red',eg5,x5,'--
b','linewidth',2)
%  xlabel ('gas volume fraction (0-1)')
%  ylabel('depth (m)')
%  title('Gas volume fraction')
%  legend('0%','1%','3%','5%','7%','location','best')
%  axis([0 0.25 -4000 0])
%  grid on

% subplot(1,2,1)
%  plot(vl1,x1,'black',vl2,x2,'g',vl3,x3,'b',vl4,x4,'red',vl5,x5,'--
b','linewidth',2)
%  xlabel ('liquid velocity (m/s)')
%  ylabel('depth (m)')
%  title('Liquid velocity')
%  legend('0%','1%','3%','5%','7%','location','best')
%  axis([-0.05 0.25 -4000 0])
%  grid on
% subplot(1,2,2)
%  plot(vg1,x1,'black',vg2,x2,'g',vg3,x3,'b',vg4,x4,'red',vg5,x5,'--
b','linewidth',2)
%  xlabel ('gas velocity (m/s)')
%  ylabel('depth (m)')
%  title('Gas velocity')
%  legend('0%','1%','3%','5%','7%','location','best')
%  axis([-0.05 0.25 -4000 0])
% %  axis([0 0.5 -4000 0])
%  grid on
```

Appendix D

Functions used in the main MATLAB codes (Appendix A and B):

pim

```
function pmvalue = pp(v,c)

  if (abs(v)<=c)
    pmvalue = (v+c)*(v+c)/(4*c)*(2.0-v/c)/c;
  else
    pmvalue = 0.5*(v+abs(v))/v;
  end
end
```

psip

```
function pmvalue = psip(v,c,alpha)

  if (abs(v)<=c)
    pmvalue = alpha*(v+c)*(v+c)/(4*c)+(1-alpha)*(v+abs(v))/2;
  else
    pmvalue = 0.5*(v+abs(v));
  end
end
```

rholiq

```
function [rhol] = rholiq(pressure,temperature)
%Simple model for liquid density
% p0 = 100000.0; % Assumed
% t0 = 20+273.15;
% beta = 2.2*10^9;
% alpha = 0.000207;
% rho0 = 1000;
% %rhol = 1000.0 + (pressure-p0)/(1500.0*1500.0);
% rhol = rho0+((rho0/beta)*(pressure-p0))-(rho0*alpha*(temperature-t0));

% SIMPLE PET 510 Model below:

if (pressure < 100000)
 pressure = 100000;
end
rhol = 1000+ (pressure-100000)/1500^2;
end
```

rogas

```
function rhog = rogas(pressure,temp)

%Simple gas density model. Temperature is neglected.
% rhogas = pressure / (velocity of sound in the gas phase)^2 = pressure /
% rT --> gas sound velcoity = SQRT(rT)
 % rhog = 4200;
%  R = 286.9;
%  rhog = pressure/(R*temp);

% SIMPLE PET 510 model below:
```

```matlab
if (pressure < 100000)
 pressure = 100000;
end

rhog = pressure/100000;
```

csound

```matlab
function mixsoundvelocity = csound(gvo,po,dlo,k)
% Note that at this time k is set to 1.0 (should maybe be
% included below

temp= gvo*dlo*(1.0-gvo);
a=1;
if (temp < 0.01)
  temp = 0.01;
end

cexpr = sqrt(po/temp);

if (gvo <= 0.5)
 mixsoundvelocity = min(cexpr,1500);
else
 mixsoundvelocity = min(cexpr,316);
end

%mixsoundvelocity = 1500*(1-gvo)+6000*gvo;
```

dpfric

```matlab
function friclossgrad =
dpfric(vlo,vgo,evo,ego,dlo,dgo,pressure,do,di,viscl,viscg)

%friclossgrad =
%dpfric(vlo,vgo,evo,ego,dlo,dgo,pressure,do,di,viscl,viscg)
% Works for two phase flow. The one phase flow model is used but mixture
 % values are introduced.

%  rhol = dlo;
%  rhog = dgo;
%  vmixfric = vlo.*evo+vgo.*ego;
%  viscmix =  viscl.*evo+viscg.*ego;
%  densmix = dlo.*evo+dgo.*ego;
%
%  % Calculate mix reynolds number
%  Re = ((densmix.*abs(vmixfric).*(do-di))./viscmix);
%
%  % Calculate friction factor. For Re > 3000, the flow is turbulent.
%  % For Re < 2000, the flow is laminar. Interpolate in between.
%
%  if (Re<0.001)
%    f=0.0;
%  else
%   if (Re >= 3000)
%    f = 0.052*Re.^(-0.19);
%   elseif ( (Re<3000) & (Re > 2000))
%    f1 = 24./Re;
%    f2 = 0.052*Re.^(-0.19);
%    xint = (Re-2000)./1000.0;
%    f = (1.0-xint).*f1+xint.*f2;
```

153

```matlab
%    else
%      f = 24./Re;
%    end
%   end
%
%   friclossgrad = ((2*f.*densmix.*vmixfric.*abs(vmixfric))./(do-di));


  vmixfric = vlo*evo+vgo*ego;
  viscmix =  viscl*evo+viscg*ego;
  densmix = dlo*evo+dgo*ego;

 % Calculate mix reynolds number
 Re = ((densmix*abs(vmixfric)*(do-di))/viscmix);

 % Calculate friction factor. For Re > 3000, the flow is turbulent.
 % For Re < 2000, the flow is laminar. Interpolate in between.

 if (Re<0.001)
   f=0.0;
 else
  if (Re >= 3000)
   f = 0.052*Re^(-0.19);
  elseif ( (Re<3000) & (Re > 2000))
   f1 = 24/Re;
   f2 = 0.052*Re^(-0.19);
   xint = (Re-2000)/1000.0;
   f = (1.0-xint)*f1+xint*f2;
  else
   f = 24/Re;
  end
 end

% if (Re<100)
%   f = 0.0;
% else
%    if (Re<200)
%      f1 = 0;
%      f2 = 24/Re;
%      xint = (Re-0)/200;
%      f = (1-xint)*f1+xint*f2;
%
%    elseif ((Re>=200)&(Re<2000))
%      f = 24/Re;
%
%    elseif ((Re>=2000)&(Re<3000))
%      f1 = 24/Re;
%      f2 = 0.052*Re^(-0.19);
%      xint = (Re-2000)/1000.0;
%      f = (1.0-xint)*f1+xint*f2;
%    else
%      f = 0.052*Re^(-0.19);
%    end
% end

   friclossgrad = ((2*f*densmix*vmixfric*abs(vmixfric))/(do-di));

%      if (friclossgrad <0)
%         friclossgrad = 0;
%      end
```

```
end
```

minmod

```matlab
function [ slope ] = minmod(x1,x2,x3,dx)
% Slopelimiter function

a = x2-x1;
b = x3-x2;

if (a*b)<=0
 slope = 0;
else
  if (abs(a)<abs(b))
    slope = a;
  else
    slope = b;
  end
end

slope = slope/dx;

end
```

pm

```matlab
function pmvalue = pm(v,c)


  if (abs(v)<=c)
    pmvalue = -1.0*(v-c)*(v-c)/(4*c)*(-2.0-v/c)/c;
  else
    pmvalue = 0.5*(v-abs(v))/v;
  end
end
```

pp

```matlab
function pmvalue = pp(v,c)

  if (abs(v)<=c)
    pmvalue = (v+c)*(v+c)/(4*c)*(2.0-v/c)/c;
  else
    pmvalue = 0.5*(v+abs(v))/v;
  end
end
```